



THE UNIVERSITY  
*of* ADELAIDE

## Final Report

UNMANNED AERIAL VEHICLE PHYSICAL HOMING RELAY  
SYSTEM FOR INTERNET OF MILITARY THINGS SYNERGY  
(UAV PHORESIS)

UNIVERSITY OF ADELAIDE SCHOOL OF MECHANICAL  
ENGINEERING

PATRICK CAPALDO (A1746146), JASON HUYNH (A1726685), DANIEL O'CONNOR (A1746088)

SUPERVISORS: ASSOCIATE PROFESSOR RINI AKMELIAWATI AND DAVID ROBERTS

Project ID: 3296

Word Count: 13312/13000

Sponsored by



**Australian Government**  
**Department of Defence**

## Executive Summary

The capability to develop an aerial vehicle to interact with, and transport, a variety of small sensors can offer increased sensing flexibility over conventional monolithic sensor platforms in terms of range, tactical positioning, and cost. An Unmanned Aerial Vehicle (UAV) Physical Homing Relay System for Internet of Military Things Synergy (PHORESIS) is proposed and prototyped in this project, with sponsorship and guidance provided by Defence Science and Technology Group (DSTG) and the University of Adelaide. The UAV PHORESIS project involves the use of a multirotor platform tasked to locate, transport, and communicate in real-time during flight with an Internet of Military Things (IoMT) payload. This report describes the systems engineering approach utilised to ensure the project meets the requirements of the project sponsor, DSTG. Furthermore, the existing academic literature, engineering theory, and currently completed designs and analytical methodologies are presented. The report is summarised with a conclusion and outline of the potential further developments in the project.

As influenced by the systems engineering approach, a set of four project objectives are defined in alignment with the client brief and the broader operational context. The objectives to be achieved are: a flyable UAV; transport of a payload; UAV, payload, and ground control station communication systems; and independent operation of the IoMT payload. These objectives form the foundation of the problem definition process. The problem definition phase considers the project as a body of subsystems, allowing for the generation of a scenario based needs analysis from which the user needs are derived. Through the use of backwards traceability, the project objectives and problem definition are distilled into a finer set of measurable targets in the form of system requirements. The satisfaction of each system requirement is able to be monitored through a verification framework consisting five categories suitable for different phases of the project: analysis, certification, demonstration, inspection, and testing. Further validation analysis is performed through regular consultation with the DSTG stakeholders and ultimately through a full flight demonstration. The system requirements strongly influence the direction of the project theory, final design, and integration, to ensure that the developed system meets the needs of the client, DSTG.

From the project direction, insights obtained through a systems engineering framework, four critical topics emerge: UAV platform selection, loaded (with payload) multirotor transportation, autonomous landing, and short-range communication. The literature pertaining to these fields indicates a need for an iterative UAV design approach for component selection. The literature regarding the load transportation problem suggests that a multirotor UAV is sufficiently controllable for transporting either rigidly-grasped or suspended loads. However, there is a lack of research in the system dynamics when initially lifting a suspended load. This research gap introduces a desire for software-in-the-loop simulation, in which ArduCopter and PX4 are found to be more suitable for augmented UAV capabilities in a real environment whilst Matlab/Simulink is suited to control-focused research scopes. It is also found that infrared homing landing systems offer reliable landing target location accuracy. A multitude of wireless short-range communication technologies are available, with trade-offs emerging between power consumption, range, bandwidth, and level of adoption. The available literature offers the academic contextual awareness from which relevant theory may be derived.

The development of the project's fundamental engineering theory arises from the directions of the system requirements and academic research identified in the literature review. The literature findings are applied in an investigation into UAV design methodologies, payload equipped UAV dynamics, short-range wireless communication, and flight simulation. It is identified that a hexacopter multirotor configuration provides an optimal solution to balance flight safety and stability with computational complexity, mechanical complexity, and cost. The behaviour of a payload-equipped UAV is investigated through analysing the equations of motion, whereby it is recommended to mount a cable-suspended payload close to the UAV centre of gravity. Simulation platforms are then utilised for preliminary testing in representative environments. The ideal short-range communication system between the UAV and payload shall utilise Bluetooth technology due to its maturity in the industry, low cost and ease of implementation. Overall, the engineering theory concepts explored provide the framework upon which the final design may be founded upon.

With influence from the supporting engineering theory, the final design demonstrates the tech-

niques used to construct the modular project subsystems: UAV platform; IoMT payload; gripper mechanism; and payload casing. The UAV platform design achieves the project's UAV flight objective through component benchmarking analysis and corroboration with physics simulations. Software considerations are made to select an open-source and mature autopilot and ground control station in ArduPilot and QGroundControl. Real-time wireless communication is enabled in the sensor module alongside a capability to independently operate the sensor payload outside of the UAV environment, hence meeting the independent payload operation objective. An electro ferro-magnet gripper is designed to be tethered to the base of the UAV, enabling up to 1kg of payload to be carried, and addresses the transport of a payload objective. Lastly, a sensor payload casing to house the IoMT sensor and increase the tolerance to UAV landing inaccuracies is 3D printed and verified to be compatible with the magnetic gripper. The synergy of the designed subsystems is further detailed in a subsystem integration analysis which investigates the physical and virtual interfaces.

A critical step in realising the final design (UAV PHORESIS) is the management of the key interfaces between and within the three key subsystems being: hardware, software/communications, and electronics. Successful integration of these subsystems completes the payload transportation and system communication objectives. Hardware integration provides a robust physical connection between the immobile payload the mobile UAV, thus allowing for the transportation of the payload objective to be met. Software/communications integration provides compatibility of signals between any transmitter and receiver pair, hence contributing towards the seamless information flow objective. Finally, electronics integration provides the foundation upon which the software/communications integration operates and power to all electrical components, thus achieving the payload transportation and system communication objectives. Ultimately, the completion of the final design and successful integration of its subsystems successfully completes all project objectives.

## Acknowledgements

The team acknowledge the invaluable in-kind support from Steele Phillips (a multirotor drone expert from Defence Science and Technology Group (DSTG)) whom offered guidance on fundamental electronic assembly techniques including soldering and crimping, in addition to displaying a range of multirotor platforms later used for benchmarking the UAV PHORESIS drone system. Further acknowledgements of DSTG staff are deserved in the supervision and guidance offered by David Roberts; flight trial organisation and support from Adrian Coulter and Martin Sniedze; manufacturing expertise and small workshop resources by Robert Comelli; and David Readman who provided an in-kind laser cut acrylic mounting plate. The team extends their sincere gratitude to DSTG for the sponsorship of the UAV PHORESIS project. The team also acknowledges the staff and support offered by the University of Adelaide in the project supervision offered by Associate Professor Rini Akmeliawati; electronics workshop support from Philip Schmidt, Lydia Zhang, and Norio Itsumi; and the Honours Project team led by Dorothy Missingham and Will Robertson. Finally, the team kindly thanks the Capaldo Family for hosting multiple project development sessions at their home.

## Disclaimer

The project group declare that all material contributed to this report is the work of the project group except where there is clear acknowledgement and reference to the work of others. The project group have read the University of Adelaide Policy Statement on Plagiarism, Collusion and Related Forms of Cheating. The project group give permission for assessment work to be reproduced and submitted to academic staff for the purposes of assessment and to be copied, submitted and retained in a form suitable for electronic checking of plagiarism.

This project is a Defence Science and Technology Group (DSTG) sponsored project and as such, DSTG will own the Project Intellectual Property (IP) and will grant to the University of Adelaide a non-transferable, non-exclusive, royalty-free licence to use the Project IP solely to perform the Project and for the Students to complete the Students' Examinable Publication (if applicable). In addition, DSTG grants to the University of Adelaide a non-transferable, non-exclusive, royalty-free licence (including the right to sub-license) to use the Project IP for research and teaching purposes. Any further IP developed by DSTG or the University of Adelaide based on the Project IP will be owned by the party that creates it.



29/10/2021

---

P. Capaldo (a1746146)

---

Date



29/10/2021

---

J. Huynh (a1726685)

---

Date



29/10/2021

---

D. O'Connor (a1746088)

---

Date

# Contents

<b>Executive Summary</b>	<b>i</b>
<b>Acknowledgements</b>	<b>iii</b>
<b>Disclaimer</b>	<b>iv</b>
<b>1 Introduction</b>	<b>1</b>
1.1 Background . . . . .	1
1.2 Motivation . . . . .	1
1.3 Client Brief . . . . .	1
1.4 Project Aims & Objectives . . . . .	1
1.5 Project Management . . . . .	2
1.6 Report Structure . . . . .	2
<b>2 Problem Definition</b>	<b>3</b>
2.1 System Context . . . . .	3
2.2 Stakeholders . . . . .	4
2.3 Scenario-Based Needs Analysis . . . . .	4
2.4 User Needs . . . . .	4
2.5 System Requirements . . . . .	4
2.6 Problem Definition Summary . . . . .	4
<b>3 Literature Review</b>	<b>12</b>
3.1 UAV Platform Selection . . . . .	12
3.2 Loaded Multirotor Transportation . . . . .	12
3.3 Autonomous Landing . . . . .	13
3.4 Short-Range Communication . . . . .	14
3.5 Literature Review Summary . . . . .	15
<b>4 Theory</b>	<b>16</b>
4.1 Airframe, Motor, and Propeller Selection . . . . .	16
4.2 Dynamics of a Multirotor UAV with a Suspended Load . . . . .	16
4.3 Bluetooth Enabled Short-Range Communication . . . . .	18
4.4 SITL Simulation . . . . .	19
4.5 Theory Summary . . . . .	21
<b>5 Final Design</b>	<b>22</b>
5.1 System Architecture . . . . .	22
5.2 Information Flow . . . . .	22
5.3 UAV Platform Subsystem . . . . .	24
5.3.1 Mechanical Component Selection . . . . .	24
5.3.2 Corroboration of Mechanical Component Selection . . . . .	25
5.3.3 Software Component Selection . . . . .	28
5.3.4 Summary . . . . .	28
5.4 IoMT Payload Subsystem . . . . .	29
5.4.1 Payload Design . . . . .	29
5.4.2 Final Payload . . . . .	31
5.4.3 UAV Integration . . . . .	34
5.4.4 Testing . . . . .	35
5.4.5 Summary . . . . .	35
5.5 Gripper Mechanism Subsystem . . . . .	35
5.5.1 Design Considerations . . . . .	36
5.5.2 Gripper Selection . . . . .	36
5.5.3 Final Gripper Design . . . . .	37
5.5.4 Summary . . . . .	37

5.6	Payload Casing Subsystem . . . . .	37
5.6.1	Conceptual Design . . . . .	38
5.6.2	Material Selection . . . . .	41
5.6.3	Infrared Beacon Detection . . . . .	41
5.6.4	Gripper Interface . . . . .	42
5.6.5	Prototyping . . . . .	42
5.6.6	Summary . . . . .	43
5.7	Final Design Summary . . . . .	44
<b>6</b>	<b>Subsystem Integration</b>	<b>45</b>
6.1	Hardware Integration . . . . .	45
6.2	Software and Communications Integration . . . . .	46
6.2.1	Sensor to Rapsberry Pi (Bluetooth) . . . . .	46
6.2.2	Raspberry Pi to UAV Radio Modem (Serial) . . . . .	46
6.2.3	UAV Radio Modem to GCS/Hand-Held Controller (Radio) . . . . .	46
6.2.4	On-Board FPV Camera to Grounded FPV Receiver (Radio) . . . . .	47
6.3	Electronics Integration . . . . .	49
6.4	UAV PHORESIS Demonstration . . . . .	51
6.5	Verification and Validation . . . . .	52
6.5.1	Verification . . . . .	52
6.5.2	Validation . . . . .	55
6.6	Subsystem Integration Summary . . . . .	55
<b>7</b>	<b>Conclusion</b>	<b>57</b>
<b>8</b>	<b>Future Work</b>	<b>59</b>
<b>A</b>	<b>Project Objectives</b>	<b>66</b>
A.1	Objective 1 - Flyable UAV . . . . .	66
A.1.1	Specific . . . . .	66
A.1.2	Measurable . . . . .	66
A.1.3	Attainable . . . . .	66
A.1.4	Relevance . . . . .	66
A.1.5	Timeframes . . . . .	66
A.2	Objective 2 - Transport of a Payload . . . . .	66
A.2.1	Specific . . . . .	66
A.2.2	Measurable . . . . .	66
A.2.3	Attainable . . . . .	66
A.2.4	Relevance . . . . .	67
A.2.5	Timeframes . . . . .	67
A.3	Objective 3 - UAV, Payload and Ground Station Communication . . . . .	67
A.3.1	Specific . . . . .	67
A.3.2	Measurable . . . . .	67
A.3.3	Attainable . . . . .	67
A.3.4	Relevance . . . . .	67
A.3.5	Timeframes . . . . .	67
A.4	Objective 4 - Independent Operation of the IoMT Payload . . . . .	67
A.4.1	Specific . . . . .	67
A.4.2	Measurable . . . . .	67
A.4.3	Attainable . . . . .	68
A.4.4	Relevance . . . . .	68
A.4.5	Timeframes . . . . .	68

<b>B Stakeholders</b>	<b>68</b>
B.0.1 The University of Adelaide (UoA)	68
B.0.2 Australian Department of Defence (ADoD)	68
B.0.3 Defence Science and Technology Group (DSTG)	68
B.0.4 Multirotor Advisor (MA)	68
B.0.5 Project Supervisor (PS)	68
B.0.6 Honours Team 3296 (HT3296)	69
<b>C Project Failure Assessment</b>	<b>70</b>
<b>D Risk Assessments and Safe Operating Procedures</b>	<b>74</b>
<b>E IoMT Payload Iterative Development</b>	<b>79</b>
<b>F MQ-2 Smoke Gas Detector Sensor Module Data Sheet</b>	<b>84</b>
<b>G XC-4438 Microphone Module Data Sheet</b>	<b>88</b>
<b>H XC-4494 Analogue Temperature Sensor Module Data Sheet</b>	<b>90</b>
<b>I Electro Ferromagnet Data Sheet</b>	<b>92</b>
<b>J SITL Simulation</b>	<b>94</b>
J.1 Ubuntu, ArduPilot, QGroundControl, FlightGear Installation	94
J.2 ArduCopter Launch	95
J.3 Add Custom Location	95
J.4 Modify Vehicle Parameters	96
J.5 Modify Environmental Parameters	96
J.6 ArduPilot and QGroundControl Launch at Location and Fly	96
J.7 ArduPilot, QGroundControl, and FlightGear Launch at Location and Fly	97
J.8 Download ArduPilot Logs	98
J.9 Download QGroundControl Logs	98
J.10 Setup a Shared Folder between Ubuntu 20LTS and Windows	98
J.11 Analyse Logs with Mission Planner	99
J.12 Create a Flight Path with QGroundControl	99
<b>K Technical Drawings</b>	<b>101</b>
<b>L IoMT Sensor Payload Code</b>	<b>105</b>
L.1 Smoke Detector Sensor Payload	105
L.2 Sound Sensor Payload	106
L.3 Temperature Sensor Payload	107
<b>M Raspberry Pi Sensor Data Receiving Code</b>	<b>108</b>
<b>N Work Breakdown Structure and Gantt Chart</b>	<b>110</b>
<b>O Detailed Flight Characteristics</b>	<b>118</b>
<b>P Mass Estimation</b>	<b>124</b>
<b>Q Budget Breakdown</b>	<b>125</b>



## Acronyms

- ABS** Acrylonitrile Butadiene Styrene. 38, 41
- ADoD** Australian Department of Defence. 4
- BEC** Battery Eliminator Circuit. 49
- CAD** Computer Aided Design. 42, 43
- CASA** Civil Aviation Safety Authority. 11, 53, 59, 66, 115
- COTS** Commercial Off The Shelf. 8, 36, 59
- DSTG** Defence Science and Technology Group. i, iii, iv, vii, x, xii, 1, 4, 7, 24, 25, 28, 51–53, 55, 59, 68, 72, 128
- FPV** First-Person Video. vi, 46, 47
- GCS** Ground Control Station. vi, 1, 2, 8, 9, 19, 22, 23, 26, 28, 34, 35, 41, 44, 46, 47, 49, 51, 54, 57, 99
- GPS** Global Positioning System. 13, 14, 19, 27, 41, 67, 71, 72, 95–97, 124–126
- GUI** Graphical User Interface. 19
- HT3296** Honours Team 3296. 4
- I2C** Inter-Integrated Circuit. 49
- ICT** Information Communication Technology. 59
- IDE** Integrated Development Environment. 29, 79, 80
- IoMT** Internet of Military Things. i, ii, v–viii, 1, 2, 19, 22, 29, 35, 37, 43–45, 51, 55, 57, 66–68, 71, 72, 79, 105
- IoT** Internet of Things. 14, 15, 67, 68, 71, 72
- IP** Intellectual Property. iv
- IR** infrared. x, 14, 15, 27, 37, 38, 41, 42, 49, 124, 125
- LAN** Local Area Network. 14, 15
- MA** Multirotor Advisor. 4
- OSD** On-Screen Display. 95
- PAN** Personal Area Network. 14, 15
- PCB** Printed Circuit Board. x, 30–33
- PHORESIS** Physical Homing Relay System for Internet of Military Things Synergy. i–iii, vi, x, 1, 4, 5, 18, 22, 45, 46, 51, 52, 57
- PID** Proportional-Integral-Derivative. 13
- PS** Project Supervisor. 4
- PWM** Pulse Width Modulation. 37, 49, 53

**SBNA** Scenario-Based Needs Analysis. x, 3–7, 55, 57

**SCD** System Context Diagram. 3, 7

**SITL** Software-in-the-Loop. 13, 15, 19, 21, 25, 28, 57, 94

**SSH** Secure Shell. 46

**SVP** Summer Vacation Placement. 59

**TWR** Thrust-to-Weight Ratio. 12, 21

**UAV** Unmanned Aerial Vehicle. i–iii, v, vi, x–xii, 1, 2, 4–6, 8–19, 21–29, 34–38, 41–47, 49–55, 57–59, 66–68, 71, 72, 82, 94, 96, 97, 99, 110, 111, 113–116, 118–122, 124

**UDP** User Datagram Protocol. 13, 28

**UoA** The University of Adelaide. 4, 28

**UWB** Ultra-wideband. 14, 15, 18, 35

**VM** Virtual Machine. 19, 98

**WBS** Work Breakdown Structure. xii, 2, 57, 59, 110, 113

## List of Figures

1	System context diagram. . . . .	3
2	UAV PHORESIS Scenario-Based Needs Analysis (SBNA) functional flow block diagram. . . . .	5
3	A suspended load modelled as a pendulum with a body-centred coordinate system defined from the UAV’s centre of gravity, where the UAV position is given by an inertial reference, $\mathbf{p} = [x \ y \ z]^T$ , and the payload position relative to the UAV is defined by the angles $\phi_L$ and $\theta_L$ (Klausen et al. 2017). . . . .	17
4	HC-05 Bluetooth module (Verma 2020). . . . .	19
5	ArduPilot and QGroundControl SITL simulation layout. . . . .	20
6	Simulated flight at St Kilda, South Australia using FlightGear and ArduPilot. . . . .	20
7	System architecture, with the inoperable payload-to-UAV communications link acknowledged with the faded dotted line. . . . .	22
8	Information flow diagram illustrating one decision cycle. . . . .	23
9	Iterative stages to Bluetooth communication system development. . . . .	29
10	Initial smoke detector sensor configuration. . . . .	30
11	Smoke detector sensor code. . . . .	30
12	Configurable PCB arrangement. . . . .	31
13	Schematic PCB design. . . . .	31
14	Final smoke detector sensor payload. . . . .	32
15	Smoke detector sensor payload output. . . . .	32
16	Final sound detector payload. . . . .	33
17	Sound detector payload output. . . . .	33
18	Final temperature sensor payload. . . . .	33
19	Temperature sensor payload output. . . . .	34
20	Sensor output when received by UAV. . . . .	34
21	Example of UAV backup flight log. . . . .	34
22	Gripper mounting implementation. . . . .	37
23	Concept sketch of payload casing solution 1. . . . .	39
24	Concept sketch of payload casing solution 2. . . . .	39
25	Concept sketch of payload casing solution 3. . . . .	40
26	Concept sketch of payload casing solution 4. . . . .	40
27	Infrared beacon detection by on-board infrared camera. The laptop screen at the top of the image displays the live picture processed by the IR camera. . . . .	41
28	Flight log showing UAV height above ground (red), IR-lock camera health (green) and IR beacon detection status (blue). . . . .	42
29	Payload casing funnel. . . . .	42
30	Iterative stages in payload casing development. . . . .	43
31	Final payload casing construction. . . . .	43
32	UAV flying with payload casing. . . . .	44
33	UAV gripper guided towards casing via funnel. . . . .	44
34	Block diagram realisation of the hardware integration interfaces. . . . .	45
35	Block diagram realisation of the software and communications interfaces. . . . .	48
36	UAV platform electrical wiring diagram. . . . .	50
37	Demonstration of UAV PHORESIS within an indoor flight arena at DSTG Edinburgh. . . . .	52
38	Power map of the six key stakeholders for this project. . . . .	69
39	Physical implementation of LED integrated boolean communication with an external power supply. . . . .	80
40	String communication between master (left) and slave (right) HC-05 modules. . . . .	81
41	Arduino function that changes the state of the transistor in order to disconnect and re-connect power to the HC-05 module. . . . .	82
43	Circuit implementation of portable master (left) and slave (right) devices with re-connect functionality. . . . .	83
42	Physical implementation of portable master (left) and slave (right) devices with re-connect functionality. . . . .	83

44	UAV platform unloaded configuration parameter inputs and basic performance characteristics. . . . .	119
45	UAV platform unloaded configuration range estimations and motor characteristics at full throttle. . . . .	120
46	UAV platform loaded configuration parameter inputs and basic performance characteristics. . . . .	121
47	UAV platform loaded configuration range estimations and motor characteristics at full throttle. . . . .	122

## List of Tables

1	User needs. . . . .	6
2	System requirements. . . . .	8
3	Communication technology signal ranges. . . . .	18
4	Generalised platform component suggestions from the DSTG advisor. . . . .	24
5	eCalc flight characteristics of the UAV in unloaded and loaded configurations. . . . .	26
6	UAV power budget. . . . .	27
7	Connection time after HC-05 Bluetooth module reset. . . . .	35
8	Gripping mechanism Pugh selection matrix. . . . .	36
9	Payload casing design morphological table. . . . .	38
10	Payload casing Pugh selection matrix. . . . .	41
11	Verification measures via analysis. . . . .	53
12	Verification measures via certification. . . . .	53
13	Verification measures via demonstration. . . . .	54
14	Verification measures via inspection. . . . .	54
15	Verification measures via testing. . . . .	55
16	Removed tasks from the WBS. . . . .	59
17	New tasks to the WBS. . . . .	59
18	Project risks. . . . .	71
19	Risk mitigation strategies. . . . .	72
20	Risk criticality matrix defined by likelihood and consequences for a project risk. . . . .	73
21	Risk evaluation impacts. . . . .	73
22	Progress key of the WBS. . . . .	110
23	Administration-based tasks of the WBS. . . . .	110
25	Designing-, building-, testing- and execution-based tasks of the WBS. . . . .	113
27	UAV on-board mass estimation, noting that the mass of certain small components are not available. . . . .	124
28	Itemised list of anticipated direct project expenditure. . . . .	125
29	Quantifiable in-kind contributions for the project. . . . .	128
30	In-kind labour contributions for the project. . . . .	128

# 1 Introduction

## 1.1 Background

The Internet of Military Things (IoMT) environment involves the use of military-purposed devices integrated into a wirelessly networked paradigm. The IoMT concept provides the capability for a multitude of networked sensors and effectors to aid operations in contested and complex environments. The easy access to low-cost, power efficient and small sensors makes them an attractive option to more conventional monolithic designs (Jasiunas 2020). However, because of their simplicity, IoMT devices are generally immobile and therefore susceptible to losing their effectiveness if the local environment evolves. Changes in the environment may threaten the survivability of the device; targets and locations of interest may migrate outside the effective range of the IoMT network; and the provided coverage from the IoMT network may no longer be appropriate.

## 1.2 Motivation

In the consideration of a typical IoMT device's susceptibility to an ever-changing environment, a development upon the IoMT concept to deliver self-forming and self-healing mesh networks is therefore incentivised. Defence Science and Technology Group (DSTG) are exploring a range of IoMT transportation methods through the use of soldiers, land vehicles, or aerial platforms to deploy and reconfigure IoMT networks.

Of particular interest is the use of a multirotor aerial platform as a transportation vehicle. The research in this transport option is primarily driven by the multirotor's capabilities and precedent usage in similar tasks such as the delivery of medical supplies for pre-hospital situations in battlefields (Braun et al. 2019), dropping fire extinguishing agents above bushfires (Saikin et al. 2020), and deliveries of parcels (Yoo et al. 2018). These applications, amongst others, offer a foundation for which an IoMT-synergistic solution may be developed.

## 1.3 Client Brief

DSTG requires an Unmanned Aerial Vehicle (UAV) solution to facilitate research into modular IoMT device integration with physical platforms. The scope of the client-driven specifications offered by the DSTG representative, David Roberts, include:

- The UAV must have comparable performance characteristics to other existing UAV research platforms operated by DSTG for future interoperability and reusability of the platform
- A prototype modular IoMT sensor device shall be developed for short-range (within 2m) standalone usage and usage within the UAV PHORESIS environment, with forethought of compatibility with other vehicular options
- The UAV shall be capable of collecting, transporting, and delivering the IoMT payload
- The communication network for the project must support real-time telemetry exchange between the IoMT payload, UAV, and Ground Control Station (GCS)
- DSTG will provide up to \$10,000 for the project
- Handover documentation must be provided to fully describe the operating procedure for all components in the project

It has been specified that the Honours Project Team shall be responsible for the distillation and refinement of the client-driven specifications. The validation elements of the project will be utilised to ensure the distilled system requirements meet the client specifications.

## 1.4 Project Aims & Objectives

This project aims to develop a directed aerial system which transports and communicates with modular, self-operable, IoMT devices in real-time. The aim of the project can be decomposed into three expected project outcomes:

1. Transport of a modular IoMT payload using a directed, multirotor UAV
2. Real-time communication systems between the payload, vehicle, and a ground station
3. Ensured operation of the IoMT payload independent of the vehicle

Each of these outcomes, alongside the Client Brief outlined in Section 1.3, influence the project objectives. Each objective can be achieved in isolation and are developed through the Specific, Measurable, Attainable, Relevance, Timeframe (SMART) methodology. The objectives are subject to reassessment in accordance with any significant change in project circumstances. The project objectives are listed below, with the full descriptions using the SMART format included in Appendix A:

O.1 Flyable UAV

O.2 Transport of a Payload

O.3 UAV, Payload, and GCS Communication Systems

O.4 Independent Operation of the IoMT Payload

## **1.5 Project Management**

A detailed Work Breakdown Structure (WBS) and Gantt Chart are included in Appendix N and form the basis of the project management. The project expenditure is presented in Appendix Q, which includes the costs of purchasing components and in-kind contributions toward the project. To ensure the achievement of the project aims and objectives, assessments of high-level project risks and mitigation strategies are tabulated in Appendix C. This is supported by the risk assessments and safe operating procedures presented in Appendix D to ensure the daily risks of assembling and operating the project are safely managed.

## **1.6 Report Structure**

The report is structured with an ultimate focus on how the modular subsystem design elements of the project are synergised using integration techniques to deliver a complete project. A systems engineering approach is presented in the Problem Definition (Section 2) to distil and quantify the project's requirements from the Client Brief, and Project Aims & Objectives. Literature Review (Section 3) subsections are guided by the project aims and objectives, and provide an academic framework for the succeeding Theory (Section 4), and Final Design (Section 5) sections. The Theory section presents the fundamental engineering knowledge from which justified and accurate designs may be developed. An outline of Subsystem Integration (Section 6) is provided subsequent to the Final Design section, where the specific details of each subsystem are described. The report is summarised with a Conclusion (Section 7) and an insight into Future Work (Section 8).

## 2 Problem Definition

The problem definition comprehensively distills and formulates the project into a measurable set of system requirements. The system requirements are fundamentally derived and influenced by various elements of the problem definition, such as the system context, stakeholders, Scenario-Based Needs Analysis (SBNA), and user needs. The dependencies are explicitly outlined through backwards traceability.

### 2.1 System Context

A system context diagram System Context Diagram (SCD) (Figure 1) defines the external entities and subsystems that interact with the system. This demonstrates the how the system interfaces with its environment and the how system is supported and constrained by varying other systems. The SCD also outlines how the system impacts and constrains other entities, and assists in the formulation of system deliverables and requirements.

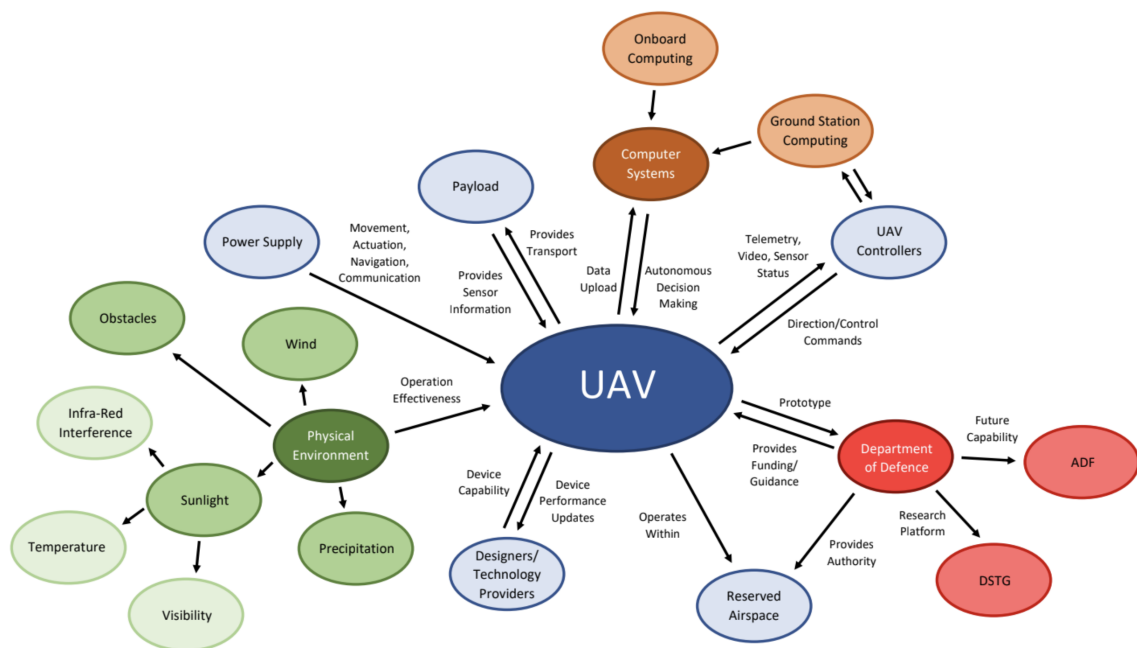


Figure 1: System context diagram.



## 2.2 Stakeholders

There are six key stakeholders identified in the project. These stakeholders are listed below, with descriptions and a stakeholder power map detailed in Appendix B:

- S.1 The University of Adelaide (UoA)
- S.2 Australian Department of Defence (ADoD)
- S.3 Defence Science and Technology Group (DSTG)
- S.4 Multicopter Advisor (MA)
- S.5 Project Supervisor (PS)
- S.6 Honours Team 3296 (HT3296)

## 2.3 Scenario-Based Needs Analysis

Scenario-Based Needs Analysis (SBNA) is a structured approach that details the interaction between various components of the system during a fully-functional scenario. From this, the needs of the users and stakeholders may be elicited. The UAV PHORESIS SBNA is displayed as a functional flow block diagram in Figure 2. It details key components of representative scenarios such as travelling to the site, deployment of the UAV and payload, interaction and communication between the UAV and payload, and pack-up of the system.

## 2.4 User Needs

The user needs (Table 1) outline the high-level stakeholder requirements to achieve full functionality and are derived from the client brief and SBNA. Each user need is separated by functional and non-functional needs. Functional needs describe services provided by the system. Conversely, non-functional needs describe critical system properties and constraints.

## 2.5 System Requirements

The system requirements (Table 2) outline the low-level requirements of the system necessary to successfully achieve the user needs. Similarly to user needs, the system requirements are separated into functional and non-functional requirements. Moreover, each system requirement is allocated a verification measure (presented in Section 6.5.1) in order to ensure its achievement.

## 2.6 Problem Definition Summary

The presented problem definition analysis provides the guiding framework for the project theory, and platform design and methodology. In particular, the comprehensive list of system requirements is referenced throughout the theory and design phases. Given the multifaceted influences on the system requirements presented in the problem definition, it is expected that continual references to the requirements throughout the project will ensure that developments remain objective-oriented and meet stakeholder expectations.

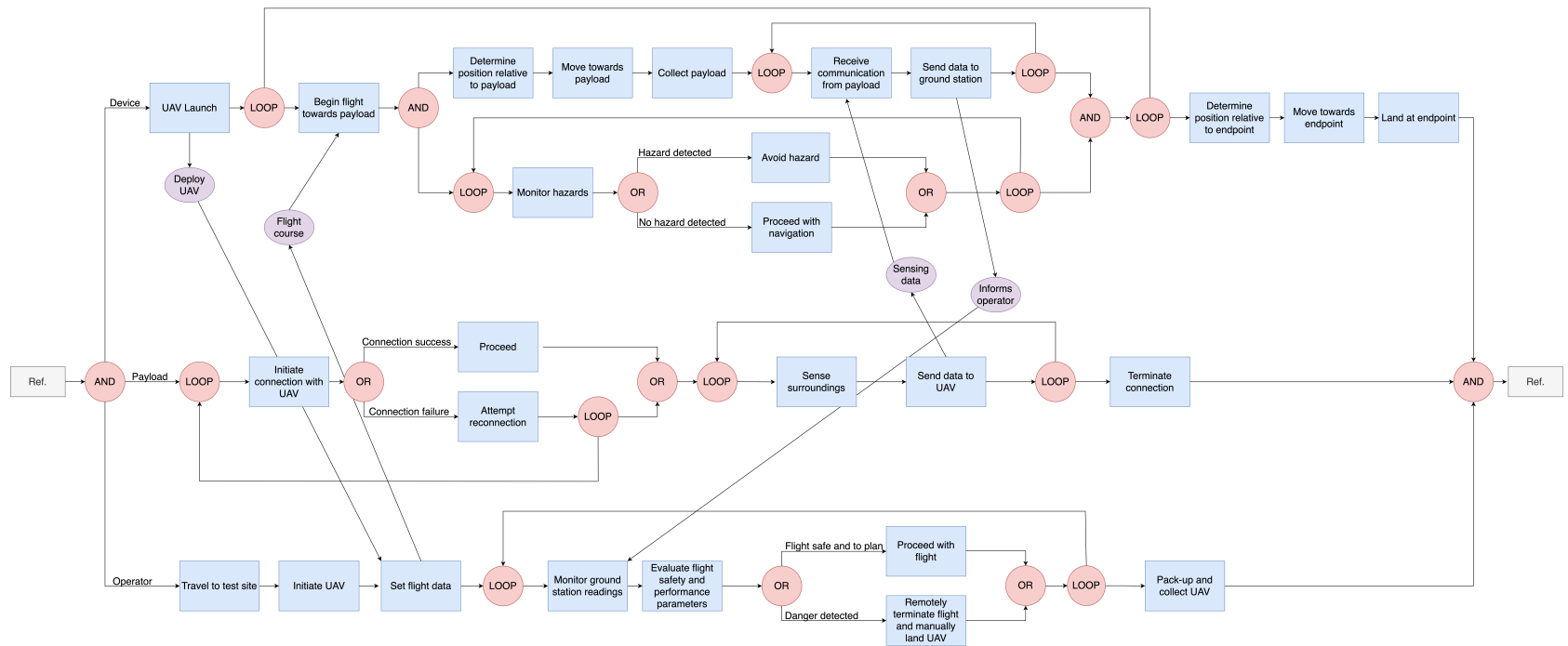


Figure 2: UAV PHORESIS Scenario-Based Needs Analysis (SBNA) functional flow block diagram.

Table 1: User needs.

Group	Sub-Group	ID	Need	Backward Traceability	Criticality
1. Functional	1. UAV Flight	UN.1.1.1	The user needs the system to maintain stable flight in light winds/turbulent conditions	Client Brief	Very Important
		UN.1.1.2	The user needs the system to successfully transport the payload from one ground location to another	Client Brief	Essential
		UN.1.1.3	The user needs the system to locate the grounded payload	sbna	Important
		UN.1.1.4	The user needs the system to descend to within a close distance of the payload	sbna	Desirable
		UN.1.1.5	The user needs the system to return to home once the payload has been transported	sbna	Important
		UN.1.1.6	The user needs the system to be remotely terminable	sbna	Essential
	2. Communication	UN.1.2.1	The user needs the system to demonstrate communication between the UAV and the attached payload in-flight	Client Brief	Essential
		UN.1.2.2	The user needs the system to demonstrate communication between the UAV and ground-station	Client Brief	Essential
		UN.1.2.3	The user needs the system to demonstrate communication between the airborne UAV and the grounded payload	Client Brief	Essential
	3. Physical Payload Interface	UN.1.3.1	The user needs the system to demonstrate the UAV picking up the payload without physical human assistance	Client Brief	Essential
		UN.1.3.2	The user needs the system to demonstrate the UAV dropping off the payload without physical human assistance	Client Brief	Essential
		UN.1.3.3	The user needs the system to maintain physical grip between the UAV and the payload during transportation	Client Brief, SBNA	Essential
	4. Payload	UN.1.4.1	The user needs the system to hold a sensor within the payload module	Client Brief, SBNA	Essential
		UN.1.4.2	The user needs the system to exhibit a separate power supply for the payload	SBNA	Very Important

2. Non-Functional	1. Physical Constraints	UN.2.1.1	The user needs the system to fit within an average-sized 4WD car	SBNA	Important
		UN.2.1.2	The user needs the system to be carried by at most two people	SBNA	Important
		UN.2.1.3	The user needs the system to exhibit an easily exchangeable power supply	SCD	Very Important
	2. Procurement and Maintenance	UN.2.2.1	The user needs the system to function within the allocated budget	Client Brief, SCD	Important
		UN.2.2.2	The user needs the system to be transferred in a completely operable state/quality	Client Brief	Very Important
		UN.2.2.3	The user needs the system to be maintainable with existing tools and materials	Client Brief	Desirable
	3. Environment	UN.2.3.1	The user needs the system to maintain functionality in direct sunlight	SCD	Desirable
		UN.2.3.2	The user needs the system to maintain functionality in light winds/turbulence	SCD	Very Important
		UN.2.3.3	The user needs the system to maintain functionality in dusty conditions	SCD	Very Important
	4. Legislation	UN.2.4.1	The user needs the system to abide by environmental protection regulations	DSTG	Important
		UN.2.4.2	The user needs the system to abide by Defence Aviation Safety Regulation (DASR) UAS.35	DSTG	Essential
		UN.2.4.3	The user needs the system to abide by DASR BR.25.A – Essential Requirements for Environmental Protection (AUS)	DSTG	Very Important

Table 2: System requirements.

ID	Requirement	Functional/ Non- Functional	Category	Backward Traceability	Criticality	Verification Measure
R.1	UAV Flight					
R.1.1	The UAV shall only operate over land controlled by Defence and comply with Defence Aviation Safety Authority, Open Category UAS Regulations (DASR UAS.40)	Functional	Legislation and standards	S.2, S.3, UN.1.6	Essential	C.1
R.1.2	The UAV shall be capable of carrying up to 1kg of payload	Functional	Functionality	S.2, S.3, UN.1.2	Very Important	T.1, I.1
R.1.3	The UAV shall have the endurance to transport a payload 50m without a change of power supply	Functional	Functionality	UN.1.2, O.2	Important	D.1, T.2
R.1.4	The UAV shall have the endurance to successfully locate, pickup, and dropoff the payload using the precision guidance and VTOL systems without a change of power supply	Functional	Functionality	UN.1.3, UN.1.4	Very Important	D.1
R.1.5	The UAV's power supply shall allow for an endurance of at least 15 minutes	Non-Functional	Technology	UN.1.1, UN.1.2, UN.1.3, UN.1.4, UN.1.5	Important	D.1, T.5
R.1.6	The UAV shall receive and act on remote instructions from the GCS within a 200m range	Functional	Technology	UN.1.5, UN.1.6	Essential	D.2
R.1.7	The UAV shall only require full system maintenance at least once every 150 hours of flight	Non-Functional	Physical Characteristics	UN.1.7	Desirable	A.1
R.1.8	The UAV shall be assembled from components which are functionally replacable with Commercial Off The Shelf (COTS) components	Non-Functional	Functionality	UN.1.7	Very Important	I.2
R.1.9	The UAV shall be autonomously controlled by a ground control station with mission planning capabilities	Functional	Functionality	UN.1.3, UN.1.4, UN.1.5	Desirable	I.3
R.2	Communication					

R.2.1	The UAV and payload shall wirelessly exchange data to a range of 2m within line of sight	Functional		UN.2.1, UN.2.3, Client Brief	Essential	T.2
R.2.2	The UAV shall locate the payload from altitude of 15m from the grounded payload	Functional	Functionality	UN.2.3, Client Brief	Essential	T.2
R.2.3	The UAV shall identify the payload from within a 35 degree angular offset from above the payload	Functional	Functionality	UN.2.3, Client Brief	Essential	T.3
R.2.4	The UAV and GCS shall wirelessly exchange data to a range of 200m within line of sight	Functional	Technology	UN.2.1 Client Brief	Essential	T.2
R.2.5	The payload shall transmit the data collected from its on-board IoMT sensor to the UAV	Functional	Technology	UN.2.1, UN.2.3	Essential	D.2
R.2.6	The UAV and GCS shall wirelessly exchange UAV telemetry and IoMT sensor data	Functional	Technology	UN.2.2	Essential	D.2
R.2.7	The UAV and payload shall maintain constant communication during transportation	Functional	Technology	UN.2.1	Essential	I.3
R.2.8	The UAV and payload shall be able to connect within 15 seconds once in range	Functional	Technology	UN.2.1	Essential	D.2
<hr/>						
R.3	Physical Payload Interface					
R.3.1	The UAV shall navigate to the payload without manual guidance from the remote pilot	Functional	Functionality	O.2	Important	D.3
R.3.2	The UAV shall keep the payload secured throughout flight	Functional	Functionality	UN.3.3	Very Important	D.1
R.3.3	The UAV shall release the payload once the payload is in contact with the ground	Functional	Functionality	UN.3.2	Very Important	D.1, D.2
R.3.4	The UAV shall collect and release the payload without physical human assistance	Functional	Functionality	UN.3.1, UN.3.2	Important	D.3
R.3.5	The UAV shall maintain stable flight upon collection and release of the payload	Functional	Functionality	UN.3.1, UN.3.3	Important	D.4
<hr/>						
R.4	Payload					
R.4.1	The payload's electrical system shall support an IoMT sensor and wireless communication module	Non-Functional	Technology	UN.4.1	Essential	I.3
R.4.2	The payload shall contain a dedicated power supply to support its independent electrical system	Non-Functional	Technology	UN.4.2	Essential	I.3
R.4.3	The payload's power supply shall support the payload's electrical systems for at least 15 minutes	Non-Functional	Technology	UN.4.3	Very Important	T.1

R.4.4	The payload shall exhibit an outer-casing that protects its electrical system from the environment	Non-Functional	Physical Characteristics	O.2	Important	I.3
R.4.5	The payload's protective casing shall not inhibit its communication capability to the UAV	Non-Functional	Physical Characteristics	O.2	Very Important	D.2, D.4
R.4.6	The payload shall not exceed a mass of 1kg	Non-Functional	Physical Characteristics	O.2	Very Important	I.1
<hr/>						
R.5	Form Constraints					
R.5.1	The combined mass of the UAV and payload shall not exceed 25kg (UAS.40)	Non-Functional	Physical Characteristics	UN.5.1, UN.5.2	Essential	I.1
R.5.2	The UAV shall have a power supply that can be exchanged	Non-Functional	Physical Characteristics	UN.5.3	Very Important	D.1
R.5.3	The payload shall have a power supply that can be exchanged	Non-Functional	Physical Characteristics	UN.5.3	Very Important	D.1
R.5.4	The UAV shall not exceed a volume storage/transportation size of 350L	Non-Functional	Physical Characteristics	UN.5.1, UN.5.2	Very Important	A.2
<hr/>						
R.6	Environment					
R.6.1	The UAV and payload shall maintain full functionality in direct sunlight for at least 15 minutes	Functional	Environment	UN.6.1	Very Important	T.4
R.6.2	The system shall exhibit full functionality after exposure to direct sunlight for at least 1 hour	Functional	Environment	UN.6.1	Important	T.4
R.6.3	The system shall maintain full functionality in light winds ( $\pm 10 m/s$ )	Functional	Environment	UN.6.2	Very Important	T.4
R.6.4	The system shall maintain full functionality in dusty conditions for at least 20 minutes	Functional	Environment	UN.6.3	Very Important	T.4
R.6.5	The system shall exhibit full functionality after exposure to dusty conditions from a full-length flight	Functional	Environment	UN.6.3	Important	D.5
<hr/>						
R.7	Administration					

R.7.1	The UAV shall abide by DASR BR.25.A – Essential Requirements for Environmental Protection (AUS)	Functional	Environment	UN.7.1	Essential	C.1
R.7.2	The system shall be operated by a person with an understanding of the entire system	Functional	Training	UN.7.1, UN.7.2, UN.7.3	Very Important	C.2
R.7.3	The system shall be operated by a person experienced in the Linux operating software	Functional	Training	O.1, O.2, O.3, O.4	Very Important	C.2
R.7.4	The system shall be flown by a pilot with a Civil Aviation Safety Authority (CASA) Remote Pilot Licence (RePL)	Functional	Training	O.1, O.2	Essential	C.2
R.7.5	The system shall be operated only over defence controlled land (UAS.40)	Functional	Security	UN.7.2, UN.7.3, O.1, O.2, S.3	Very Important	C.1
R.7.6	The system shall be designed, procured, operated and maintained within the allocated budget of AUD\$10,000	Non-Functional	Legislation and standards	UN.7.4, UN.7.5	Very Important	I.2

---



### 3 Literature Review

An analysis of the problem definition reveals four critical topics for research: UAV platform selection, loaded multirotor transportation, autonomous landing, and short-range communication. Each topic presented in the literature review investigates existing capabilities, standards, and contradictory findings to form a foundation of understanding and refine the scope of this project.

#### 3.1 UAV Platform Selection

The rapid proliferation of multirotor UAVs has introduced the need for their performance-oriented and application-specific technical design, yet despite this, there is a noticeable lack of design methodology standardisation and recognition of component interdependencies. The majority of proven methodologies agree that the first factor to evaluate when designing a UAV is its expected total weight (Abarca et al. 2017; Bryceson et al. 2016; Javir et al. 2015; Reid 2019; Yudho et al. 2017). However, the authors fail to provide any analytical reasoning to justify their choice of frame size and rotor count - opting for a brief qualitative statement instead. For example, Yudho et al. (2017) justifies their choice of designing a hexacopter with the lack of redundancy of quadcopters and the expense of octocopters; whilst Javir et al. (2015) rationalises their quadcopter selection based purely on their popularity. Reid (2019) is the only of the four authors who begins the design process without such assumptions, yet the frame size and rotor count selections are never systematically addressed. To further contradict the authors aforementioned, Achtelik et al. (2012) argue that the motors should be selected prior to the total UAV weight estimation as they determine the maximum lifting force of the UAV and hence its expected total weight. The vast majority of the aforementioned authors (Abarca et al. 2017; Bryceson et al. 2016; Javir et al. 2015; Reid 2019; Yudho et al. 2017) agree that the next step in the design process is the motor type selection. However, their methods of analysis differ between a combination of two key factors: thrust-to-weight ratio (TWR) and "KV" value. The TWR is a measure of the vehicle's acrobatic ability and ease of control in challenging environments, such as wind gusts (Szyk 2018). The KV value states the number of rotations per minute (RPM) achieved by an unloaded motor (without propeller) with one volt (1V) of potential across it (Tengfei et al. 2016) - this value is critical to selecting an appropriate propeller to match the motor. To select an appropriate motor, Bryceson et al. (2016) and Abarca et al. (2017) use only the KV value, whilst Javir et al. (2015) use only the TWR. Yudho et al. (2017) and Reid (2019) consider both TWR and KV values to conduct a more detailed motor and propeller selection. The multitude of contradictory design methodologies indicate the presence of ambiguous industry standards and strong interdependencies between components that prevent them from being selected independently. For example, estimated weight determines the thrust required, which determines the number of rotors, which determines the frame size, which cyclically determines the estimated weight. The limitations of this architecture are recognised by Magnussen et al. (2015) and Idres et al. (2015) who suggest the use of an iterative design process where the selection of each component is revisited several times to approach an optimal design. This approach is desirable as it offers a standard selection methodology that can be applied in various technical spaces, and because it overcomes the limitation of component interdependencies through reiteration and re-evaluation of the system design.

#### 3.2 Loaded Multirotor Transportation

The multirotor UAV load transportation problem investigates the extents of stability and maneuverability for loaded UAVs. The two primary approaches to multirotor load transportation include directly grasping the load from the airframe or utilising a cable-suspension linkage (Villa et al. 2020). The directly-grasped load transport approach typically introduces a poorer flight endurance and slower control response when compared to a cable-suspended load strategy (Pounds et al. 2011). However, a cable-suspended approach poses a fundamentally more complex problem in the introduction of unactuated states related to the swaying of the load (Klausen et al. 2017). Angelis et al. (2019) observe the similarities between the relatively modern suspended load control problem in multirotor UAVs and overhead cranes in the construction industry, the latter of which has been extensively studied. A more modern comparison than overhead cranes, but with

greater research precedent that multirotor UAV platforms may include the design of helicopter slung-load systems (Omar 2013). A grasped-load approach involves a rigid connection of a load onto the vehicle frame. Therefore, the aggregated system may still be modelled as a single body after acknowledging changes to the mass parameters (Villa et al. 2020). Lindsey et al. (2012) demonstrate the usage of mechanical grippers positioned below a quadcopter to provide a construction capability for cubic structures. It was shown that the quadcopters have the necessary dynamic control to grab structural members for precise delivery upon landing. Pounds et al. (2012) utilise a Proportional-Integral-Derivative (PID) flight controller to also demonstrate the capability of multirotor platforms to transport grasped loads. It was calculated that there exists a permissible centre of gravity-offset radius which the PID controller can accommodate. This has implications in the precision in the positioning of a grasped load with respect to a UAV’s geometric centre. The suspended-load approach is presented as another primary alternative to the UAV load transport problem (Villa et al. 2020). Cruz et al. (2017) note that the initial lifting phase of the suspended-load collection process has not been widely studied in literature. Their work aims to precisely track the trajectory of a payload during collection from a slack to taut cable suspension state. The proposed approach was verified with a quadrotor and suspended load. In scenarios where a multirotor platform is already loaded with a load, research has been performed in the tracking of the load and the manoeuvrability potential of the system. Sreenath et al. (2013) present methods to minimise the swaying of a suspended load, and have also developed a method to exploit the swinging motion to enhance acrobatic motions of the UAV. Recently, further work performed by Guo et al. (2020) utilises a Proportional-Derivative trajectory tracking controller to accurately manipulate the trajectory of a suspended load. The approach is demonstrated by flying the loaded UAV system through a narrow window requiring the payload to be swinging upwards to allow for a smaller profile for successful passage. It is noted that Proportional-Derivative controllers are comparatively simpler and more accessible than other control methodologies, and are widely implemented.

The existence of the aforementioned loaded multirotor configurations within fields of active research introduces limitations regarding their real-world prototyping due to the safety risks and financial costs of hardware. These problems can be overcome with the use of Software-In-The-Loop (SITL) simulation which mimics real-world UAV operation by continuously interfacing virtual models of the plant (vehicle and environment) and controller - hence allowing for comprehensive testing without hardware-related overheads (Opal-RT 2021). The three most common approaches to SITL simulation include Matlab/Simulink, ArduPilot and PX4. Matlab/Simulink is a closed-source software and is generally used to investigate low-level control dynamics of a particular traditional UAV platforms, independent of the surrounding environment or any non-traditional UAV capability augmentation (Marks et al. 2012; Notter et al. 2016; H. T. Nguyen et al. 2018; Fogelberg 2013). However, Ribeiro et al. (2010) and Aschauer et al. (2015) warn that custom User Datagram Protocols (UDPs) are required to allow Matlab/Simulink to interface with 3D visualisation programs such as FlightGear and X-Plane. Conversely, ArduPilot is an open-source vehicle control software which generally cooperates with non-traditional vehicle models, 3D visualisation programs, and flight planning software (ArduPilot 2016). Unlike Matlab/Simulink, this approach favours virtual testing in real geospatial locations, as well as camera integration for 3D environment mapping, in-flight ground vehicle tracking, and computer vision-enabled autonomous landing and takeoff (Apriaskar et al. 2017; Nugraha et al. 2017; Riansyah et al. 2017; Ridlwan et al. 2017). Finally, PX4 is a similarly capable open-source, autopilot software to ArduPilot with its key differences being commercialisation-encouraging licensing, reduced platform support, and a smaller user-base.

### 3.3 Autonomous Landing

When landing autonomous UAVs, accuracy is a significant consideration due to the accuracy required for payload collection and deposit (Wubben et al. 2019). The traditional approach to autonomous landing is performed using a Global Positioning System (GPS)-based landing system. This is simple to implement and can be integrated with the same flight-based GPS system used in the UAV (T. H. Nguyen et al. 2018). However, due to the error in the tracking of the position of the UAV during flight, significant offsets from the actual position are experienced and thus the landing of the UAV is inaccurate (Pluckter et al. 2018). Furthermore, GPS systems become less accurate

in the presence of tall buildings and over uneven terrain such as when flying over trees (Safadinho et al. 2020). Accuracy for GPS-based UAV landing is regularly recorded to be between 1-3m of the target with some GPS systems utilising a base station achieving under 0.5m accuracy (Macron et al. 2018; Wubben et al. 2019). This accuracy can be improved by implementing a precision landing system utilising numerous varieties of sensors, such as cameras or infrared (IR) sensors, in order to aid in direction towards the target. One common precision landing system uses multiple cameras with a computer vision enabled computer attached to the UAV. The cameras search for the target, estimate the UAV's distance from the target using stereo vision and navigate the UAV towards it. This process is repeated until the target has been reached (Safadinho et al. 2020). This procedure is cost effective, accurate and can reliably navigate to within 11cm of the target (Wubben et al. 2019). However, the system is prone to many sources of error. Namely, lighting conditions and weather, both of which greatly negatively influence the effectiveness of detecting the target. Similarly, target detection effectiveness and probability decreases when the UAV is outside of the range 2.5-10m from the target (Safadinho et al. 2020). A reliable alternative is the utilisation of an IR landing system which detects a ground-based IR beacon with an IR camera attached to the UAV. It behaves similarly to the computer vision enabled approach by detecting the location of a beacon, navigating towards it and repeating. Moreover, the IR-guided approach is significantly less susceptible to error as it is less prone to uncontrollable events such as weather (Nowak et al. 2017). The IR-guided approach can reliably land within 30cm of a beacon. Although less accurate than the vision-based approach, the beacon can be reliably detected if the UAV is within 15m, thus the detection of the target is more accurate (ArduPilot 2020a). This accuracy is confirmed by Marcon et al. (2018) who experimentally maintained under 30cm of deviation from the intended target when equipped to a multicopter uav. Marcon et al. (2018) maintained an average deviation of 12.4cm through the use of a base-station enabled GPS and an improved accuracy of 8cm deviation average with the addition of an IR-enabled landing system. Conversely, results demonstrated by Kong et al. (2013) show a lesser accuracy improvement with the addition of the IR sensor with an average deviation of 10.4cm. This is contrasted to the accuracy achieved through the use of a computer vision approach as demonstrated by Lange et al. (2008) with an improved average deviation of 2cm and a maximum deviation of 5cm. Nevertheless, IR-guided precision landing systems are simpler to implement than vision-guided systems as most off-the-shelf devices are compatible with open source microcontrollers such as Arduino and autonomous UAV systems such as ArduPilot (IR-Lock 2021). Moreover, the success of computer vision based approaches are incredibly dependent on algorithm quality and are difficult to adapt to multiple flight scenarios and conditions (Lange et al. 2008; Nowak et al. 2017). In order to maximise vision accuracy and improve adaptation to varying flight scenarios, Lange et al. (2008) and Dergachov et al. (2020) encourage the implementation of a consistent landing pad or target design. This most commonly manifests in a large "H" being placed in the centre of the landing pad and allows the vision algorithm to search for the same template in all scenarios.

### 3.4 Short-Range Communication

The most commonly used technologies for wireless short-range communication between devices are Bluetooth, Zigbee and Ultra-wideband (UWB) (Yu et al. 2018). Each of these have the capability to transmit data quickly across short distances. That is, transmitting data at a rate of at least 250Kb/s at a distance of at least 10m (Yu et al. 2018). The most widely used technology for short-distance communication is Bluetooth. As Bluetooth is universal and well established in its domain, it is secure and low cost (Yu et al. 2018). In many cases, the cost of Bluetooth is lower than wired communication. Furthermore, due to Bluetooth's maturity, it is compatible with most microcontrollers, such as Arduino and Raspberry Pi, and is ultimately simple to implement (Coleman et al. 2015). Bluetooth operates on a 2.4GHz frequency and is able to transmit data at a rate of 10Mb/s (Yu et al. 2018). However, generally, Bluetooth only has a range of approximately 10m and has a power consumption of 1W which is significantly large for most Internet of Things (IoT) applications (Ray 2015). A more widely used technology for IoT applications, also operating on 2.4GHz, is Zigbee. This is primarily due to its low power consumption of approximately 100mW and its larger range of up to 100m (Zigbee 2021). Furthermore, Zigbee operates on Local Area Network (LAN) as opposed to Personal Area Network (PAN), like Bluetooth does, thus

it can access more nodes at once than Bluetooth can (Ray 2015). Nevertheless, Zigbee has a lower communication speed than Bluetooth and can only transmit up to 250Kb/s (Yu et al. 2018). Zigbee is ideal for two-way communication between devices due to its reliance on LAN and is easily compatible with most microcontrollers (Baddeley 2016). Lee et al. (2007) argue that Bluetooth and Zigbee are ideal for low data-rate applications in which the data-rate is less than 250Kb/s, and are intended for portable, short-range situations in which battery power is limited. Kumar et al. (2017) argues in favour of Zigbee as Bluetooth uses a master-slave methodology in which one master is connected to numerous slaves. Although this decreases the computational complexity of the communication implementation, it limits the possibility for two way communication. As Zigbee is connected in a self-healing mesh between numerous nodes, back-and-forth communication is commonplace. Moreover, due to the self-healing mesh orientation of Zigbee, if one node is damaged, the network remains operational. This is contrasted from Bluetooth, where if the master-node is damaged then the network fails. One argument Kumar et al. (2017) gives in favour of Bluetooth is that Bluetooth can transmit more varieties of data than Zigbee such as strings and multimedia whereas Zigbee can generally only transmit simple data types. Another alternative for short-range communication is UWB. UWB operates between 3.1GHz-10.6GHz and as such, is incredibly resistant to interference from other signals (Yu et al. 2018). Furthermore, UWB has the capability to operate at varying communication speeds. For example, UWB can operate at 480Mb/s over 2m or 100Mb/s over 10m (Gislason 2008). As discussed by Lee et al. (2007) and Kumar et al. (2017), due to UWB's high data rate, it is suitable for a larger range of data type transmission than Zigbee, such as multimedia. Similarly to Bluetooth, UWB operates using PAN connectivity. However, UWB has a relatively low maturity thus the ease of integration with off-the-shelf micro controllers is currently low and its IoT capabilities have not been fully explored (Frenzel 2017). This is confirmed by Slamich (2020) who outlines that that primary hindrance to UWB at the current moment is the lack of existing infrastructure. This is not an issue for Bluetooth, as a well established technology with widespread device compatibility.

### 3.5 Literature Review Summary

The literature indicates a need for an iterative UAV design approach for component selection. The literature regarding the load transportation problem suggests that a multirotor UAV is sufficiently controllable for transporting either grasped or suspended loads. A desire for SITL simulation arises as an intermediate step between theory and physical implementation, in which ArduCopter and PX4 are found to be more suitable for augmented UAV capabilities in a real environment whilst Matlab/Simulink is suited to control-focused research scopes. It is also found that IR beaconing landing systems offer reliable landing target location. A multitude of wireless short range communications are available, with trade-offs emerging between power consumption, range, bandwidth, and level of adoption.

## 4 Theory

To apply the reviewed literature to the project design, the findings from Section 3 will inform the development of the fundamental engineering theory for the project. The literature is evaluated with respect to the project objectives and system requirements. The literature findings are applied in an investigation into UAV design methodologies, payload-equipped UAV dynamics, short-range wireless communication and flight simulation.

### 4.1 Airframe, Motor, and Propeller Selection

The airframe, motors, and propellers of a multicopter are among the three most critical mechanical components to select. Referring to Section 3.1, a desirable selection methodology is via cyclic analysis of such components in any given order. Beginning with the airframe, the most common and economical number of motors to achieve directional and stable flight of a multicopter is four (Feist 2018). However, using more than four motors allows the UAV to exhibit more actuators than control inputs - introducing a degree of actuator redundancy that allows the UAV to maintain stability despite motor failure(s) (Yang et al. 2016). This also improves the thrust load distribution as the increased number of arms allows each to experience a smaller load (Mckay et al. 2018). Both of these factors increase safety by reducing the probability of loss of UAV stability (Achtelik et al. 2012). However, increasing the size and number of arms/motors of the airframe significantly increases financial costs, mechanical complexity, and storage requirements (Gortolev 2014). Consideration of these limitations further supports the utilisation of a hexacopter to optimise safety, redundancy, complexity, and cost compared to a quadcopter or octocopter. The propeller size is highly dependent on the rotor count and frame size where maximum performance is achieved by avoiding blade overlap over other blades and the UAV frame. The motor type is dependent on the total weight of the UAV and the propeller size, which is often influenced by three key parameters: KV value, thrust-to-weight ratio, and specific thrust. When finding an appropriate KV value, it is generally true that large propellers rotating at a slower speed can generate the same amount of thrust as small propellers rotating at a faster speed (Achtelik et al. 2012). Additionally, motors that spin small propellers fast, exhibit fewer windings of thicker wires - allowing them to carry larger electrical currents at smaller voltages (high KV, low torque). Conversely, motors that spin large propellers slowly, exhibit more windings of thinner wires - allowing them to carry smaller electrical currents at higher voltages (low KV, high torque) (Abarca et al. 2017). These properties introduce a trade-off between increasing motor efficiency (low KV, high torque) and increasing agility (high KV, low torque). Another important motor size parameter is the UAV's thrust-to-weight ratio, which is recommended to be at least 2:1 for gentle flying (Szyk 2018). This allows for hovering at approximately half throttle and hence provides adequate manoeuvrability and control authority in unpredictable environments (e.g., strong winds, turbulence). Finally, the specific thrust of a motor and propeller pair provides a proportional measurement of their efficiency by defining the amount of thrust produced for a given amount of airflow (units of g/W) (NASA 2021). The distinct advantages of utilising a hexacopter airframe, as well as the three key motor and propeller selection parameters of KV value, thrust-to-weight ratio, and specific thrust will support a detailed component selection process in Section 5.3.

### 4.2 Dynamics of a Multicopter UAV with a Suspended Load

To understand the behaviour of a multicopter UAV with a payload suspended beneath, it is worthwhile to consider the fundamental equation of motion for the system. A well-grounded understanding of the system dynamics will support the design phase of the project in alignment with Objectives 1 and 2, a flyable UAV and the transport of a payload, respectively.

As concluded in Section 5.5 (Gripper Mechanism Subsystem), the scope of the UAV dynamics analysis shall relate to the use of a cable-tethered payload approach. A multicopter carrying a tethered load can be conceptualised with the load dynamics modelled as a pendulum. A key assumption in doing so is that the tether must remain taut, hence recommending that the operational envelope of the UAV shall be restricted to non-aerobatic maneuvers. This model is illustrated in Figure 3.

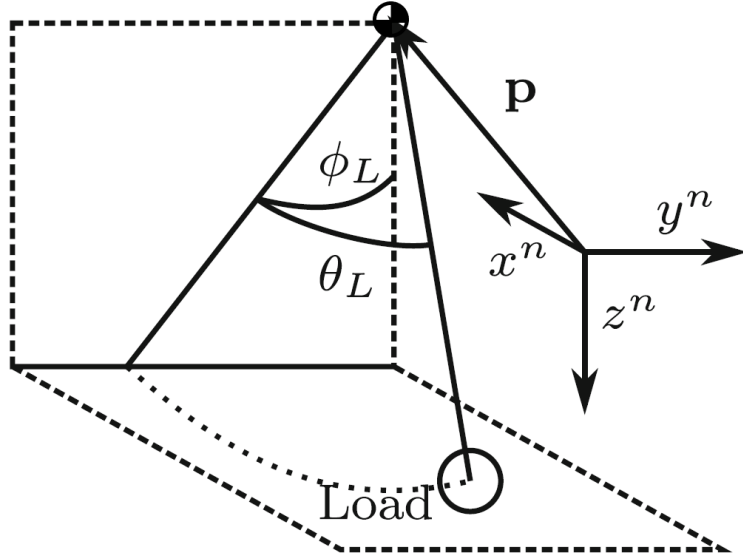


Figure 3: A suspended load modelled as a pendulum with a body-centred coordinate system defined from the UAV's centre of gravity, where the UAV position is given by an inertial reference,  $\mathbf{p} = [x \ y \ z]^T$ , and the payload position relative to the UAV is defined by the angles  $\phi_L$  and  $\theta_L$  (Klausen et al. 2017).

The governing equation of motion for a multirotor with a suspended load modelled as a pendulum is obtained via Kane's equation (Klausen et al. 2017):

$$\mathbf{M}\dot{\boldsymbol{\nu}} + \mathbf{C}\boldsymbol{\nu} + \mathbf{G} + \mathbf{D}\boldsymbol{\nu} = \boldsymbol{\tau} + \boldsymbol{\tau}_a, \quad (1)$$

where,

$$\boldsymbol{\nu} = \begin{bmatrix} \dot{x} \\ \dot{y} \\ \dot{z} \\ \dot{\phi}_L \\ \dot{\theta}_L \end{bmatrix}, \dot{\boldsymbol{\nu}} = \begin{bmatrix} \ddot{x} \\ \ddot{y} \\ \ddot{z} \\ \ddot{\phi}_L \\ \ddot{\theta}_L \end{bmatrix},$$

$$\mathbf{M} = \begin{bmatrix} m_L + m_c & 0 & 0 & 0 & Lm_L \cos\theta_L \\ 0 & m_L + m_c & 0 & -Lm_L \cos\phi_L \cos\theta_L & Lm_L \sin\phi_L \sin\theta_L \\ 0 & 0 & m_L + m_c & -Lm_L \cos\theta_L \sin\phi_L & -Lm_L \cos\phi_L \sin\phi_L \\ 0 & -Lm_L \cos\phi_L \cos\theta_L & -Lm_L \cos\theta_L \sin\phi_L & L^2 m_L \cos^2\theta_L & 0 \\ Lm_L \cos\theta_L & Lm_L \sin\phi_L \sin\theta_L & -Lm_L \cos\phi_L \sin\theta_L & 0 & L^2 m_L \end{bmatrix},$$

$m_c$  is the mass of the UAV,  $m_L$  is the mass of the suspended payload,  $L$  is the length of the tether,

$$\mathbf{C} = \begin{bmatrix} 0 & 0 & 0 & 0 & -L\dot{\theta}_L m_L \sin\theta_L \\ 0 & 0 & 0 & Lm_L (\dot{\phi}_L \cos\theta_L \sin\phi_L + \dot{\theta}_L \cos\phi_L \sin\theta_L) & Lm_L (\dot{\phi}_L \cos\phi_L \sin\theta_L + \dot{\theta}_L \cos\theta_L \sin\phi_L) \\ 0 & 0 & 0 & -Lm_L (\dot{\phi}_L \cos\phi_L \cos\theta_L - \dot{\theta}_L \sin\phi_L \sin\theta_L) & -Lm_L (\dot{\theta}_L \cos\phi_L \cos\theta_L + \dot{\phi}_L \sin\phi_L \sin\theta_L) \\ 0 & 0 & 0 & -\frac{1}{2}L^2 \dot{\theta}_L m_L \sin(2\theta_L) & -\frac{1}{2}L^2 \dot{\phi}_L m_L \sin(2\theta_L) \\ 0 & 0 & 0 & \frac{1}{2}L^2 \dot{\phi}_L m_L \sin(2\theta_L) & 0 \end{bmatrix},$$

$$\mathbf{G} = \begin{bmatrix} 0 \\ 0 \\ -g(m_L + m_c) \\ Lgm_L \cos\theta_L \sin\phi_L \\ Lgm_L \cos\phi_L \sin\theta_L \end{bmatrix},$$

$g$  is the acceleration due to gravity,

$$D = \begin{bmatrix} 0 & 0 & 0 & 0 & 0 \\ 0 & 0 & 0 & 0 & 0 \\ 0 & 0 & 0 & 0 & 0 \\ 0 & 0 & 0 & d & 0 \\ 0 & 0 & 0 & 0 & d \end{bmatrix},$$

$d$  is an assumed constant drag coefficient related to the payload,

$$\boldsymbol{\tau} = \begin{bmatrix} F_x \\ F_y \\ F_z \\ 0 \\ 0 \end{bmatrix}, \boldsymbol{\tau}_a = \begin{bmatrix} w_x \\ w_y \\ w_z \\ 0 \\ 0 \end{bmatrix},$$

$F$  are the inertial control forces of the UAV, and  $w$  are unknown disturbance forces acting on the UAV, such as gusts.

A critical step in the derivation of the governing equation of motion (1) is that the payload tether is attached close to the UAV's centre of gravity. Configuring the tether as such restricts the impact of the load dynamics to the translational motion of the UAV, hence leaving the pitch, roll, and yaw dynamics unaffected. This has a significant influence on the UAV PHORESIS platform, in providing design incentive to integrate a tether mount as close to the UAV's centre of gravity as possible.

### 4.3 Bluetooth Enabled Short-Range Communication

The design of a communication system between the UAV and payload will advance Project Objective 3. A design which is adaptable to varying payloads provides a robust modular-orientated solution. The selected short-range communication technology for further investigation is Bluetooth, which has been selected over Zigbee and UWB from reviewing the literature presented in Section 3.4.

Zigbee and UWB have further signal ranges than Bluetooth, as given in Table 3. However, the extended range is not required for the short-range communication component of Objective 3 (Gislason 2008; Ray 2015; Zigbee 2021).

Table 3: Communication technology signal ranges.

Communication Technology	Range (m)
Bluetooth	10
Zigbee	100
UWB	100

This is primarily because the communication range between the UAV and payload is required to be no larger than approximately 1m thus the range achieved by Bluetooth is sufficient. Similarly, the greater data rate of UWB when compared to Bluetooth is not required for most proposed payload applications which involve only integer and string data transmission as opposed to multimedia (Kumar et al. 2017; Lee et al. 2007). In the future expansion of the project, multimedia enabled payload applications may be investigated thus UWB may become a more viable option. Nevertheless, the primary reason Bluetooth is selected over Zigbee and UWB is for its dominance in maturity and existing infrastructure. Bluetooth has a lower cost than its competitors as it is well established in the market and it is easily configurable with off-the-shelf microcontrollers as compatible modules have been well developed (Slamich 2020). Bluetooth's ease of integration makes it the ideal candidate for versatile short-range communication in a dynamic ever-changing environment.

One method to implement communication between the UAV and payload is through an HC-05 Bluetooth Module (Figure 4). The HC-05 Module is a Bluetooth Serial Port Protocol Module

which can send and receive data between microcontrollers. The HC-05 operates on a 4-6V supply and can reliably communicate 1Mb/s to a range of approximately 10m (Verma 2020). An HC-05 module can be connected to an Arduino to enable wireless communication via Bluetooth. This will therefore facilitate the IoMT payload sensor data transfer to an on-board microcontroller on the UAV.

The two HC-05 modules can be connected to an Arduino Uno or Raspberry Pi microcontroller which in turn are connected to the a payload or the UAV. The microcontroller on the payload processes the data retrieved by the sensor and communicates it to the HC-05 on the payload in real-time thus achieving the intended UAV-payload short-range communication. An alternative to using two HC-05 modules is to use one with a Bluetooth-enabled microcontroller.

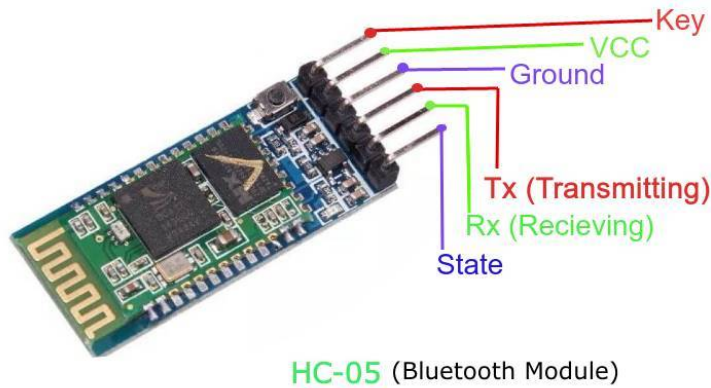


Figure 4: HC-05 Bluetooth module (Verma 2020).

#### 4.4 SITL Simulation

To conduct meaningful testing through SITL simulation, the use of a GCS is highly recommended to easily employ complex UAV flight paths both in the real world and in virtual environments. The two most popular GCS platforms being Mission Planner which is only available on Windows, and QGroundControl which is available on Windows, Mac OSX, or Linux (Wallich 2012). Support by the Linux operating system is desirable as it allows program usage through a virtual machine (VM), such as VirtualBox, which minimises the risk of damaging the host machine by providing an experimentation-dedicated virtual environment (Vissarion 2020). Furthermore, GCSs utilise Graphical User Interfaces (GUIs) to support intuitive UAV flight planning, control, and supervision. Firstly, the in-built, overhead GPS-mapped GUI allows the user to intuitively create, save, and execute complex flight paths which can be applied to virtual or real UAV platforms - a capability not offered by the control software, such as ArduPilot, alone. Secondly, GCSs provide a separate GUI that simplifies UAV control commands from terminal entries to straightforward button interactions which reduces the cognitive burden on the operator and hence the chances of an accident. Finally, the following capabilities are presented over a real-time track of the UAV over the GPS map with the relevant telemetry (e.g., orientation, altitude, speed, flight time elapsed) displayed numerically and graphically to improve situational awareness. Figure 5 displays the QGroundControl program (top left) supervising a simulaUAV flight. To further improve the visualisation of the UAV's movement, flight simulators such as FlightGear or X-Plane can interface with the control software to display a 3D model of the UAV and its surroundings (ArduPilot 2020b) (an example is displayed in Figure 6).



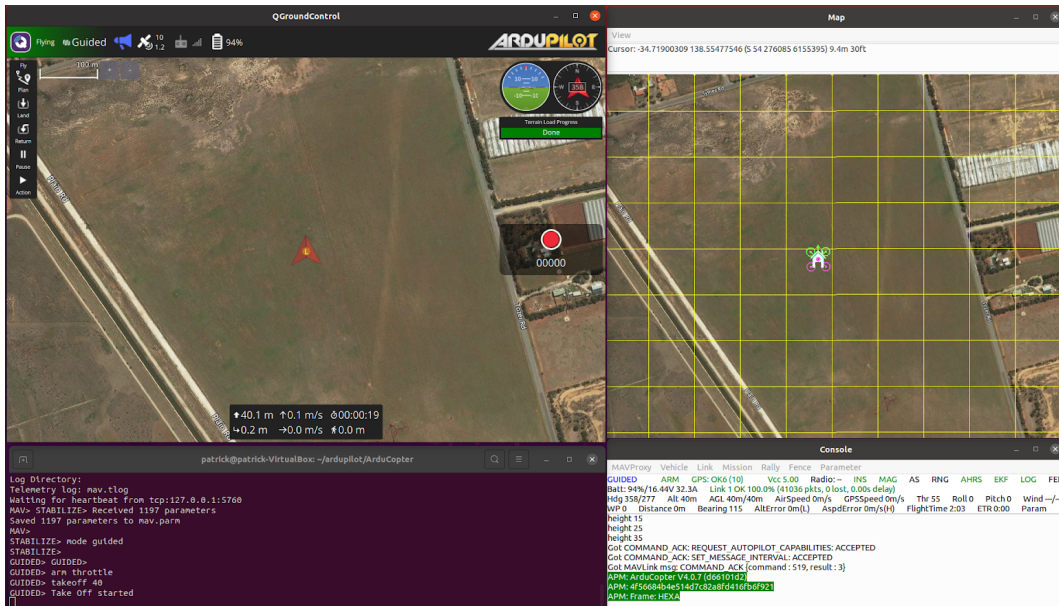


Figure 5: ArduPilot and QGroundControl SITL simulation layout.

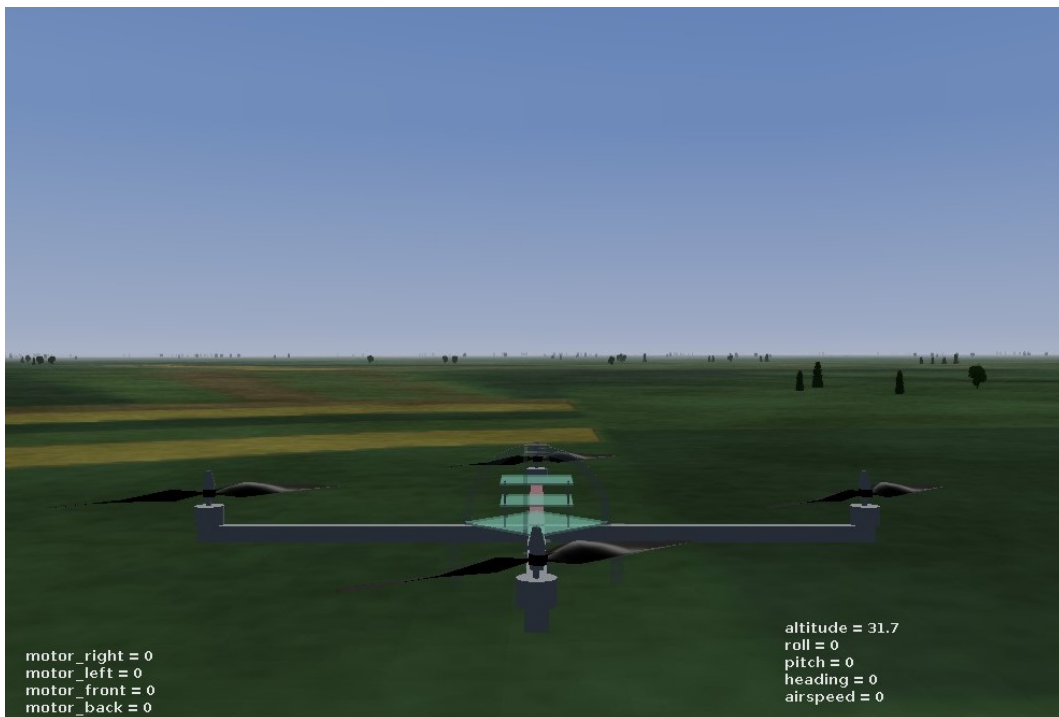


Figure 6: Simulated flight at St Kilda, South Australia using FlightGear and ArduPilot.

## 4.5 Theory Summary

The component theory investigation demonstrates that a hexacopter provides an optimal solution to balance flight safety and stability with computational, mechanical complexity, and cost. Moreover, it is indicated that in motor size selection, a UAV TWR of at least 2:1 should be maintained and specific thrust should be maximised. It is determined, that the ideal short range communication system between the UAV and payload utilises Bluetooth technology due to its maturity in the industry, low cost, and ease of implementation. The behaviour of a payload-equipped UAV is investigated through analysing the equations of motion, whereby it is recommended to mount a cable close to the UAV's centre of gravity. The SITL simulation platforms, Mission Planner, and QGroundControl, then enable the UAV to be thoroughly tested in representative environments.

## 5 Final Design

The UAV PHORESIS final design incorporates the engineering technical detail presented in Section 4, and is guided by the problem distillation presented in Section 2. The definition of the project’s subsystems enables an objective-orientated solution while also facilitating a modular design philosophy. Establishing modularity in the first implementation of the project is critical, as future developments can be implemented iteratively and be scoped to individual subsystems. The project’s individual subsystems include the: UAV platform; IoMT payload; gripper mechanism; and payload casing. Through the successful design and implementation of each subsystem, significant progress is achieved in meeting all project objectives defined in Section 1.4, with the following subsystem integration (Section 6) achieving complete satisfaction of objectives.

### 5.1 System Architecture

The UAV PHORESIS subsystems are defined with the use of a system architecture diagram presented in Figure 7. The system architecture of the project identifies the relevant mechanical and digital interfaces between subsystems and the surrounding environment. This encourages the adherence to contextual boundaries between subsystems, ultimately enforcing the modular design philosophy of the project. A limitation experienced in the implementation of the payload-to-UAV interface resulted in an inability to directly communicate between the two platforms. The technical hurdle is elaborated upon in Section 5.4. Despite the difficulty, a facet of the project’s highly modular design philosophy enables a redundancy plan to communicate with the payload to be enacted. Instead of utilising the UAV and its on-board antennas as an intermediate communications bearer, the payload transmits sensor information directly to the GCS, however the range is limited to approximately 20 metres due to the smaller antennas. While this is a short-term solution, it critically demonstrates the resilience of the system to failure.

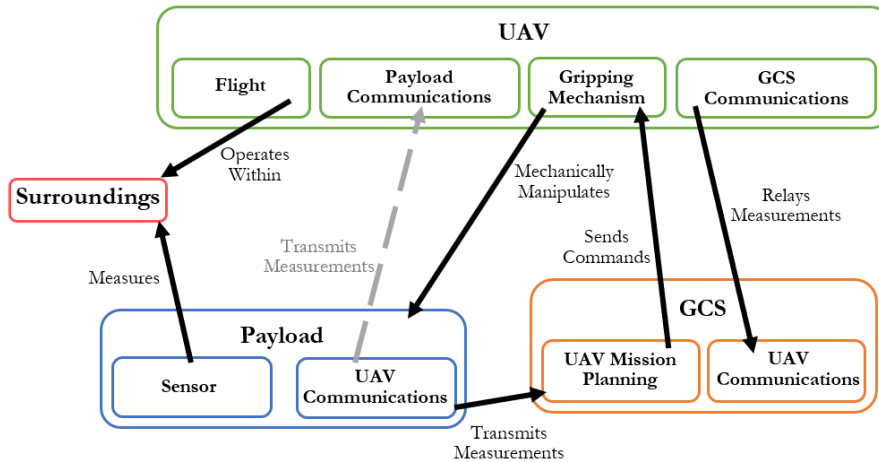


Figure 7: System architecture, with the inoperable payload-to-UAV communications link acknowledged with the faded dotted line.

### 5.2 Information Flow

The mapping of information transfer is represented by an information flow diagram presented in Figure 8 and serves as a diagrammatic representation of subsystem interface implementations alongside processing bottlenecks. The information flow diagram is demonstrative of the cyclical nature of information processing within the system whereby the diagram captures a decision cycle at one instance. A sensor payload device deployed in the field collects data and transmits the information in real-time to the GCS. Note that the transmission from payload to GCS utilises the redundancy plan instead of the more ideal transmission path with the UAV and its antennas as an intermediate to boost signal strength. A mission operator manning the GCS is able to

interpret the received data and assess whether a payload shall be repositioned. If it is required that a payload be collected, mission waypoints and mission commands may be sent to the UAV by the mission operator via the GCS. Additionally, the GCS facilitates live monitoring of the UAV health by receiving continuous data such as the UAV's battery levels. Once the UAV receives a command, the flight computer forwards the action to either of its two primary effectors in the gripping mechanism or motors. Additionally, the mission operator monitoring the UAV telemetry feed can observe whether the UAV has located a payload via its location beacons. If it is deemed appropriate to collect a payload once located, the operator has the authority to trigger a “precision land” mission command to set the UAV into an autonomous payload landing mode. The decision cycle concludes as new environmental data is sought, allowing the mission operator to interrupt or let the UAV continue on its mission plan.

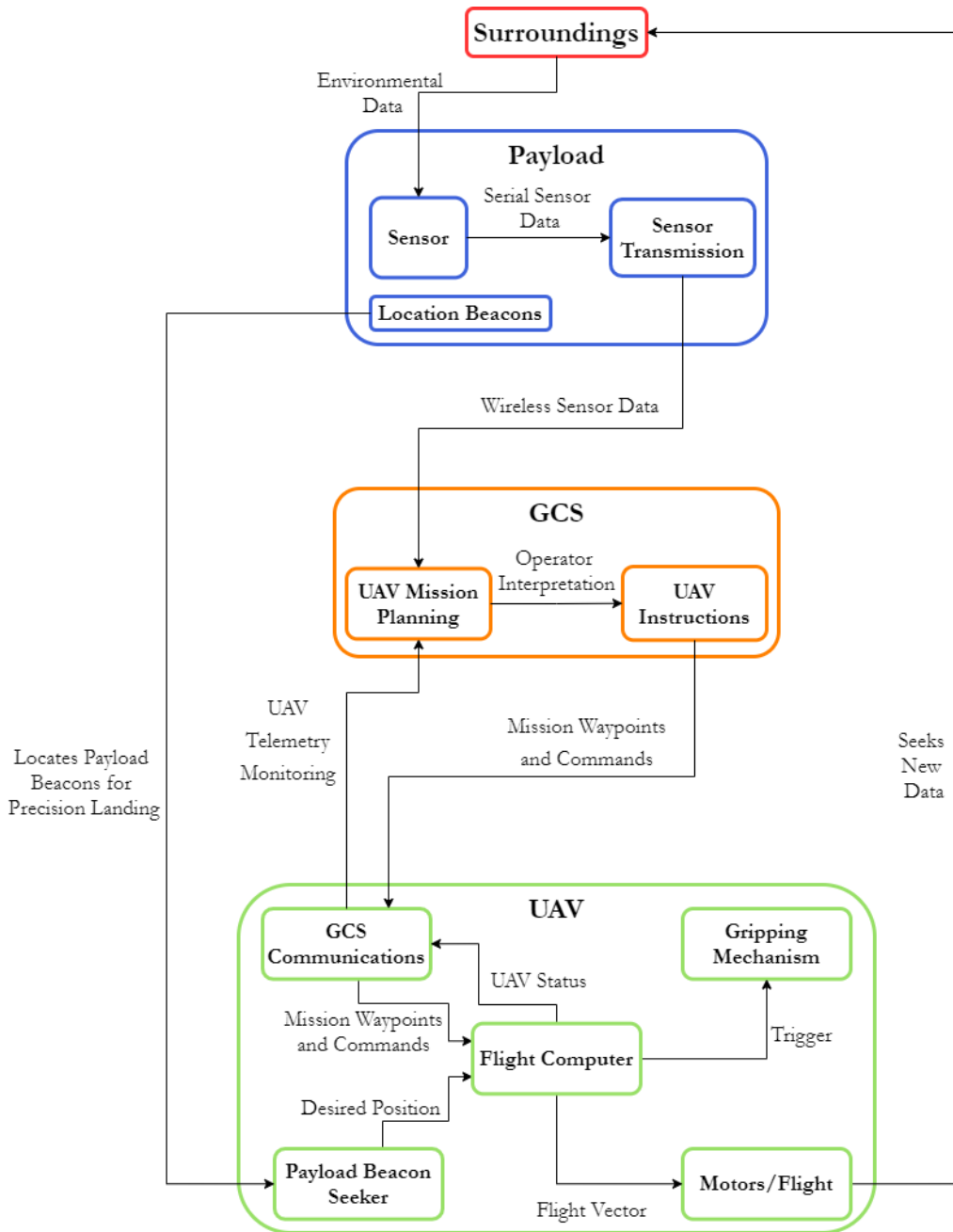


Figure 8: Information flow diagram illustrating one decision cycle.

### 5.3 UAV Platform Subsystem

The UAV platform represents the primary components required for its unloaded (without payload) operation (Objective 1): airframe, motors, propellers, and programming software. The literature review of Section 3.1 describes the utility of a cyclic design/selection process for the mechanical components, whilst Section 3.2 provides proven examples and capabilities of multirotor control software. Both of these selection methodologies are employed in conjunction with initial guidance from the DSTG representative to approach a platform design that satisfies the necessary system requirements. The approximate component suggestions from the DSTG advisor are adapted from an operational model at DSTG Edinburgh with similar capabilities to those required for this project. This guidance provides a shortlist for the following selection processes.

#### 5.3.1 Mechanical Component Selection

The initial suggestions for the key mechanical components (airframe, motors, and propellers) are displayed in Table 4 with a brief justification for each. Using Table 4 as a baseline, the cyclic design approach is employed to find an optimal mechanical UAV design. Additionally, for the purposes of this design analysis, the remaining UAV components (Appendix P, Table 27: Ma.1, Ma.2.2, Ma.2.3, Ma.2.4, Ma.2.7, Ma.3, Ma.4) have a combined mass of approximately 3.4kg in addition to the maximum payload mass of 1kg (R.4.6).

Table 4: Generalised platform component suggestions from the DSTG advisor.

Component	High-Level Suggestion	Justification
Airframe	Tarot Hexacopter	As mentioned in Section 3.1, the hexacopter optimises redundancy, lifting capabilities, and cost compared to a quadcopter or octocopter. Tarot is a reputable supplier of aviation technology <sup>1</sup> .
Motors	T-Motor MN4010	The T-Motor <sup>1</sup> MN40 series is optimal for a hexacopter configuration as it supports large, heavy, and low speed UAV platforms with reduced cost, power consumption, and size compared to larger motors that may be better suited for larger airframes (T-Motor 2019b).
Propellers	T-Motor 12in - 16in	Using the same brand as the motors will guarantee compatibility and reliable performance. The minimum and maximum sized blades for the T-Motor MN4010 motor are 12in and 16in, respectively (T-Motor 2019b).

There are three potential candidate models for the Tarot hexacopter airframe: T680, T810, and T960 (where the number represents the distance in mm between opposing motor mounts). The T680 is initially considered since its highest performing configuration exhibits a maximum takeoff mass of 6kg (including the 2.8kg airframe mass) which allows for approximately 3.2kg of additional components to be lifted (Helipal 2021). However, this is less than the 5kg required for the payload and other physical components and thus the T680 airframe is not suitable. The selection process is repeated for the T810 airframe, which has a mass of 1.02kg (HobbyTech 2021a) and is recommended to utilise 320KV motors with 15in diameter (5.5in pitch), carbon fibre propellers (HobbyTech 2021b). Applying the closest approximation of this configuration in accordance with Table 4 (T-Motor MN4010 370KV, 14.8V motors and T-Motor 15in diameter (5in pitch), carbon fibre propellers) gives a maximum takeoff mass of approximately 7kg and a maximum lifting mass (excluding airframe, motors, and propellers) of about 5kg (T-Motor 2019a). This maximum lifting mass satisfies the 5kg required for the payload and other components and is thus deemed suitable. However, redundant lifting capacity is desirable for the UAV’s performance (to avoid

<sup>1</sup>Whilst Tarot and T-Motor are each owned and operated by separate international companies, the components sourced from them are not involved in any communication protocols within the system and thus are not considered security vulnerabilities.

consistent high-throttle flight) and for the end-user, DSTG, who plan to further augment the system. Therefore, a platform with greater lifting capacity is desirable. The selection process can again be repeated for the T810 airframe, now selecting the MN4010 580KV, 14.8V motors with the same propellers to provide a lifting mass of about 10kg. This lifting mass far exceeds the 5kg required and provides a 5kg buffer for future augmentation in the interests of DSTG - therefore, this configuration is deemed suitable. Finally, the remaining UAV components are less critical regarding its capability and thus can simply be benchmarked using the proven model specified by the DSTG advisor. Whilst this manual selection methodology maintains merit in defining a basic platform through a simple cyclic process, it lacks important performance/flight characteristics such as the UAV's platform temperature, flight time, electrical load, and specific thrust.

### 5.3.2 Corroboration of Mechanical Component Selection

To calculate detailed flight characteristics of the UAV platform, Biczyski et al. (2020) suggest the use of programs such as "eCalc" (Müller 2018) which achieve this task by utilising comprehensive component databases and SITL physics simulations. The program's parameters were input according to Appendix O under two primary configurations: unloaded and loaded. The difference between the configurations was represented as a simple mass discrepancy regarding the payload's presence on the vehicle. The major flight characteristics and a brief analysis for each is displayed in Table 5. The hover endurance flight characteristic can be corroborated through power budget calculations (Table 6) using the 15 minute flight time requirement (R.1.5, R.4.3, R.6.1) and the electrical components' masses in Appendix P (Table 27: Ma.1.1, Ma.1.2, Ma.1.6, Ma.2.5, Ma.4.1, Ma.4.3, Ma.4.4, Ma.4.5, Ma.4.6). To calculate a total flight time, all motors are assumed to operate on average at 65% throttle, which accommodates standard hover at 50% throttle and gentle adjustments performed at greater throttle levels. Under this assumption, the total flight time is calculated to be approximately 17.9 minutes, which is similar to the hover flight times of 19.1 minutes and 17.2 minutes for the unloaded and loaded configurations, respectively. The relatively small discrepancy between the hover flight time results from eCalc and the power budget provide confidence in their estimates.

Table 5: eCalc flight characteristics of the UAV in unloaded and loaded configurations.

<b>Flight Characteristic</b>	<b>Unloaded</b>	<b>Loaded</b>	<b>Analysis</b>
Hover Flight Time [mins]	19.1	17.2	The flight time for both configurations satisfies the system requirements R.1.5, R.4.3, and R.6.1 of 15 minutes. The criticality of this requirement is listed as "Important" which indicates that values near what is estimated by eCalc may be acceptable.
Thrust-to-Weight Ratio [-]	2.4	2.2	The thrust-to-weight ratios of the unloaded and loaded configurations are equal to or above the recommended value of 2.0 (Section 4.1) which implies that hovering can be achieved at approximately 50% throttle. This bolsters the mechanical components selection by providing confidence that the total mass of the vehicle can be lifted (with a significant safety margin) whilst maintaining manoeuvrability (Müller 2021).
Specific Thrust [g/W]	7.47	7.20	The specific thrust is greater than 6g/W for both configurations which indicates that both exhibit higher than average hover efficiencies (Müller 2021).
Range [m]	4082	3794	The range of flight distance for both configurations is far greater than that specified in the system requirements (R.1.3, R.1.6, R.2.4) of 50m for the transport of the payload and 200m for communication between the vehicle and GCS.
Temperature [°C]	44	44	The estimated temperature of the motors during maximum-performance flight profiles, in unloaded and loaded configurations, is 48 °C. This value is below the 70 °C safety limit and hence there is a minimal risk of overheating and any performance decrease associated with overheating (Müller 2021).
Electric Power [W]	451	451	The electric power requirement for all six motors is less than 70% of the limiting value specified by the manufacturer. This indicates that the choice of motors and propellers is appropriate for the total mass of the vehicle in both unloaded and loaded configurations (Müller 2021).
Rotor Failure [-]	Resistant	Resistant	The presence of 6 rotors and their ability to hover using less than 80% throttle enables the vehicle to maintain stability in the event of a single motor failure (or two motor failures on opposing rotors) (Müller 2021).

Table 6: UAV power budget.

Component	Quantity Needed	Maximum Current per Component [mA]	Maximum Current Subtotal [mA]	Voltage [V]	Battery Capacity Subtotal (mAh)
Cube Orange Standard Set (ADS-B Carrier Board)	1	2500	2500	5.7	625
Here3 GPS <sup>2</sup>	1	55	55	5	13.75
RFD900x Modem Bundle	1	800	800	5	200
Raspberry Pi 4	1	3000	3000	5.1	750
T-Motor MN4010 580kV (Assuming 65% average throttle)	6	10000	60000	14.8	15000
Caddx Turtle V2	1	380	380	5	95
25-200-600mW Adjustable Power Video Transmitter (SPMVT1000)	1	176	176	12	44
IR-Lock Sensor <sup>2</sup>	1	0	0	5	0
LW20/B (50 m) Serial+I2C (Lidar Rangefinder)	1	110	110	5.5	27.5
NicaDrone Electro Permanent Magnet (OPEN-GRAB EPM V3 R5C)	1	10	10	6.5	2.5
<b>Total</b>	-	-	<b>67031</b>	-	<b>16757.75</b>

<sup>2</sup>Component specifications lack a current draw value, thus an estimate from a similar product is used or the current draw is assumed to be negligible.



### 5.3.3 Software Component Selection

There are three primary software options to form the basis of the UAV's control architecture as specified in Section 3.2: Matlab/Simulink, ArduPilot, and PX4. A crucial factor to consider regarding software selection is the benchmarked flight controller for the UAV platform which is the Pixhawk Cube Orange. Matlab does support Pixhawk autopilot capabilities via the UAV Toolbox which, whilst being closed-source, is openly available to Honours Project 3296 due to the licensing provided by the University of Adelaide (UoA). However, in consideration of the future use of this platform outside of the UoA and within Defence fields, closed-source software is undesirable. Additionally, Matlab's requirement for customised UDPs to interface with SITL simulators adds unnecessary complexity to platform testing. Therefore, open-source software with SITL simulation support and high transferability to hardware testing, such as ArduPilot or PX4, are preferable options. However, compared to PX4, ArduPilot exhibits greater product maturity, more diverse platform support, and a larger user-base (Baidya et al. 2018). The latter two factors are important with the use of a GCS, such as QGroundControl, as advocated in Section 4.4. Furthermore, ArduPilot's slightly stricter licensing than PX4 (GNU General Public License versus Berkeley Source Distribution) does not hinder the applicability of this UAV platform since it is already owned by DSTG and will not be commercialised. Therefore, ArduPilot, specifically its dedicated multirotor derivative, ArduCopter, and QGroundControl are the software platforms of choice for the control of the UAV in real-world and simulated environments.

### 5.3.4 Summary

This section specifies a UAV platform to achieve Objective 1 (UAV flight). The hardware was selected by firstly considering components already proven and in use by DSTG, then conducting a high-level performance analysis to select specific components, and finally corroborating the selections with eCalc. Specific hardware components are given by item identifiers Ma.1, Ma.2, and Ma.3 in Table 27. The software (autopilot and GCS) were selected with the following desirable criteria: open source, maturity, large platform support, large user-base, and SITL simulation support. The selected autopilot and GCS software are Ardupilot and QGroundControl, respectively.

## 5.4 IoMT Payload Subsystem

In the achievement of Objective 3, as discussed in Section 4.3, the selected method for short-range communication between the UAV and payload is Bluetooth. Utilising inexpensive off-the-shelf Arduino sensor modules, HC-05 Bluetooth modules and numerous electronic components, multiple distinct communicable IoMT sensor payloads are developed. This is achieved through an iterative approach (Figure 9) with incremental improvement in complexity and capability. To demonstrate a proof of concept, preliminary designs featured two independent devices each with HC-05 Bluetooth modules. These devices allowed for the set-up of the communication framework which the final payload devices could be built upon. The initial two-device iterative development is detailed in Appendix E. This capability is then extended to allow for payload to UAV communication. All programming is performed through the Arduino Integrated Development Environment (IDE) (Appendix L). Moreover, preliminary testing of range and connection speed has also been performed.

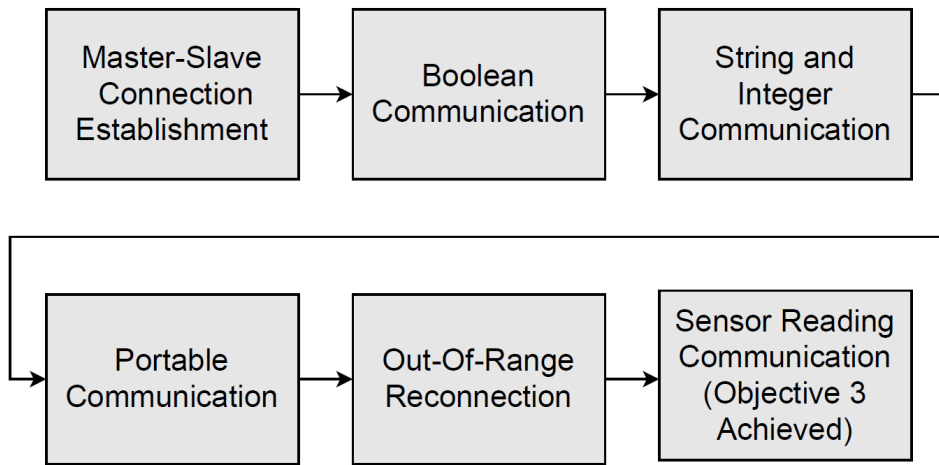


Figure 9: Iterative stages to Bluetooth communication system development.

### 5.4.1 Payload Design

After the successful achievement of Boolean communication, string and integer communication, portable communication and out-of range re-connection as detailed in Appendix E, inexpensive off-the-shelf Arduino compatible sensor modules may be integrated with ease into the wireless Bluetooth enabled payload device. Off-the-shelf Arduino compatible sensor modules, such as a smoke detector sensor, are connected to the HC-05-Arduino circuitry as shown in Figure 10. The Arduino is then able to take the sensor's reading, interpret it and ultimately transmit a message. In Figure 11, an example is given in which a smoke detector sensor payload transmits different messages depending on whether the smoke detector reading reaches a set tolerance. The messages are transmitted at a baud rate of 9600 to be then received by any paired Bluetooth device.

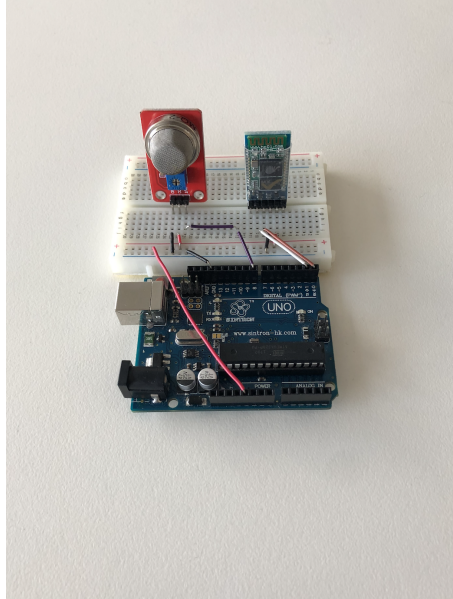


Figure 10: Initial smoke detector sensor configuration.

```
sensorValue=analogRead(smokeA0);           //Smoke detection reading
if(sensorValue > 300)                       //Tolerance for smoke detection
{
  Serial.println("Smoke detected");
}
else
{
  Serial.println("No smoke detected");
}
```

Figure 11: Smoke detector sensor code.

In order to increase the durability and robustness of the sensor payload shown in Figure 10, Printed Circuit Boards (PCBs) are designed and manufactured. The durability of the payload device is critical as the payload will be constantly in motion whilst being collected, transported and deposited - thus developing the payload device into a PCB is essential. In order to maintain the configurability provided by breadboards, the PCB is designed such that different Arduino compatible sensor modules may be seamlessly integrated into the circuit. This is shown in Figure 12 where there are different slots for different varieties of sensors. A schematic representation of the designed PCB is shown in Figure 13.

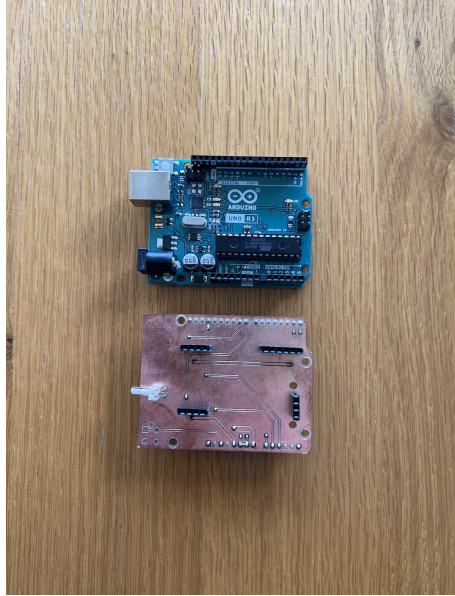


Figure 12: Configurable PCB arrangement.

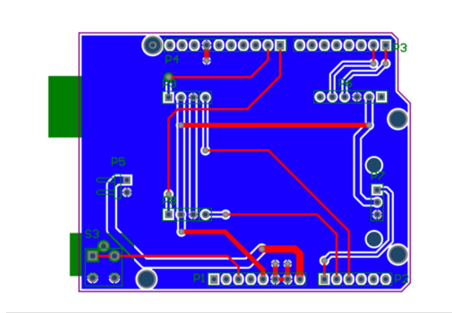


Figure 13: Schematic PCB design.

#### 5.4.2 Final Payload

##### Smoke Detector Payload

The smoke detector sensor payload (Figure 14) utilises the configurable PCB arrangement as detailed as the final iteration in Section 5.4.1. The sensor has the capability to detect smoke, as well as LPG, alcohol, propane, hydrogen, methane and carbon monoxide from 200 to 10000 parts per million in air (LME 2021). The sensitivity of the sensor payload may be changed with ease by rotating a screw. Similarly, by programming a tolerance, different messages may be sent for varying quantities of detected smoke. When smoke is detected, messages are communicated via Bluetooth as shown in Figure 15. The data sheet for the smoke detector sensor module used in the sensor payload may be found in Appendix F.

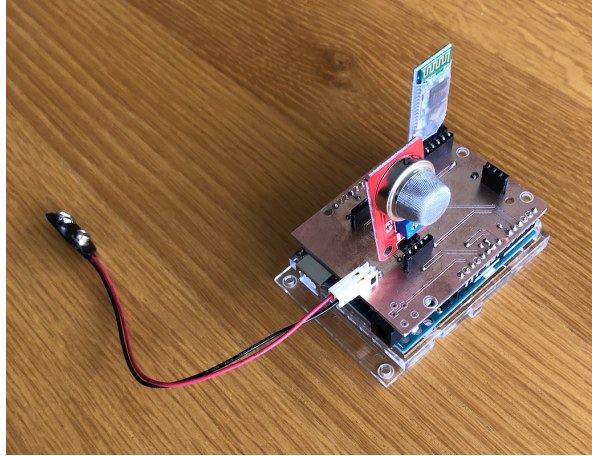


Figure 14: Final smoke detector sensor payload.

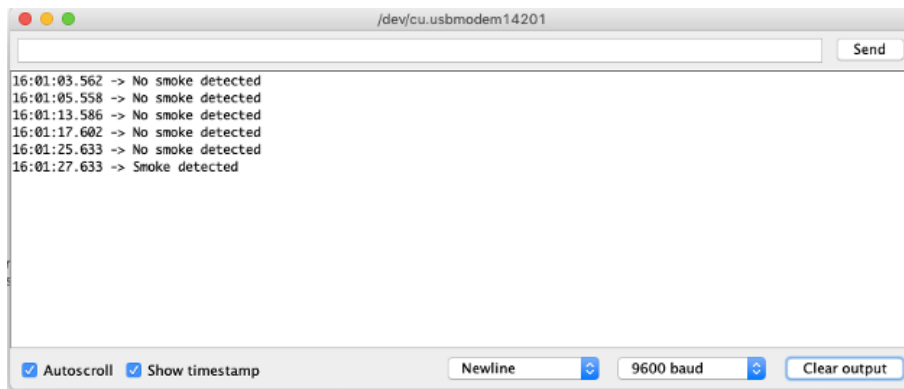


Figure 15: Smoke detector sensor payload output.

### Sound Detector Payload

Similarly to the smoke detector sensor payload, the sound detector sensor payload (Figure 16) utilises the configurable PCB arrangement. The sensor is able to detect sound from a range of 44-66dB (David 2021). Again, the sensitivity of the sensor payload may be changed by rotating a screw. Similarly, by programming a tolerance, different messages may be sent for varying sound levels. When sound is detected, messages are communicated via Bluetooth as shown in Figure 17. The data sheet for the sound sensor module used in the sensor payload may be found in Appendix G.

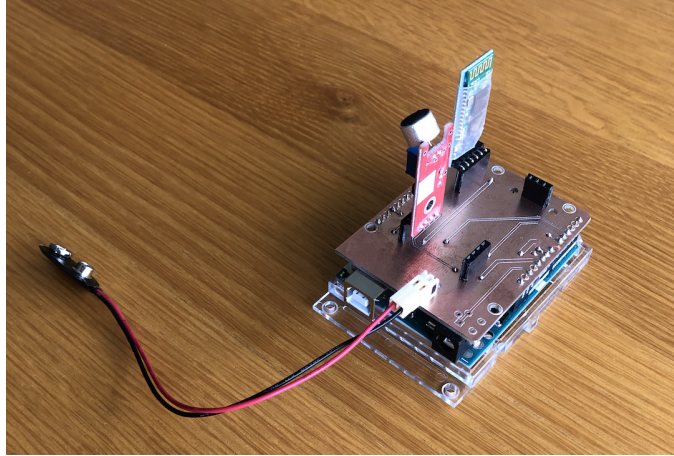


Figure 16: Final sound detector payload.



Figure 17: Sound detector payload output.

### Temperature Sensor Payload

The temperature sensor payload (Figure 18) also utilises the configurable PCB arrangement. The sensor is able to accurately detect temperature to  $0.1^{\circ}\text{C}$ . Every 2 seconds, the sensor payload refreshes and outputs the current recorded temperature. Messages are communicated via Bluetooth as shown in Figure 19. The data sheet for temperature sensor module used in the sensor payload may be found in Appendix H.

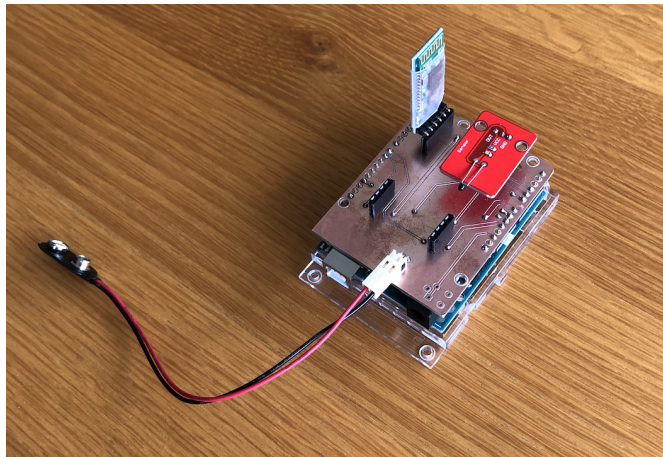


Figure 18: Final temperature sensor payload.

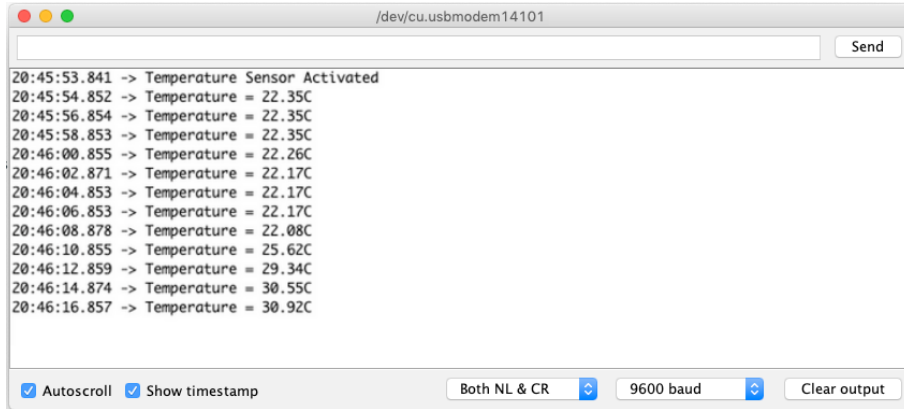


Figure 19: Temperature sensor payload output.

### 5.4.3 UAV Integration

Using a similar approach as taken in the first iteration of sensor payload development (Appendix E), the Bluetooth-enabled payload device can be paired with the on-board Raspberry Pi such that it may communicate its sensed data to the UAV as opposed to another HC-05 enabled Arduino. The sensed data is received via the Raspberry Pi's Bluetooth serial communication, with the readable a display presented in Figure 20 (the Raspberry Pi code is included in Appendix M. The sensor data may then be interpreted and further communicated to the ground station utilising the MAVLink protocol, as discussed in Section 6.2.2. Being conscious of redundancy, that is, if the UAV is not able to further communicate the sensed data to the GCS, a sensor log (Figure 21) is recorded throughout the flight such that all sensor messages with timestamps are recorded to be retrieved after the flight is completed.

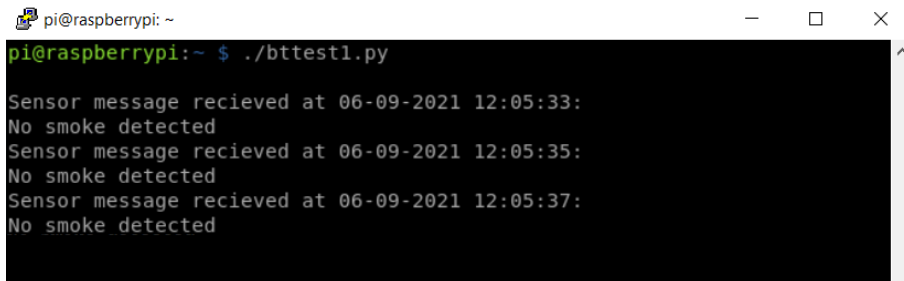


Figure 20: Sensor output when received by UAV.

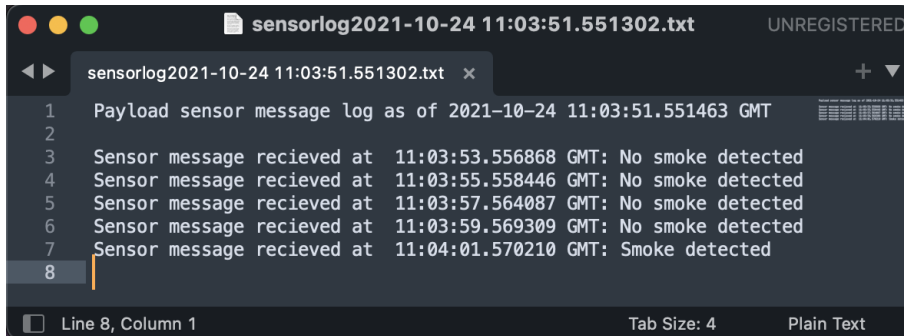


Figure 21: Example of UAV backup flight log.

#### 5.4.4 Testing

The pairing time of Bluetooth devices is critical, as it is important to ensure the payload is operational throughout flight. Moreover, if a problem causes the UAV and payload lose connection, the reconnection time must be minimised. To determine the time taken for the sensor payload to connect, the device is reset, and connection time recorded. To minimise error, numerous trials are performed, and the same timer is used each time. The results are tabulated in Table 7, which demonstrates that the connection time of the payload device has a mean of 4.775s which is successfully meets the minimum connection time of 15s outlined in system requirement R.2.8.

Table 7: Connection time after HC-05 Bluetooth module reset.

<b>Test</b>	<b>Connection Time (Seconds)</b>
1	4.22
2	4.72
3	4.79
4	3.71
5	4.74
6	9.22
7	4.54
8	4.80
9	2.88
10	4.13
<b>Mean</b>	4.775
<b>Standard Deviation</b>	1.590

As the payload and UAV will constantly be within 2m when connected, as per R.2.1, a large maximum communication range is not a priority. Nevertheless, a range of 2m is required and should be verified. After incremental range testing in open spaces, the device range is verified to be approximately 20m which is greater than the predicted range of 10m as discussed in Section 4.3. As evidenced in Section 5.4.2, each designed payload successfully performs its expected operations of successful smoke detection, temperature detection, and sound detection. The connection time and range is not noticeably affected by altering the sensor payload. Through sensor payload demonstrations seen in Section 5.4.2, it is seen that the sensor is able to communicate in real-time with the UAV with negligible delay.

#### 5.4.5 Summary

Through verified communication between the IoMT sensor payload and UAV it is evident that the payload is effective at sensing and communicating data. The IoMT sensor payload is able to communicate in real time to the UAV which then communicates the sensed data to the GCS, and thus contributes towards achieving Objective 3. Moreover, as demonstrated in Section 5.4.1, the sensor payload is also able to collect sensed data, temporarily store the sensed data and then communicate this data to Bluetooth enabled devices other than the UAV. That is, it is also independently operable, achieving Objective 4. Future requirements of the project may necessitate a longer range communication protocol for communication between the UAV and payload. This may be facilitated via technologies such as UWB or LoRaWAN (Gislason 2008) (Lavric et al. 2017).

### 5.5 Gripper Mechanism Subsystem

The development of a gripping mechanism solution is fundamental in creating the capability for the UAV to collect, carry, and deposit the IoMT payload. As such, the gripping mechanism design addresses Objective 2, the transport of a payload, whilst aiming to have minimal detriment to the flight characteristics of the UAV which constitute Objective 1.



### 5.5.1 Design Considerations

In alignment with the literature presented in loaded multirotor transportation (Section 3.2) and theory pertaining to multirotor suspended load dynamics presented in Section 4.2, the mounting of the magnetic gripper shall be achieved via cables. This is considered preferable to completely rigid or semi-rigid linkages, as a cable attached close to the UAV’s centre of gravity will introduce comparably minimal moments when the UAV pitches, hence allowing for greater stability, endurance, and faster control response.

### 5.5.2 Gripper Selection

A set of selection criteria to evaluate various gripper design options may be developed with reference to the system requirements presented in Table 2. The mechanical operational complexity of the gripper system is significant, as a reduction in complexity will address system requirement R.1.8 in making it cheaper and easier to find COTS replacement pieces in the case of a failure. Similarly, a simpler design addresses system requirement R.1.7 which concerns the frequency of maintenance for the system. The level of compatibility between the on-board UAV flight controller and the gripping module is important in coordinating each of the collection, transport, and delivery phases of flight. A high compatibility would allow the system to easily meet system requirements R.3.2, R.3.3, and R.3.4, which all concern the interaction between the UAV and payload at various phases of flight. The load carrying capacity of the gripper mechanism is necessary to directly address system requirement R.1.2. The functionality of the gripper design in rugged environments is critical for outdoors operation and to meet all environment-related system requirements presented in R.6. The combined mass of the gripper and its interface on the payload is also important to minimise the impact on the UAV flight characteristics. A well-designed gripper shall meet the payload mass system requirement R.4.6, and the legislative system requirement R.5.1. Finally, the gripper mechanism shall be tolerant of landing position inaccuracies to an extent, given the expectations of a moderate environmental disturbances upon the flight operating conditions. An inaccuracy-tolerant gripper module would address system requirements R.1.4, R.6.3, and R.3.5. The developed selection criteria are applied to five gripper design options and evaluated in a Pugh selection matrix in Table 8.

Table 8: Gripping mechanism Pugh selection matrix.

Criteria	Snap Fit Mating	Clamps for Form-Fixed Payload	Claw for Free Form Payload	Standard Electromagnet	Electro Ferromagnet
Mechanical Complexity	S	–	–	++	++
Command Integration Complexity with Flight Controller	S	S	–	S	+
Load Carrying Capacity	S	S	+	–	S
Functionality in Rugged Environments	S	+	+	+	+
System Mass	S	--	--	–	–
Landing Accuracy Tolerance	S	++	+	+	+
<b>Total</b>	0	0	–1	2	4

### 5.5.3 Final Gripper Design

As indicated through the selection analysis process, an electro ferromagnet gripper is most suited for the project's requirements. The commercially available OpenGrab EPM v3 is selected for its proven capabilities in prior usage with drones, a 1kg carrying capacity during flight manoeuvres, and the availability of a Pulse Width Modulation (PWM) interface allowing it to be controlled similarly to a servo and other common drone electronic attachments. The component data sheet is provided in Appendix I. Unlike a standard electromagnet, the electro ferromagnet does not require a constant power supply to remain magnetic and instead only requires power to change its state to become magnetised (Kirienko 2018). From empirical results presented by ArduPilot, it is advised that the magnet shall be positioned at least 5-10cm away from the flight computer to avoid magnetic field interference of navigation systems (ArduPilot 2021). Therefore, the electro ferromagnet is mounted 10cm below the UAV frame, effectively increasing the distance between the magnet to the flight computer to approximately 15cm for additional precautions. An intended benefit of utilising a long tether is to enable extra slack for compliance with misaligned landings. A short-term solution for prototyping the tether involves the use of string threaded through the magnet's mounting plate with high-strength tape to secure the connection as shown in Figure 22. An engineering drawing of the magnet and mounting plate with drilled holes for the tether is provided as PRT03 in Appendix K. It was experimentally verified that the string can carry up to 2kg individually. Alongside the tether is a cable to connect the PWM terminals from the flight computer to the gripper to facilitate actuation signals.

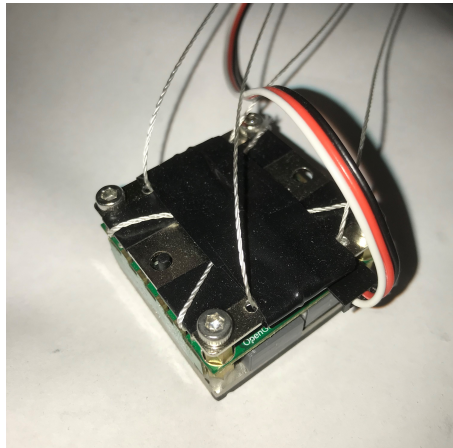


Figure 22: Gripper mounting implementation.

### 5.5.4 Summary

It is concluded from the selection analysis that an electro ferromagnet is the most preferable gripper option for the project. The availability of a PWM interface port allows for immediate compatibility with the flight computer system. The gripper implementation enables the capability for the UAV to transport a payload, hence progress is made towards Objective 2, the transport of a payload. Objective 2 will be fully satisfied through the development of the payload casing described in Section 5.6. Future developments of the magnet tether may utilise a more weather-proof material, such as nylon fishing line instead of string, to ensure the carrying capacity does not degrade overtime especially when exposed to outdoor environments.

## 5.6 Payload Casing Subsystem

In order to successfully achieve Objective 2, transport of a payload, the safety of the payload must be ensured throughout flight. Thus, a casing is desired such that the IoMT device payload may remain secured to the gripper throughout flight as per system requirement R.3.2, but also remain a safe distance from the electromagnet gripper such that it is not affected by the magnetic field. Moreover, the payload casing will incorporate IR beacons making it easier to be located by

the UAV as per system requirement R.2.2. A cube shaped casing is desired in order to ensure stability in picking up and dropping off the payload. Furthermore, a cube casing will increase ease of manufacture and will increase symmetry which ultimately minimises the added complexity on the UAV's flight dynamics caused by the payload.

### 5.6.1 Conceptual Design

In formulating potential solutions for a payload casing, numerous concepts are developed for key considerations in the design, and explored through the utilisation of a morphological table (Table 9). Four potential solutions are selected by considering four selection priorities: minimising the mass of the system, minimising the cost of the system; maximising the performance in terms of strength, durability, aerodynamics, and collection accuracy; and a balanced priority which attempts to find a mix of each of the other priorities. These solutions are developed through concept sketches as detailed in Figures 23 - 26. Using a Pugh selection matrix (Table 10), it is identified that an ideal payload casing solution (Figure 26) is constructed from 3D printable Acrylonitrile Butadiene Styrene (ABS) and features a steel plate and cone on the top such that the gripper can be guided toward its magnetic target plate. The ideal casing features internally-cabled symmetrical IR beacons. The sides of the casing are kept open in order to minimise the mass and to aid in ease of payload sensor changeover.

Table 9: Payload casing design morphological table.

Component	Concept 1	Concept 2	Concept 3	Concept 4
Material	ABS (3D Printing)	Aluminium	Plywood	
Number of IR Beacons	1	2		
Wall Type	Enclosed	Not Enclosed		
Payload Fastening Method	Glue	Screw	Tape	Mount
Gripper Interface	Cone	Flat		

Key: Solution 1 – Low Mass, Solution 2 – Low Cost, Solution 3 – High Performance, Solution 3 – Balanced

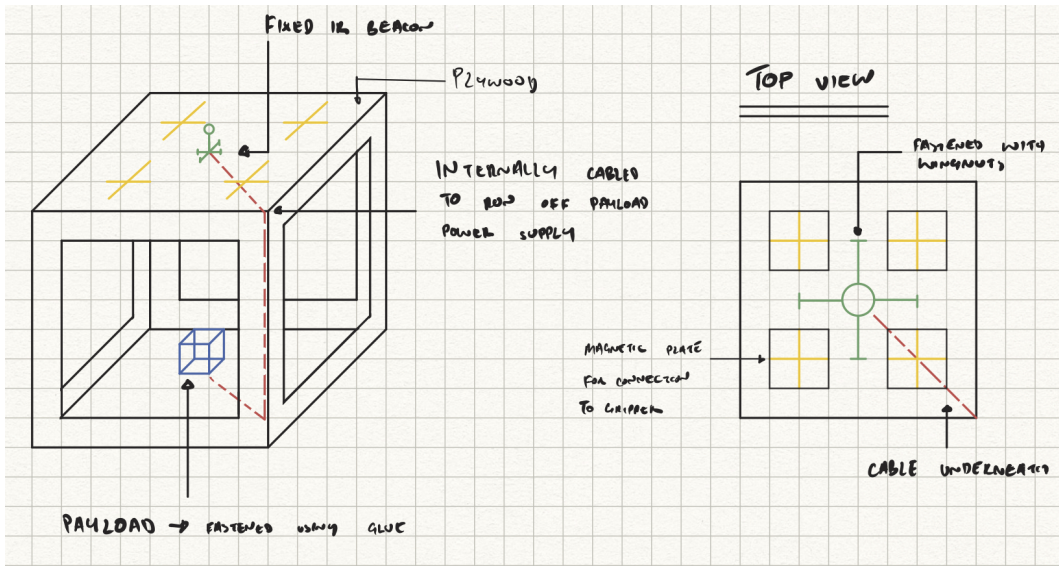


Figure 23: Concept sketch of payload casing solution 1.

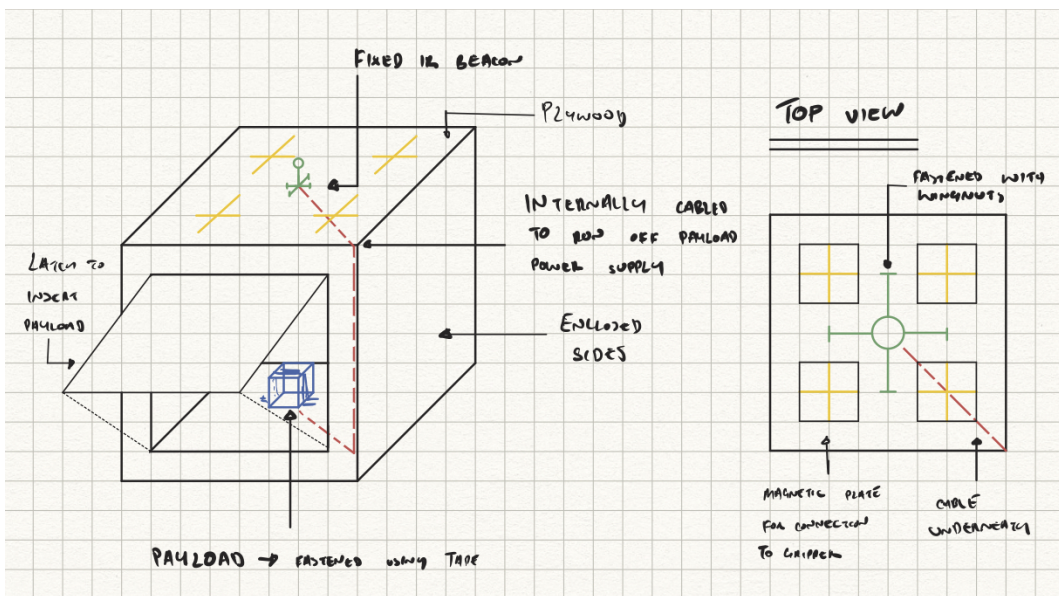


Figure 24: Concept sketch of payload casing solution 2.

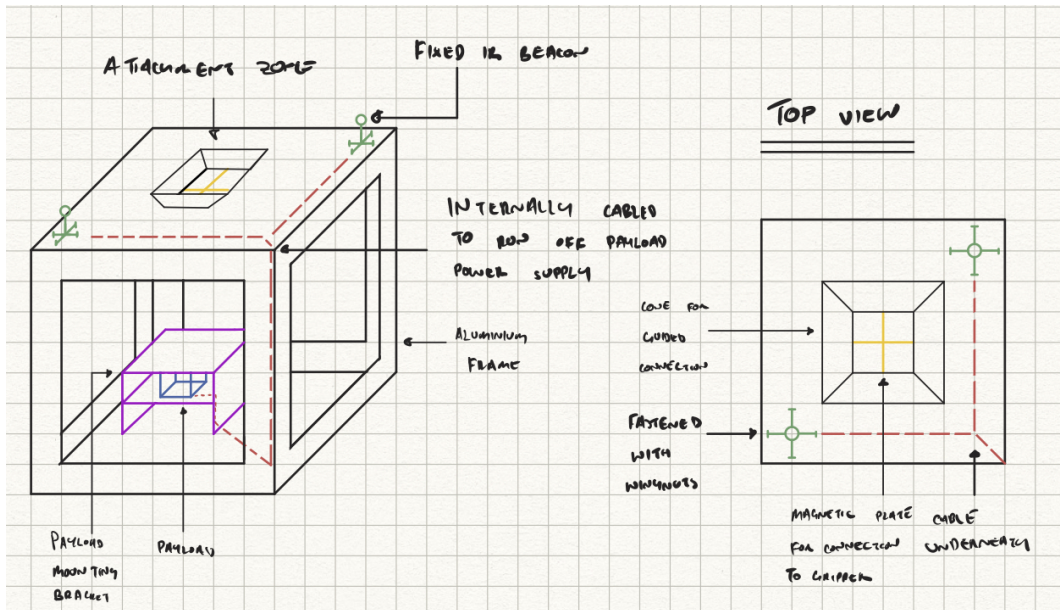


Figure 25: Concept sketch of payload casing solution 3.

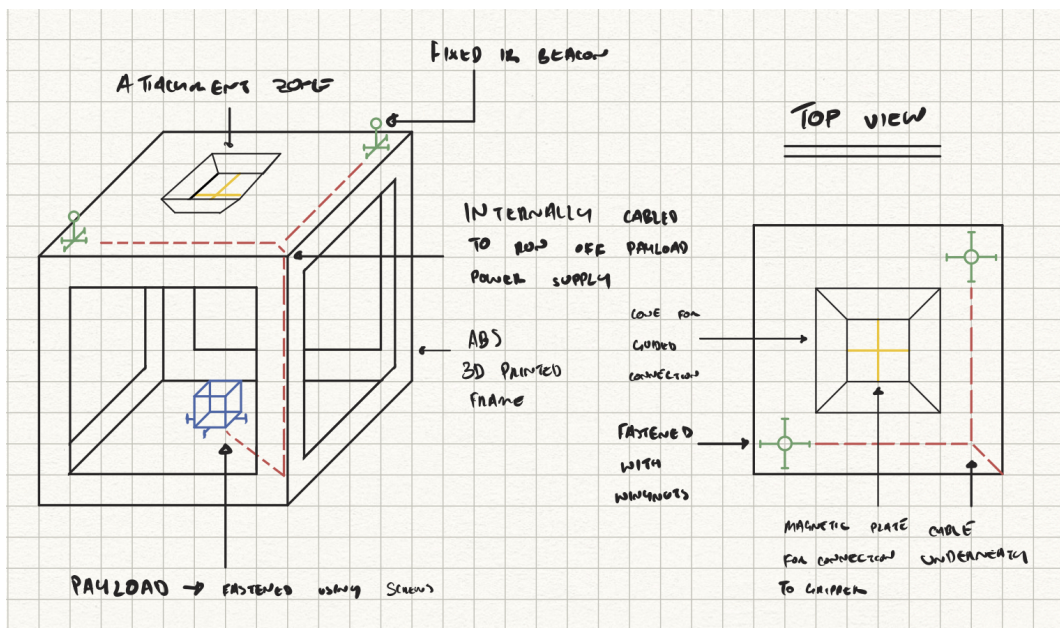


Figure 26: Concept sketch of payload casing solution 4.

Table 10: Payload casing Pugh selection matrix.

Criteria	Solution 1	Solution 2	Solution 3	Solution 4
Mechanical Complexity	S	–	–	+
Computational Complexity	S	S	–	–
Strength and Durability	S	S	++	+
Aerodynamics	S	S	+	+
Cost	S	S	–	–
Collection Accuracy	S	S	+	+
<b>Total</b>	0	–1	1	2

### 5.6.2 Material Selection

As detailed in Table 9, the three investigated casing materials are ABS, aluminium, and plywood. These materials were considered primarily due to their low density thus they would not add significant mass to the payload. This is critical as the mass of the payload could not exceed 1kg as detailed in system requirement R.4.6. This is distinct in the option of plywood, which has a density of  $500\text{kg/m}^3$  (Plywoods 2021). However, plywood’s low density is significantly overshadowed by its low compressive strength (41MPa) thus if the UAV were to land on top of the casing it would likely break (Laboratory 1990). This is contrast to aluminium which has a significantly higher compressive strength (280MPa) but also a higher density ( $2500\text{kg/m}^3$ ) (AZO 2019). The primary disadvantage of using aluminium for a payload casing is that it has a high manufacturing complexity where methods such as welding are required to construct it. A material that finds a balance between plywood and aluminium is ABS with a density of ( $1000\text{kg/m}^3$ ) and compressive strength of up to 60MPa (R. et al. 2016) (BPF 2021). Furthermore, ABS has a low manufacturing complexity as it may be rapidly prototyped using 3D printing. Thus, ABS is the selected payload casing material.

### 5.6.3 Infrared Beacon Detection

As investigated in the literature review of Section 3.3, an infrared detection camera is to be mounted on the UAV to ensure more accurate detection of the payload. As discussed in Section 3.3, it has been established that the addition of an IR beacon has the potential to increase the UAV’s detection accuracy from 12.4cm (GCS enabled GPS) to 8cm. To further increase this accuracy, two IR beacons (Figure 27) are placed symmetrically on top of the payload casing such that the UAV may detect both beacons. One potential future application of two IR beacons being placed on top of the payload casing is that the centre location of the casing may be calculated and ultimately more reliably detected. The distance between the UAV and payload will also be more accurately known through the utilisation of stereo vision.

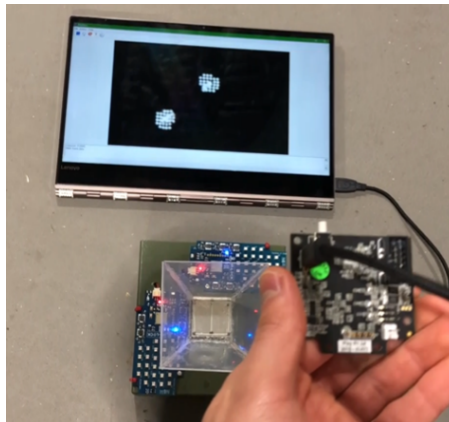


Figure 27: Infrared beacon detection by on-board infrared camera. The laptop screen at the top of the image displays the live picture processed by the IR camera.

At present, the IR-lock functionality is non-operational but it is being troubleshooted. As shown in Figure 27, successful calibration of the IR-lock with the accompanying payload casing IR beacons was achieved. However, during flight, the beacons are unable to be detected. As demonstrated in the flight log shown in Figure 28, although the IR-lock beacons are connected, calibrated and operational (confirmed by a health reading of "1"), the IR beacons are unable to be detected (as indicated by the IR beacon detection status of "0"). Nevertheless, beacon detection refinement is a primary area for future development. Currently, manual guided flight is being utilised to collect the payload, thus removing the burden of the non-operational IR-beacon detection.



Figure 28: Flight log showing UAV height above ground (red), IR-lock camera health (green) and IR beacon detection status (blue).

#### 5.6.4 Gripper Interface

In order to ensure secure collection of the payload via the magnet, a funnel-shaped guide (Figure 29) is to be placed around the attachment zone such that misaligned landings may still achieve complete gripper contact with the payload. Moreover, the funnel design accommodates for the minor swaying motion experienced by the UAV due to the ground effect turbulence when hovering close to the ground. The funnel is constructed using IR-transparent acrylic and acrylic glue.

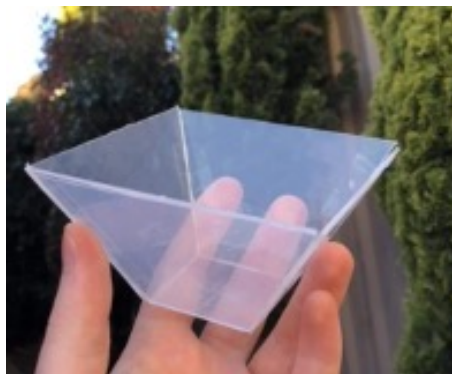


Figure 29: Payload casing funnel.

#### 5.6.5 Prototyping

To first gain a conceptual understanding of the designed payload casing, a basic Computer Aided Design (CAD) model (Figure 30a) is developed. This is refined with a detailed CAD model (Figure

30b) which may be 3D printed (Figure 30c). This print features numerous holes throughout such that the beacons, a steel attachment plate, and guiding funnel may be secured using screws and zip-ties. A technical drawing of the 3D printed payload casing body is shown in PRT01 of Appendix K. Figure 31 shows the final construction of the payload casing.

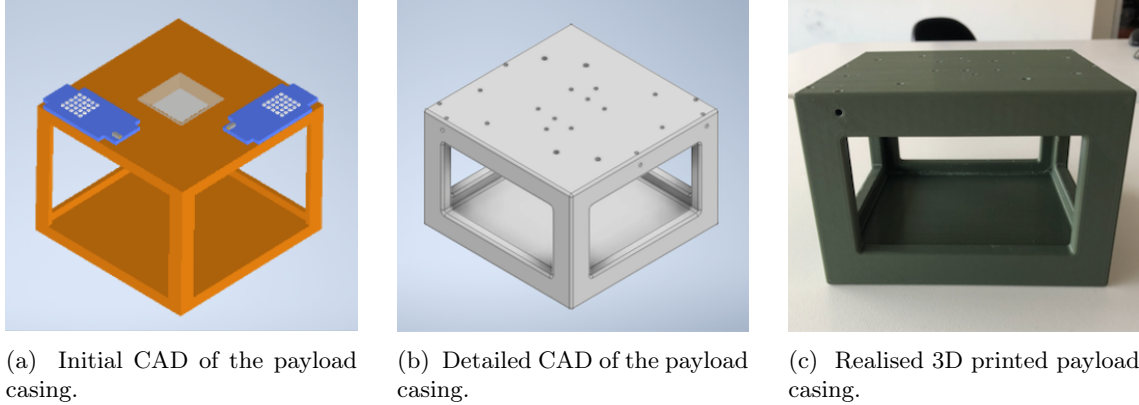


Figure 30: Iterative stages in payload casing development.



Figure 31: Final payload casing construction.

### 5.6.6 Summary

Through flight demonstrations (to be presented in Section 6.4), it is evident that the payload casing is effective in housing the IoMT payload during flight (Figure 32). Moreover, it is evident that the guiding funnel is effective in ensuring accurate and secure collection by the electro ferromagnet gripper (Figure 33). The payload casing allows the IoMT payload to be effectively transported by the UAV and ensures safe and secure transportation.





Figure 32: UAV flying with payload casing.

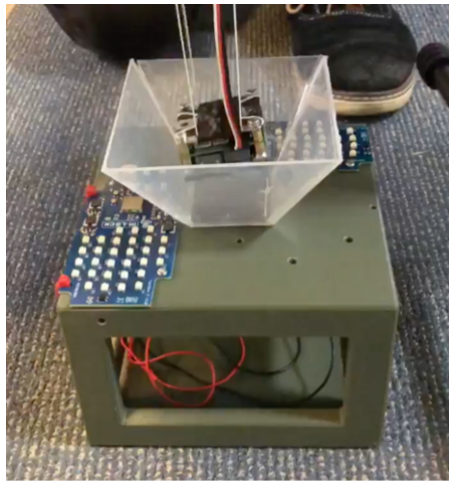


Figure 33: UAV gripper guided towards casing via funnel.

## 5.7 Final Design Summary

The final design demonstrates the processes used to construct the modular project subsystems: UAV platform; IoMT payload; gripper mechanism; and payload casing. The UAV platform design achieves the project's Objective 1 (UAV flight) through component benchmarking analysis and corroboration with eCalc approximations. Software considerations are made to select an open-source and mature autopilot and GCS in ArduPilot and QGroundControl. Real-time wireless communication is enabled in the sensor module, which makes progress towards Objective 3. Independent operation of the sensor payload is additionally possible, hence meeting Objective 4. An electro ferromagnet gripper is designed for a tethered grasping configuration, allowing up to 1kg of payload to be carried, and addresses Objective 2. Lastly, the payload casing is 3D printed and is tested to be compatible with the magnetic gripper. The details of the separate subsystems' synergy provided in subsystem integration (Section 6).

## 6 Subsystem Integration

This section discusses the means through which the four key subsystems (UAV platform, IoMT payload, gripper mechanism, and payload casing) are integrated to achieve UAV PHORESIS. Integration of these subsystems is achieved through three mediums: hardware, software/communications, and electronics. Hardware integration involves the mechanical relationships between components; software/communication integration regards the routing of instructions/data throughout the system; and electronic integration realises the physical wiring that permits communication links. The systems are further synthesised through verification and validation analysis to ensure the integrated platform meets the defined requirements.

### 6.1 Hardware Integration

All four key subsystems exhibit interdependent mechanical interfaces which magnify the importance of high-quality hardware integration across all subsystems. A block diagram illustrating the hardware interfaces is presented in Figure 34. The primary mechanical interfaces include: IoMT payload contained within the payload casing, payload casing mating with the gripper, and the gripper suspended by the UAV platform. Firstly, the payload is secured within the payload casing using double-sided mounting tape. The tape sufficiently negates vibration within the casing whilst being relatively simple, lightweight, and affordable to remove and replace when alternating payloads. Secondly, the payload casing features a squared funnel around a metal plate on its top surface to support accurate and reliable gripper mating (as discussed in Section 5.6). Finally, the gripper is attached to the UAV platform and sufficiently displaced from sensitive electrical components via two loops of cotton twine. The cotton twine provides sufficient strength to hold the payload, whilst being lightweight, highly affordable, and highly flexible. Whilst a flexible material increases the chances of significant payload movement during flight, it is ultimately beneficial by reducing airframe moments during manoeuvres, not transmitting compressive disturbing forces, and permitting passive mating accuracy augmentation via the squared funnel on the payload casing. Successful integration of the latter two interfaces directly contributes towards the completion of Objective 2, transport of a payload.

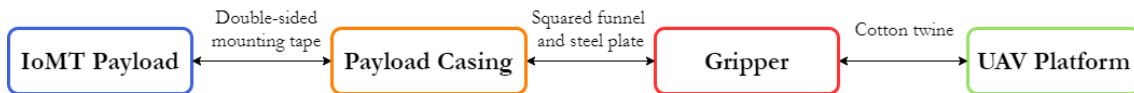


Figure 34: Block diagram realisation of the hardware integration interfaces.

## 6.2 Software and Communications Integration

Four primary software/communication links are present during the UAV PHORESIS operation (as illustrated in the block diagram in Figure 35): Bluetooth between the sensor and Raspberry Pi; serial between the Raspberry Pi and the autopilot; radio between the autopilot and controller (GCS or remote controller); and radio between the on-board First-Person Video (FPV) camera and grounded video receiver.

### 6.2.1 Sensor to Raspberry Pi (Bluetooth)

As discussed in Section 5.4.3, the sensor data is routed through an Arduino and transmitted using an HC-05 Bluetooth module; this signal is then received by the Raspberry Pi's native Bluetooth receiver and routed to its General Purpose Input/Output pins, specifically the transmit (TXD) pin.

### 6.2.2 Raspberry Pi to UAV Radio Modem (Serial)

The sensor data from the Raspberry Pi's TXD pin is serially routed through the autopilot, using the MAVLink messaging protocol, to one or both of the UAV's radio modems. If the UAV is being controlled via the hand-held controller (FrSky Taranis X9D), the FrSky RX8R Pro radio modem is used for UAV platform instructions whilst the RFD900x Modem is used for UAV status monitoring. Conversely, if the UAV is being controlled via the GCS, then the RFD900x Modem is used for both UAV platform instructions and status monitoring. The open source nature of MAVLink allows for its customisation to augment the communication capability. Such augmentation was attempted by embedding the sensor data received by the Raspberry Pi from the sensor payload in a MAVLink message, and sending this to the autopilot to then be transmitted to the GCS.

The radio link between the UAV radio modem (on-board the UAV) and the controller (grounded) also utilises the MAVLink protocol to exchange UAV control instructions and status. An attempt was made to combine the augmented MAVLink message (containing the sensor variable) with the default autopilot MAVLink message to allow the variable to be read from the GCS in real-time. However, a failure to correctly modify the MAVLink source code prevented this from being achieved. It is believed that the error is likely due to compatibility issues between the transmitted and received MAVLink messages. Given the highly modular nature of the UAV PHORESIS system, a redundancy plan to bypass the usage of a MAVLink-augmented sensor data message is conveniently achieved. A similarly configured Raspberry Pi is placed at the GCS to leverage the already proven communication capabilities between the sensor payload and Raspberry Pi. The received data at the Raspberry Pi can then be displayed at the GCS through utilising a laptop to Secure Shell (SSH) into the Raspberry Pi. This redundancy plan (signified by the dashed line in Figure 35) limits the range the UAV and payload can travel (approximately 20m) whilst offering real-time sensor payload data, as the sensor data can no longer leverage the larger antennas on-board the UAV which would have been accessible via the on-board Raspberry Pi. However, the UAV remains controllable from the GCS beyond the 20m GCS Raspberry Pi-sensor payload Bluetooth communication range. This critically enables the locally stored data within the sensor payload to be retrieved once the payload is brought back within Bluetooth range of the GCS-based Raspberry Pi.

### 6.2.3 UAV Radio Modem to GCS/Hand-Held Controller (Radio)

The sensor data routed through the autopilot is then combined with UAV status variables and is received by the UAV radio modem via an FTDI serial connection. The sensor and UAV status data is then transmitted as a radio signal by the one of the modems on-board the UAV. If the RFD900x Modem is utilised, the signal is received by the GCS and serially routed to QGroundControl for display and monitoring by the human operator. Similarly, if the FrSky RX8R Pro modem is used, the signal is received by the hand-held controller and displayed for monitoring by the operator. Additionally, the GCS/hand-held controller communicates UAV control and gripper actuation instructions to the radio modem on-board the UAV. These instructions are then serially routed to

the autopilot where they are interpreted and converted into regulated voltages to actuate specific motors to specific rotational speeds, and to actuate the gripper.

#### **6.2.4 On-Board FPV Camera to Grounded FPV Receiver (Radio)**

It is desirable to provide a real-time video feed of the area beneath the drone - improving safety via human monitoring and the accuracy of manual landings. Thus, hardware to transmit video footage from on-board the UAV is established; however, an appropriate ground receiver was unable to be obtained and hence the video was instead recorded, stored locally, and collected after landing the UAV. Integrating these software/communication links contributes towards the completion of Objective 3, UAV, payload, and GCS communication systems.

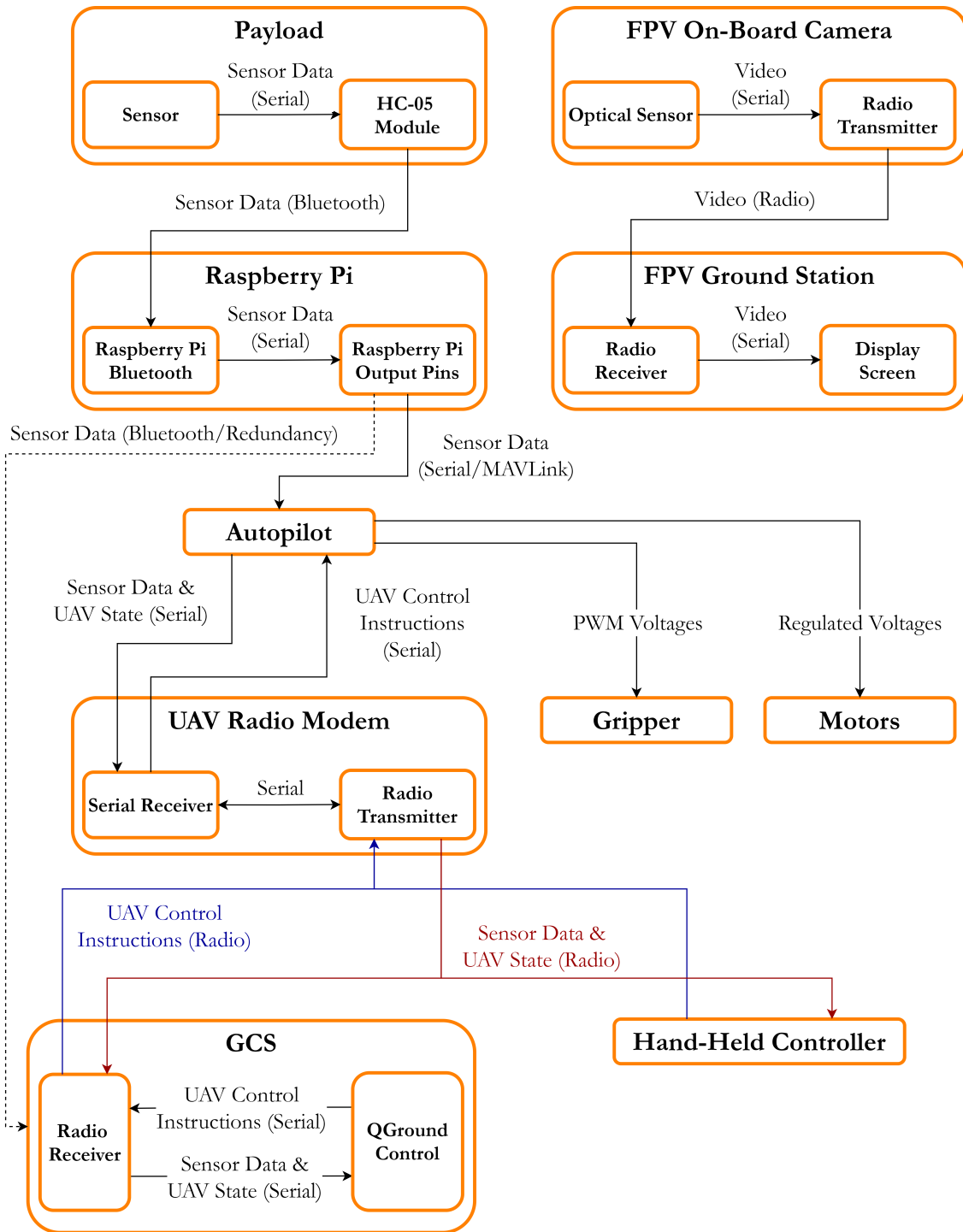


Figure 35: Block diagram realisation of the software and communications interfaces.

### 6.3 Electronics Integration

On-board the UAV platform, various electronic systems to achieve gripper control, augment flight control and sensor data communication are integrated (refer to the wiring diagram in Figure 36) to complete Objectives 2 and 3. The gripper is wired to the autopilot via a PWM connection, allowing for actuation from the GCS. The Bluetooth signal from the sensor payload is received by a Raspberry Pi 4 at the Ground Control Station (GCS). Despite enacting the redundancy plan to operate the Raspberry Pi from the GCS, electronics integration for operating it on-board the UAV has been performed to enable easier synergy in the future. The gripper and Raspberry Pi are both powered in parallel via the 5V output from the BEC. Another electronic system integrated into the UAV platform is the on-board, downward-looking optical video camera. The system involves a camera connected to an on-board wireless transmitter to a ground video receiver station. The camera also contains a micro-SD card slot to allow for local video storage which acts as a contingency for wireless transmission, as discussed in Section 6.2. Finally, the integration details to achieve an autonomous precision landing capability involve an on-board IR-homing camera and lidar - both connected to the autopilot via an Inter-Integrated Circuit (I2C) connection and both powered via the 5V output from the BEC. All electrical components and wiring are physically supported by an acrylic mounting plate that is suspended below the carbon fibre body of the UAV. This mounting plate is detailed in PRT02 of Appendix K.

UAV PHORESIS Wiring Diagram

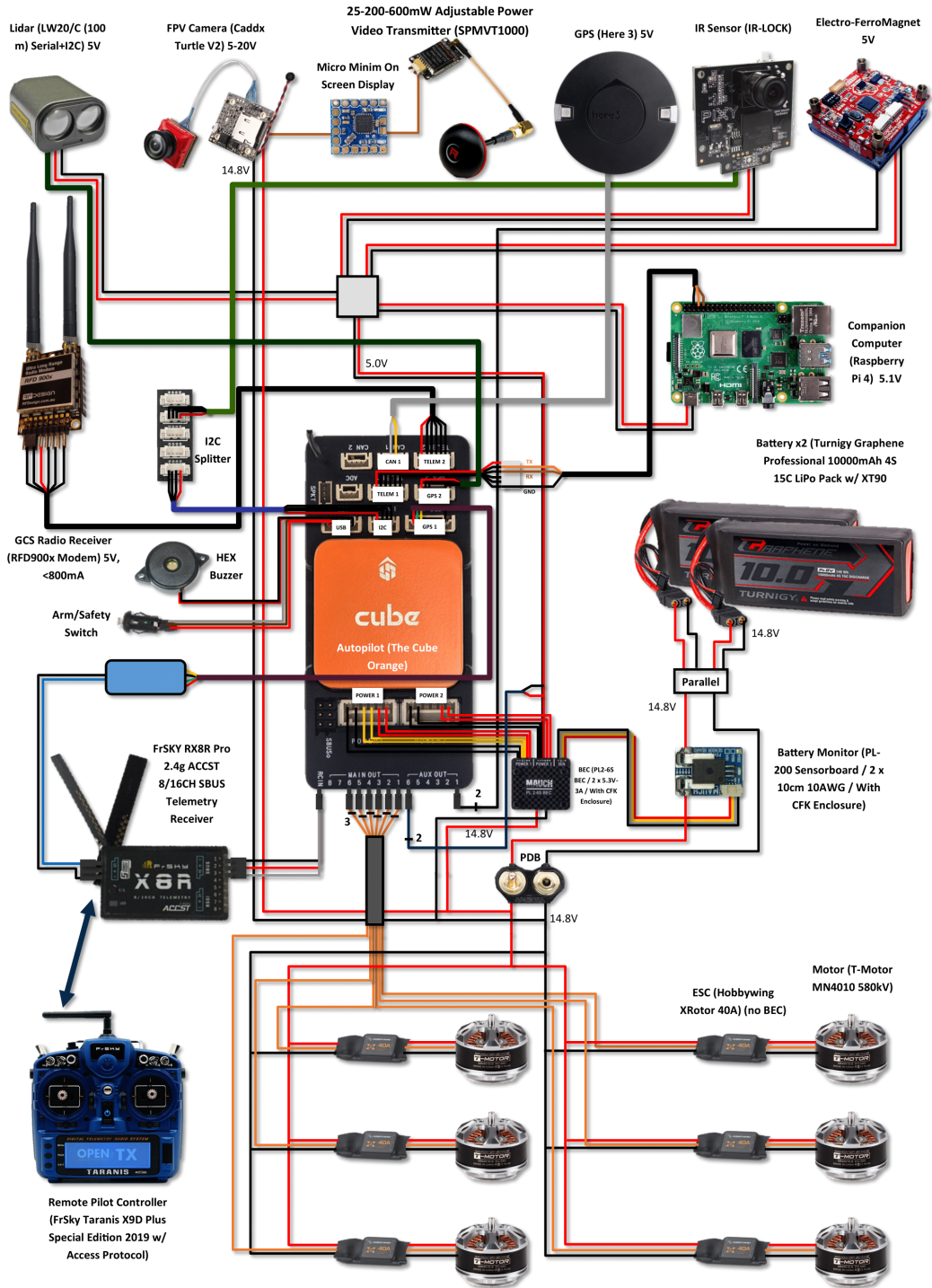
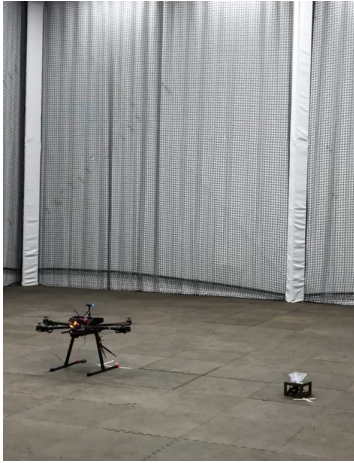


Figure 36: UAV platform electrical wiring diagram.

## 6.4 UAV PHORESIS Demonstration

An indoor flight trial was conducted at DSTG Edinburgh that successfully demonstrates UAV PHORESIS and hence evidences the achievement of all four project objectives (flyable UAV; transport of a payload; UAV, payload, and GCS communication; and independent operation of the IoMT payload) in a single flight. The demonstration involves four stages: unloaded flight, payload collection, loaded flight, and payload deposit (refer to Figure 37). Objective 1 is demonstrated with unloaded flight and Objective 2 is demonstrated with payload collection, loaded flight, and payload deposit. Objectives 3 and 4 are demonstrated throughout as the UAV status is received and its position controlled, whilst a continuous stream of sensor data was received throughout the trial. The Risk Assessment and Safe Operating Procedure for this flight trial may be found in Appendix D.

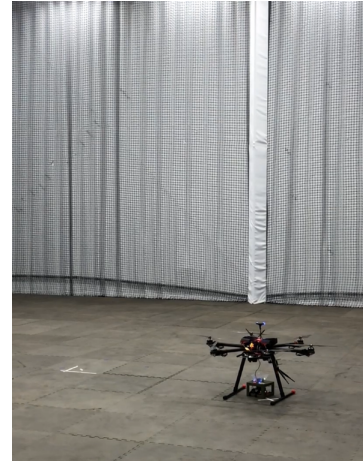




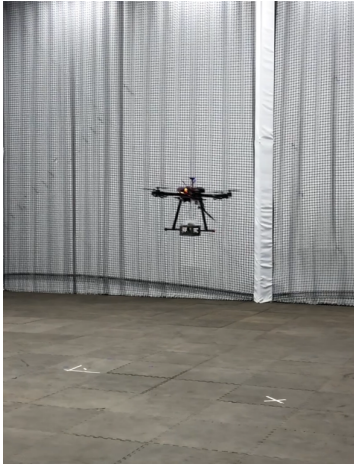
(a) Initial positions of UAV and payload.



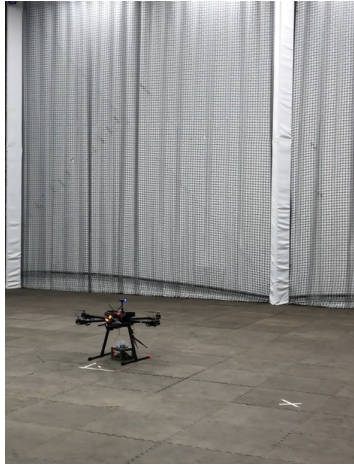
(b) Unloaded flight of the UAV approaching the payload.



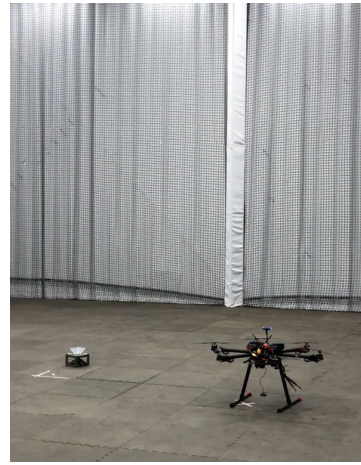
(c) Collection of payload by UAV.



(d) Loaded flight of the UAV transporting the payload.



(e) Deposit of the payload by UAV.



(f) Final positions of the UAV and payload.

Figure 37: Demonstration of UAV PHORESIS within an indoor flight arena at DSTG Edinburgh.

## 6.5 Verification and Validation

Verification and validation are critical quality control processes which ensure that the problem is solved logically and correctly. They also provide an easily documented basis upon which the successful completion of tasks can be determined. The verification and validation for UAV PHORESIS comprehensively demonstrate the successful completion of the project.

### 6.5.1 Verification

Verification measures aim to prove that the system meets all of its specified requirements. To acknowledge the interrelation between system requirements and verification measures, backwards traceability of verification measures for each system requirement are presented in Table 2 within the problem definition, Section 2.5. The verification measures must be enacted throughout the entirety of the project, including the planning, design, construction, operation, and retirement of the product. The verification measures are divided into five categories suitable for different phases of the project: analysis, certification, demonstration, inspection, and testing. The measures presented below in Tables 11 - 15 include descriptions of tasks to verify the design meets the requirements, alongside examples of the verification being implemented during the project.

## Analysis

Collect data using a sensor, evaluate the data using a mathematical calculation or simulation, then check for the accuracy of the calculation.

Table 11: Verification measures via analysis.

<b>Analysis</b>	<b>Description</b>	<b>Implementation</b>
A.1	Investigate the expected maintenance requirement or lifetime of a critical UAV component	A severed motor control PWM cable was identified and rapidly repaired with solder and heatshrink for insulation
A.2	Investigate the sizing of a component and how this may impact other components/functions it may interface with	The tether length separating the magnet from sensitive electronics was measured to a length greater than the empirically recommended 10cm

## Certification

Written assurance that the component's expected development, manufacture, operation, and/or retirement plan adheres to the appropriate legal or industrial standards.

Table 12: Verification measures via certification.

<b>Certification</b>	<b>Description</b>	<b>Implementation</b>
C.1	Consult with the representative for DSTG to ensure the device adheres to the relevant DASR requirements	Consulted three CASA-approved drone specialists at DSTG who regularly operate under DASR regulations. The airworthiness of the UAV and appropriate risk management procedures were verified
C.2	Consult with the representative for the University of Adelaide or Honours Group 3296 to ensure that the device is operated by licensed individuals	The UAV was remotely piloted by a CASA-approved DSTG specialist flying within DASR regulations

## Demonstration

Operate the system against a set of criteria which must be satisfied and witnessed by any necessary parties. This measure must not require any specialised equipment that does not constitute part of the system’s normal operating componentry.

Table 13: Verification measures via demonstration.

<b>Demonstration</b>	<b>Description</b>	<b>Implementation</b>
D.1	Manually operate the UAV and perform a critical task within its fully operational, physical capability	The sensor payload transportation task was successfully completed during the flight trial
D.2	Manually operate the UAV and perform a critical task within its fully operational, communicative capability	The real-time payload communication task was successfully completed during the flight trial, alongside real-time wireless actuation of the magnet from the GCS
D.3	Autonomously operate the UAV and perform an important task within its fully operational, physical and communicative capability	The automated guided infrared landing camera failed when connected to the autopilot, despite calibration measures being successful from the GCS
D.4	Operate the UAV for a full-length flight that exhibits full-functionality	During the flight trial, all expected tasks including unloaded flight, payload collection and deposit, loaded flight, and real-time communications were achieved

## Inspection

Refer to the readings of a sensor to examine the state of the system.

Table 14: Verification measures via inspection.

<b>Inspection</b>	<b>Description</b>	<b>Implementation</b>
I.1	Weigh a physical component using a weighing scale	The payload module including the casing, electronics, and battery were weighed as less than 600g, enabling a margin of safety to the magnet’s nominal 1kg carrying capacity
I.2	Review the procurement source of a component and its maintenance or replacement requirements	All utilised components remain available online, and manufactured components requiring the use of 3D printing, laser cutting, and drilling may be performed at local mechanical workshops
I.3	Review the operational nature of a component, its capabilities, and how this influences any components it may interface with	The magnet was noted to be a source of electromagnetic interference and was consequently placed greater than 10cm away from sensitive electronics according to empirical recommendations

## Testing

Operate the system against a set of criteria which must be satisfied and witnessed by any necessary parties. This measure is highly likely to involve the use of specialised equipment to assess the level of satisfaction of the criteria.

Table 15: Verification measures via testing.

Testing	Description	Implementation
T.1	Operate the UAV with a payload of well-known physical characteristics whilst maintaining stability	The UAV remained controllable during flight when performing non-acrobatic aerial manoeuvres loaded with a payload
T.2	Operate the UAV with respect to a distance-travelled measurement	The UAV flew the 15m length of the Indoor Flight Arena over 5 times with negligible draw from the power supply
T.3	Operate the UAV with respect to an angular displacement measurement from a ground location	The UAV hovered at the Indoor Flight Arena wall separating the UAV from the operator, hence placing it at an angle of approximately $60^\circ$ from the operator
T.4	Operate the UAV with respect to adverse environmental conditions	As the UAV flight was demonstrated within an indoor arena, outdoor environmental conditions were unable to be assessed. However, adverse environmental conditions existed due to the enclosed nature of the arena reflecting propeller downwash similarly to an outdoor wind gust. The UAV was visibly affected by the disturbances but control was rapidly re-asserted by the autopilot stabilisation.
T.5	Operate the UAV with respect to a temporal measurement	The UAV was airborne for greater than 20 minutes without a change of power supply during the trial

### 6.5.2 Validation

Validation measures aim to ensure that the correct problem has been solved. The nature of the validation process is more qualitative than the verification measures aforementioned. This is achieved by comparing the operation of the system to the high-criticality user needs (e.g., essential, very important, important), the Scenario-Based Needs Analysis (SBNA), and with reflection upon the conclusions of the problem definition (Section 2). Primarily, validation was achieved through regular progress discussions with the DSTG representative, who provides guidance and feedback on behalf of the project client, DSTG. Furthermore, the final flight demonstration conducted at DSTG (as photographed in Figure 37) served as an opportunity to showcase the project meeting the defined objectives in front of the DSTG stakeholders. The satisfaction and feedback offered by the DSTG stakeholders adds to the validation of the project. It is ultimately concluded through the verification and validation process that the project meets all objectives by satisfying all system requirements labelled as "Very Important" and "Essential", and that the project fundamentally offers a design platform from which further research may be performed regarding the transportation and real-time communication with IoMT sensors.

## 6.6 Subsystem Integration Summary

The integration of various hardware, software/communications, and electronic subsystems and components directly contributes most significantly to Objectives 2 and 3. Hardware integration ensures that a suitable physical connection between the immobile payload and mobile UAV exists which allows for the payload to be transported (Objective 2). Software/communications integration ensures that signals transmitted from one component are detectable and readable on the receiving component which allows for seamless information flow through each subsystem (Objective 3). Elec-

tronics integration provides the foundation upon which the software/communications integration operates whilst providing power and control signals to hardware components (Objectives 2 and 3). Furthermore, the verification and validation analysis provides a cohesive framework to assess how well the project meets the requirements and needs of the client - from this it was concluded that the project meets all objectives.

## 7 Conclusion

This report documents the development of a UAV-implemented physical homing relay system for the transportation of modular, self-operable IoMT devices. More specifically, the achievement of the four project objectives, as detailed in Appendix A, are discussed. A systems engineering approach was adopted to methodically achieve the project objectives in a solution-agnostic manner. This commenced with considering the project as a system with various interacting subsystems and allowed for an effective Scenario-Based Needs Analysis (SBNA) (Section 2.3) in which the interactions between subsystems were contextualised and the needs of the users and stakeholders were elicited. The needs of the user (Section 2.4) were derived from the client brief and SBNA and define what the stakeholders need from the system. Moreover, through developing the user needs into system requirements (Section 2.5), specific requirements were identified which created a clear direction towards objective achievement.

To satisfactorily achieve the system requirements, numerous components of the system were thoroughly investigated through a literature review (Section 3). Namely, four topics of research were identified as critical areas for investigation to thoroughly understand each component: UAV platform selection, loaded multirotor transportation, autonomous landing, and short-range communication. Each topic investigated existing capabilities, standards, and contradictory findings in order to accurately evaluate how each requirement can be adequately met and ultimately successfully achieve each project objective. The findings from the reviewed literature were contextualised and tailored to the project such that they could inform solution development. Specifically, the development of project theory (Section 4) gives insight into UAV motor design, short-range communication evaluation, UAV flight dynamics, and simulation techniques. The project theory culminates into the final design (Section 5) with numerous operational communicable IoMT sensor payloads with a payload casing and the physical development of a flyable UAV following in the subsystem integration (Section 6). A systems engineering approach was again utilised to make informed, solution-agnostic selections for the UAV-payload interface, payload casing, and the UAV platform. As evidenced by Table 25 of the Work Breakdown Structure (WBS) (Appendix N), the engineering design detailed in Section 5, and subsystem integration in Section 6, it is observed that the four objectives detailed in Appendix A are complete. Section 5.3 explores the achievement of Objective 1, a flyable UAV, through the application of SITL simulation and corroboration of mechanical and software components. This design is verified via the successful flight trial documented in Section 6.4. An appropriate UAV platform is explored in Section 5.3 to progress Objective 2, transport of a payload. Sections 5.5 and 5.6, on the gripper mechanism and payload casing, respectively, contribute to the achievement of Objective 2 when coupled with the synergy provided through hardware and electronics integration in Sections 6.1 and 6.3, respectively. The IoMT payload subsystem section (Section 5.4) advances the achievement of Objective 3 and completes Objective 4, UAV, payload and GCS communication systems and independent operation of the IoMT payload. Three distinct IoMT payloads have been developed, each independently operable and communicable: a smoke detector sensor, temperature sensor, and sound sensor. The software and communications integration presented in Section 6.2 synthesises the information flow throughout the project and ultimately completes Objective 3.

There are two potential limitations of the proposed UAV PHORESIS solution: the mode of transportation and the independent operation of the payload. The nomination of a UAV as the designated sensor transport vehicle for the project offers considerable advantages in augmenting sensing capabilities by enabling a highly mobile and aerial sensor platform. However, a UAV has payload weight capacity limitations compared to alternate vehicles such as land-based rovers or maritime ships. Therefore, the breadth of compatible sensor payloads is inherently limited for UAV PHORESIS. An additional limitation concerns the independent operation of the sensor payload module. While an independently operable payload offers enhanced sensing flexibility by not being physically constrained to the UAV, the independence imposes a limitation on sensor payload operational endurance. Difficulties are experienced, particularly if a sensor has a large power demand or if the environment adversely affects battery life.

The engineering detailed in this report unequivocally demonstrates the capability for a low-cost solution to problems like bushfire monitoring but also countless other sensor enabled problems such as medical or agricultural applications. It is clear that modular sensors integrated with a

communicable UAV have strong potential to accurately and adequately monitor situations removing involvement or danger from human operators who might otherwise be directly monitoring the situation.

## 8 Future Work

The progress of the project is measured by assessing the completion of tasks specified in the Work Breakdown Structure (WBS) (refer to Appendix N) and their combined impact on the completion of the four project objectives. To date, all of the WBS tasks have been completed which has ensured the successful completion of all four project objectives. Continual reassessment of the salience of WBS tasks has led to some designing, building, testing, and execution-based tasks (Table 25) being removed (if a task has become irrelevant/inaccurate) and added (if an unforeseen task has been recognised). Lists of all removed and added tasks from the outset of the project are presented in Tables 16 and 17, respectively.

Table 16: Removed tasks from the WBS.

Section	Task	Justification
4.6.	CASA Certification to Pilot the UAV	Whilst this is still a requirement to ensure flight safety, the task could not be completed by Patrick Capaldo or Jason Huynh due to their unavailability to complete the course. Instead, a licensed pilot at DSTG will pilot the UAV.
5.2.	Deliver Gripping Mechanism Design to Workshop Team	The gripping mechanism (electro ferromagnet) does not require further functional augmentation from its off-the-shelf state. Thus, it is not necessary to seek design advice or service from the workshop team at DSTG or the University of Adelaide.
5.3.	Payload and Gripping Mechanism Manufacture	The payload is assembled using simple and inexpensive Commercial Off The Shelf (COTS) components and hence does not require the manufacture of new components or the functional augmentation of existing components. The gripping mechanism does not require functional augmentation from its off-the-shelf state.

Table 17: New tasks to the WBS.

Section	Deliverable	Justification
2.3.1.	Payload-UAV Communication	Communication between the payload and UAV was considered only from the perspective of physical circuitry, and not from that of the programming required to utilise the circuitry.
2.3.2.	Ground Station-UAV Communication	Similarly to 2.3.1, the software required to utilise the electrical circuitry that connects the ground station and the UAV was not previously considered.
3.2.	Component Approval	All information communication technology (ICT) components must be rigorously assessed prior to their purchase through DSTG. This assessment unexpectedly delayed purchases by at least two weeks.
4.6	Reserving a UAV Pilot with a CASA UAV License	Since Patrick Capaldo and Jason Huynh were unable to find a suitable period to complete the CASA UAV licensing course, a pilot from DSTG is to be reserved instead.

Further development of this project is expected to occur via the DSTG Summer Vacation Placement (SVP) program and potentially in subsequent Honours projects within the University of Adelaide. The DSTG SVP will generally aim to integrate the UAV with existing hardware and software platforms used by DSTG. Subsequent Honours projects may aim to implement artificial intelligence-based route planning, computer vision-enabled navigation, and refine the tether and payload sensor designs. The route planning and navigation augmentations will likely reduce the



human labour required to operate the system by increasing its autonomy, and improve the robustness of payload identification and collection. Refinement of the tether design (e.g., material and geometry) may improve the accuracy and stability of payload collection, transportation, and deposit. Finally, refinement of the payload sensor (e.g., fine-tuning for application or expected environment, weather-proofing) may increase the survivability of each payload module and improve the reliability of the sensor measurements.

## References

- Abarca, M., Saito, C., Angulo, A., Paredes, J., and Cuellar, F. (2017). “Design and development of an hexacopter for air quality monitoring at high altitudes”, pp. 1457–1462.
- Achtelik, M., Doth, K., Gurdan, D., and Stumpf, D. (2012). “Design of a Multi Rotor MAV with regard to Efficiency, Dynamics and Redundancy”.
- Amazon (2016). *Amazon Prime Air*. <https://www.amazon.com/Amazon-Prime-Air/b?ie=UTF8&node=8037720011>. Accessed: 13-03-2021.
- Angelis, E. L. de, Giulietti, F., and Pipeleers, G. (2019). “Two-time-scale control of a multirotor aircraft for suspended load transportation”. eng. *Aerospace science and technology* 84, pp. 193–203. ISSN: 1270-9638.
- Apriaskar, E., Nugraha, Y. P., and Trilaksono, B. R. (2017). “Simulation of Simultaneous Localization and Mapping Using Hexacopter and RGBD Camera”. *2nd International Conference on Automation, Cognitive Science, Optics, Micro Electro-Mechanical System, and Information Technology (ICACOMIT) 2017*, pp. 48–53.
- ArduPilot (2016). *ArduPilot: About*. <https://ardupilot.org/index.php/about>. Accessed: 12-03-2021.
- (2020a). *Precision Landing and Loiter with IR-LOCK*. <https://ardupilot.org/copter/docs/precision-landing-with-irlock.html>. Accessed: 13-03-2021.
- (2020b). *Setting up SITL on Windows*. <https://ardupilot.org/dev/docs/sitl-native-on-windows.html>. Accessed: 13-05-2021.
- (2021). *Electro Permanent Magnet Gripper (EPM688)*. <https://ardupilot.org/copter/docs/common-electro-permanent-magnet-gripper.html>. Accessed: 21-05-2021.
- Aschauer, G., Schirrer, A., and Kozek, M. (2015). “Co-Simulation of Matlab and FlightGear for Identification and Control of Aircraft”. 48.1, pp. 67–72. ISSN: 2405-8963. DOI: <https://doi.org/10.1016/j.ifacol.2015.05.071>.
- AZO (2019). *Aluminum - Advantages and Properties of Aluminum*. <https://www.azom.com/article.aspx?ArticleID=1446>. Accessed: 13-07-2021.
- Baddeley, B. (2016). *Which Wireless Tech is Right for You?* <https://hackaday.com/2016/05/05/which-wireless-tech-is-right-for-you/>. Accessed: 13-03-2021.
- Baidya, S., Shaikh, Z., and Levorato, M. (2018). “FlyNetSim: An Open Source Synchronized UAV Network Simulator Based on Ns-3 and Ardupilot”. MSWIM '18, pp. 37–45. DOI: 10.1145/3242102.3242118. URL: <https://doi.org/10.1145/3242102.3242118>.
- Biczyski, M., Sehab, R., Whidborne, J., Krebs, G., and Luk, P. (2020). “Multirotor Sizing Methodology with Flight Time Estimation”. *Journal of Advanced Transportation* 2020.9689604.
- BoM (2020). *Adelaide (Kent Town), South Australia May 2020 Daily Weather Observations*. <http://www.bom.gov.au/climate/dwo/202005/html/IDCJDW5002.202005.shtml>. Accessed: 13-05-2021.
- Bose, M. (2019). *How to Use VirtualBox: Quick Overview*. <https://www.nakivo.com/blog/use-virtualbox-quick-overview/>. Accessed: 13-05-2021.
- BPF (2021). *Acrylonitrile Butadiene Styrene (ABS) and Other Specialist Styrenics*. [https://www.bpf.co.uk/plastipedia/polymers/ABS\\_and\\_Other\\_Specialist\\_Styrenics.aspx](https://www.bpf.co.uk/plastipedia/polymers/ABS_and_Other_Specialist_Styrenics.aspx). Accessed: 13-07-2021.
- Braun, J., Gertz, S. D., Furer, A., Bader, T., Frenkel, H., Chen, J., Glassberg, E., and Nachman, D. (2019). “The Promising Future of Drones in Prehospital Medical Care and its Application to Battlefield Medicine”. eng. *The journal of trauma and acute care surgery* 87.1S, S28–S34. ISSN: 2163-0755.
- Bryceson, K., Borrero, K., Camilleri, C., and Vasuian, F. (2016). “Small Quadcopter Drones as Educational Tools in Agriculture at the University of Queensland”, pp. 8052–8060.
- Coleman, Don, Mistry, Sandeep, and Allan, Alasdair (2015). *Make: Bluetooth*. Make Community, LLC.
- Cruz, P. J. and Fierro, R. (2017). “Cable-suspended load lifting by a quadrotor UAV: hybrid model, trajectory generation, and control”. eng. *Autonomous robots* 41.8, pp. 1629–1643. ISSN: 0929-5593.
- David, Christopher (2021). *Sound Sensor*. <https://diyi0t.com/sound-sensor-arduino-esp8266-esp32/>. Accessed: 13-07-2021.

- Dergachov, K., Bahinskii, S., and Piavka, I. (2020). “The Algorithm of UAV Automatic Landing System Using Computer Vision”. *2020 IEEE 11th International Conference on Dependable Systems, Services and Technologies (DESSERT)*, pp. 247–252. DOI: 10.1109/DESSERT50317.2020.9124998.
- DHL (2021). *DHL’S Parcelcopter: Changing Shipping Forever*. <https://www.dhl.com/discover/business/business-ethics/parcelcopter-drone-technology>. Accessed: 12-03-2021.
- Feist, J. (2018). *How many propellers does your drone need? – how to fly, the science of flight*. <https://dronerush.com/propellers-drone-need-science-of-flight-10733/>. Accessed: 28-04-2021.
- Fogelberg, J. (2013). “Navigation and Autonomous Control of a Hexacopter in Indoor Environments”. ISSN: 0280-5316.
- Frenzel, L. (2017). *UWB for IoT?* <https://www.mwrf.com/technologies/systems/article/21848479/uwb-for-iot>. Accessed: 13-03-2021.
- “Zigbee Wireless Networking” (2008). Ed. by Drew Gislason. Newnes, pp. 45–63.
- Gortolev, M. (2014). *Quadcopter vs Hexacopter vs Octocopter: The Pros and Cons*. <http://dronebly.com/quadcopter-vs-hexacopter-vs-octocopter-the-pros-and-cons>. Accessed: 28-04-2021.
- Guo, M., Gu, D., Zha, W., Zhu, X., and Su, Y. (2020). “Controlling a Quadrotor Carrying a Cable-Suspended Load to Pass Through a Window”. eng. *Journal of intelligent robotic systems* 98.2, pp. 387–401. ISSN: 0921-0296.
- Helipal (2021). *Tarot 680 Pro Hexacopter Build Kit*. <http://www.helipal.com/tarot-fy680-pro-hexacopter-frame-set.html>. Accessed: 13-05-2021.
- HobbyTech (2021a). *TAROT T810 Foldable Hexacopter Frame Kit*. <https://www.hobbytech.com.au/products/rc-multi-rotors/kit-frame/tarot-t810-foldable-hexacopter-frame-kit/>. Accessed: 13-05-2021.
- (2021b). *TAROT T810 Foldable Hexacopter Frame Kit*. <https://hobbyhobby.com/product/362599/tarot-t810-foldable-hexacopter-frame-kit/>. Accessed: 13-05-2021.
- Idres, M., Makame, B., Ahmad, B., Alsubari, S., and Safiuddin, A. (Mar. 2015). “Design, Fabrication and Flight Testing of a Surveillance UAV”. *Advanced Materials Research* Vol 1115, pp 450–453.
- Jasiunas, M. (Nov. 20, 2020). “The Internet of Things: Here, There and Everywhere”. *Defence Science Technology Group*. URL: <https://www.dst.defence.gov.au/news/2020/11/20/internet-things-here-there-and-everywhere> (visited on 03/18/2021).
- Javir, A.W., Pawar, K., Dhudum, S., Patale, N., and Patil, S. (2015). “Design, Analysis and Fabrication of Quadcopter”. *Journal of Advance Research in Mechanical Civil Engineering (ISSN: 2208-2379)* 2.3.
- Kirienko, P. (2018). *OpenGrab EPM v3*. [https://kb.zubax.com/display/MAINKB/OpenGrab+EPM+v3#Mode\\_and%20status%20codes](https://kb.zubax.com/display/MAINKB/OpenGrab+EPM+v3#Mode_and%20status%20codes). Accessed: 21-05-2021.
- Klausen, K., Fossen, T. I., and Johansen, T. A. (2017). “Nonlinear Control with Swing Damping of a Multirotor UAV with Suspended Load”. eng. *Journal of intelligent robotic systems* 88.2, pp. 379–394. ISSN: 0921-0296.
- Kong, W., Zhang, D., Wang, X., Xian, Z., and Zhang, J. (2013). “Autonomous landing of an UAV with a ground-based actuated infrared stereo vision system”. *2013 IEEE/RSJ International Conference on Intelligent Robots and Systems*, pp. 2963–2970. DOI: 10.1109/IROS.2013.6696776.
- Kumar, N., Rajeev, V., Bhuvana, C., and Anushya, S. (2017). “Comparison of ZigBee and Bluetooth wireless technologies-survey”. *2017 International Conference on Information Communication and Embedded Systems (ICICES)*, pp. 1–4. DOI: 10.1109/ICICES.2017.8070716.
- Laboratory, Forest Products (1990). *Wood Engineering Handbook, Second edition*. Prentice Hall.
- Lange, S., Sünderhauf, N., and Protzel, P. (Jan. 2008). “Autonomous Landing for a Multirotor UAV Using Vision”. In *Workshop Proceedings of SIMPAR 2008 Intl. Conf. on Simulation, Modeling and Programming for Autonomous Robots*.
- Lavric, A. and Popa, V. (2017). “A LoRaWAN: Long Range Wide Area Networks Study”. *International Conference on Electromechanical and Power Systems*.
- Lee, J., Su, Y., and Shen, C. (2007). “A Comparative Study of Wireless Protocols: Bluetooth, UWB, ZigBee, and Wi-Fi”. *IECON 2007 - 33rd Annual Conference of the IEEE Industrial Electronics Society*, pp. 46–51. DOI: 10.1109/IECON.2007.4460126.

- Lindsey, Q., Mellinger, D., and Kumar, V. (2012). “Construction with quadrotor teams”. eng. *Autonomous robots* 33.3, pp. 323–336. ISSN: 0929-5593.
- LME (2021). *MQ2 Gas Sensor*. <https://lastminuteengineers.com/mq2-gas-sensor-arduino-tutorial/>. Accessed: 13-07-2021.
- IR-Lock (2021). *IR-LOCK Sensor*. <https://irlock.com/products/ir-lock-sensor-precision-landing-kit>. Accessed: 13-03-2021.
- Magnussen, Ø., Ottestad, M., and Hovland, G. (2015). “Multicopter Design Optimization and Validation”. *Modeling, Identification and Control: A Norwegian Research Bulletin* 36, pp. 67–79.
- Marcon, P., Janousek, J., and Kadlec, R. (2018). “Vision-Based and Differential Global Positioning System to Ensure Precise Autonomous Landing of UAVs”. *2018 Progress in Electromagnetics Research Symposium (PIERS-Toyama)*, pp. 542–546. DOI: 10.23919/PIERS.2018.8598179.
- Marks, A., Whidborne, J. F., and Yamamoto, I. (2012). “Control Allocation for Fault Tolerant Control of a VTOL Octorotor”. *UKACC International Conference on Control 2012*.
- Mckay, M. E., Niemiec, R., and Gandhi, F. (2018). “Analysis of Classical and Alternate Hexacopter Configurations with Single Rotor Failure”. *Journal of Aircraft* 55.6. ISSN: 2372-2379. DOI: <https://doi.org/10.2514/1.C035005>.
- Mercedes (2016). *Vans and Drones in Zurich*. <https://www.mercedes-benz.com/en/vehicles/transporter/vans-drones-in-zurich/>. Accessed: 12-03-2021.
- Müller, M. (2018). *eCalc - the most reliable electric motor calculator on the web for RC pilots*. <https://www.ecalc.ch/>. Accessed: 12-03-2021.
- (2021). *eCalc*. <https://www.ecalc.ch/calcinclude/help/xcoptercalchelp.htm>. Accessed: 13-05-2021.
- NASA (2021). *Glenn Research Center: Specific Thrust*. <https://www.grc.nasa.gov/www/k-12/airplane/specth.html>. Accessed: 13-05-2021.
- Nguyen, H. T., Yang, G., Nielsen, A. H., Jensen, P. H., and Coimbra, C. (2018). “Control parameterisation for POD via software-in-the-loop simulation”. *The 7th International Conference on Renewable Power Generation, Journal of Engineering* 2019.18, pp. 4864–4868. ISSN: 2051-3305. DOI: 10.1049/joe.2018.9331.
- Nguyen, T. H., Cao, M., Nguyen, T., and Xie, L. (2018). “Post-Mission Autonomous Return and Precision Landing of UAV”. *2018 15th International Conference on Control, Automation, Robotics and Vision (ICARCV)*, pp. 1747–1752.
- Notter, S., Heckmann, A., Mcfadyen, A., and Gonzalez, F. (2016). “Modelling, Simulation and Flight Test of a Model Predictive Controlled Multirotor with Heavy Slung Load”. *IFAC* 49 17, pp. 182–187. DOI: 10.1016/j.ifacol.2016.09.032.
- Nowak, E., Gupta, K., and Najjaran, H. (2017). “Development of a Plug-and-Play Infrared Landing System for Multirotor Unmanned Aerial Vehicles”. *14th Conference on Computer and Robot Vision (CRV)*, pp. 256–260.
- Nugraha, Y. P., Ridlwan, H. M., Riansyah, M. I., and Trilaksono, B. R. (2017). “Autonomous Tracking of Hexacopter on Moving Mobile Robot Using Gazebo ROS Simulation”. *Proceedings of the 9th International Conference on Machine Learning and Computing* 2017, pp. 498–501. DOI: <http://dx.doi.org/10.1145/3055635.3056657>.
- Omar, H. M. (2013). “Designing anti-swing fuzzy controller for helicopter slung-load system near hover by particle swarms”. eng. *Aerospace science and technology* 29.1, pp. 223–234. ISSN: 1270-9638.
- Opal-RT (2021). *SOFTWARE-IN-THE -LOOP*. <https://www.opal-rt.com/software-in-the-loop/>. Accessed: 19-04-2021.
- Pluckter, K. and Scherer, S. (2018). *Precision UAV Landing in Unstructured Environments*. Robotics Institute, Carnegie Mellon University, Pittsburgh, PA.
- Plywoods, Austral (2021). *Characteristics of Plywood*. <https://www.australply.com.au/technical/characteristics>. Accessed: 13-07-2021.
- Pounds, P. E., Bersak, D. R., and Dollar, A. M. (2011). “Grasping from the air: Hovering capture and load stability”. eng. *2011 IEEE International Conference on Robotics and Automation*. IEEE, pp. 2491–2498. ISBN: 9781612843865.
- (2012). “Stability of small-scale UAV helicopters and quadrotors with added payload mass under PID control”. eng. *Autonomous robots* 33.1-2, pp. 129–142. ISSN: 0929-5593.

- R., Hernandez, Slaughter, R., Whaley, D., Tate, J., and Asiabanpour, B. (2016). “Analysis the Tensile, Compressive, and Flexural Properties of 3D Printed ABS P430 Plastic Based on Printing Orientation Using Fused Deposition Modeling”. eng. *Solid Freeform Fabrication Symposium – An Additive Manufacturing Conference*. Ingram School of Engineering, Texas State University, pp. 939–950.
- Ray, B. (2015). *A Bluetooth ZigBee Comparison For IoT Applications*. <https://www.link-labs.com/blog/bluetooth-zigbee-comparison>. Accessed: 13-03-2021.
- Reid, J. (2019). *Multicopter Motor Guide*. <https://www.rotordronepro.com/guide-multicopter-motors/>. Accessed: 10-03-2021.
- Riansyah, M. I., Nugraha, Y. P., Ridlwan, M. H., and Trilaksono, B. R. (2017). “3D Mapping Hexacopter Simulation using Gazebo and Robot Operating System (ROS)”. *Proceedings of the 9th International Conference on Machine Learning and Computing 2017*, pp. 507–510. DOI: <http://dx.doi.org/10.1145/3055635.3056659>.
- Ribeiro, L. R. and Oliveira, N. M. (2010). “UAV autopilot controllers test platform using Matlab/Simulink and X-Plane”, S2H-1-S2H-6. DOI: 10.1109/FIE.2010.5673378.
- Ridlwan, H. M., Nugraha, Y. P., Riansyah, M. I., and Trilaksono, B. R. (2017). “Simulation of Vision-Based For Automatic Takeoff and Landing Hexacopter on a Moving Ground Vehicle”. *Proceedings of the 9th International Conference on Machine Learning and Computing 2017*, pp. 502–506. DOI: <http://dx.doi.org/10.1145/3055635.3056657>.
- Safadinho, D., Ramos, J., Ribeiro, R., Filipe, V., Barroso, J., and Pereira, A. (2020). “UAV Landing Using Computer Vision Techniques for Human Detection”. *Sensors* 20.3.
- Saikin, D. A., Baca, T., Gurtner, M., and Saska, M. (2020). “Wildfire Fighting by Unmanned Aerial System Exploiting Its Time-Varying Mass”. eng. *IEEE robotics and automation letters* 5.2, pp. 2673–2680. ISSN: 2377-3766.
- Slamich, M. (2020). *Bluetooth vs Ultra-Wideband*. <https://www.pointr.tech/blog/bluetooth-vs-ultra-wideband-which-technology-to-use-for-indoor-location>. Accessed: 25-04-2021.
- Sreenath, K., Michael, N., and Kumar, V. (2013). “Trajectory generation and control of a quadrotor with a cable-suspended load - A differentially-flat hybrid system”. eng. *2013 IEEE International Conference on Robotics and Automation*. IEEE, pp. 4888–4895. ISBN: 1467356417.
- Szyk, B. (2018). *Drone Motor Calculator*. <https://www.omnicalculator.com/other/drone-motor>. Accessed: 12-03-2021.
- T-Motor (2019a). *MN4010 KV370*. <https://store-en.tmotor.com/goods.php?id=341>. Accessed: 13-05-2021.
- (2019b). *T-Motor: MN4010 KV580*. <https://store-en.tmotor.com/goods.php?id=343>. Accessed: 13-05-2021.
- Tengfei, S., Pengfei, M., Xin, J., Ximao, C., and Xinhui, D. (2016). “Proceedings of the 2016 International Conference on Advanced Electronic Science and Technology (AEST 2016)”, pp. 881–890.
- Tucakov, D. (2020). *How to Install Ubuntu 20.04 LTS Desktop (Focal Fossa)*. <https://phoenixnap.com/kb/install-ubuntu-20-04>. Accessed: 13-05-2021.
- UPS (2017). *UPS Flight Forward Drone Delivery*. <https://www.ups.com/us/en/services/shipping-services/flight-forward-drones.page#:~:text=UPS%20has%20tested%20launching%20drones,driver%20continues%20along%20the%20route..> Accessed: 12-03-2021.
- Verma, A. (2020). *All about HC-05 Bluetooth Module*. <https://www.geeksforgeeks.org/all-about-hc-05-bluetooth-module-connection-with-android/>. Accessed: 02-05-2021.
- Villa, D. K., Brandão, A. S., and Sarcinelli-Filho, M. (2020). “A Survey on Load Transportation Using Multicopter UAVs”. eng. *Journal of intelligent robotic systems* 98.2, pp. 267–296. ISSN: 0921-0296.
- Vissarion, Y. (2020). *Virtual Machine and its Benefits | Parallels Insights*. <https://www.parallels.com/blogs/ras/virtual-machine/>. Accessed: 13-05-2021.
- Wallich, P. (2012). “Arducopter parenting”. *IEEE Spectrum* 49.12, pp. 26–28. DOI: 10.1109/MSPEC.2012.6361754.
- Wubben, J., Fabra, F., Calafate, C. T., Krzeszowski, T., Marquez-Barja, J. M., J.Cano, and Manzoni, P. (2019). “Accurate Landing of Unmanned Aerial Vehicles Using Ground Pattern Recognition”. *Electronics* 8.1532.

- Yang, Y., Wang, W., Iwakura, D., Namiki, A., and Nonami, K. (2016). “Sliding Mode Control for Hexacopter Stabilization with Motor Failure”. *Journal of Robotics and Mechatronics* 28.6, pp. 936–948. ISSN: 1883-8049. DOI: <https://doi.org/10.20965/jrm.2016.p0936>.
- Yoo, W., Yu, E., and Jung, J. (2018). “Drone delivery: Factors affecting the public’s attitude and intention to adopt”. eng. *Telematics and informatics* 35.6, pp. 1687–1700. ISSN: 0736-5853.
- Yu, Y., Zheng, L., Zhu, J., Cao, Y., and Hu, B. (2018). “Technology of short-distance wireless communication and its application based on equipment support”. *AIP Conference Proceedings* 1955.1.
- Yudho, B., Heryanto, M., Suprijono, H., Muliadi, J., and Kusumoputro, B. (2017). “Design and development of heavy-lift hexacopter for heavy payload”, pp. 242–247.
- Zigbee (2021). *Zigbee FAQ*. <https://zigbeealliance.org/zigbee-faq/#:~:text=Transmission%20distances%20range%20from%2010,in%20the%202.4GHz%20band..> Accessed: 13-03-2021.

## Appendix A Project Objectives

### A.1 Objective 1 - Flyable UAV

#### A.1.1 Specific

Developing a stable, controllable and repeatable flying regime for the towed payload UAV configuration. This will involve the research and integration of a general, multirotor control architecture and its modification to support the towed payload configuration in all three flight states: take-off, airborne movement, and landing.

#### A.1.2 Measurable

The UAV must sustain stable and controlled flight for at least 10 minutes and at an altitude of at least 10m, and radially away from the grounded control station. Testing these benchmarks will require UAV control by an individual holding a CASA Remote Pilot Licence and the reservation and use of UAV-approved airspace.

#### A.1.3 Attainable

The viability of this objective relies on the integration of a general, multirotor control architecture and a specialised, towed payload control architecture. The former will be highly achievable as it is supported by significant open-source research and proven examples, whilst the latter will require additional theoretical knowledge and programming to implement, making this objective moderately attainable. Multirotors are capable of flying in trim with payloads offset from the centre of gravity (Pounds et al., 2012)

#### A.1.4 Relevance

The stable and controlled flight of the UAV is essential to addressing Expected Outcome 1 and Objective 2.

#### A.1.5 Timeframes

This objective will be completed by the 5th of September, 2021.

### A.2 Objective 2 - Transport of a Payload

#### A.2.1 Specific

Controlling the multirotor UAV to pickup, carry and deposit the modular IoMT payload from one ground location to another. This behaviour will be achieved independently of any manual human interaction between the UAV or payload and will not impede the normal performance of either the UAV or payload.

#### A.2.2 Measurable

The payload must be transported 100m linearly (parallel to ground surface) from one ground location to another ground location. The payload must not sustain any damage that deteriorates its communication performance, structural integrity, or ability to be transported to another location.

#### A.2.3 Attainable

Parcel delivery systems such as those demonstrated by Amazon Prime Air (Amazon 2016), UPS (UPS 2017), Mercedes (Mercedes 2016), and DHL (DHL 2021) have achieved ranged transport of payloads. The Amazon Prime Air and DHL services prove that automatic payload collection and depositing is possible with the support of significant mechanical infrastructure. Due to this additional complexity, this objective is classified as moderately attainable.

#### **A.2.4 Relevance**

The physical transportation of the payload addresses Expected Outcome 1 and supports the completion of Objective 3.

#### **A.2.5 Timeframes**

This objective will be completed by the 9th of September, 2021.

### **A.3 Objective 3 - UAV, Payload and Ground Station Communication**

#### **A.3.1 Specific**

This objective seeks to achieve real-time communication between the payload and the vehicle, and between the vehicle and a ground station. As the payload will be a modular, self-operable IoMT device, the communication between the vehicle and the payload will service as an interface for the vehicle to subscribe to the information gathered by the payload. For example, if the payload is a smoke detector, the vehicle will communicate with the payload in order gain an update on the status of how the smoke detector is responding. This information, as well as UAV flight telemetry data, such as GPS positional information, will be relayed to the ground station.

#### **A.3.2 Measurable**

As the communication between the payload and the vehicle will only occur whilst the payload is attached, the measurable communication distance is within 1m. The communication between the ground station and the vehicle must occur throughout the entire flight. As outlined in Objective 1, the expected range of flight is 100m, thus, the ground station-UAV communication must span 100m.

#### **A.3.3 Attainable**

As discussed in Section 3, short- and long-range communication is achievable through various technologies. The communication between the UAV and payload, and UAV and ground station will be achieved through radio frequency transmission. Another potential method for short-range communication between the UAV and payload is wired communication.

#### **A.3.4 Relevance**

This objective directly relates to the communication aspect of the aim in which the aerial system can communicate with modular, self-operable, IoMT devices in real-time.

#### **A.3.5 Timeframes**

This objective will be completed by the 30th of July.

### **A.4 Objective 4 - Independent Operation of the IoMT Payload**

#### **A.4.1 Specific**

The IoMT payload must be able to function in the absence of the UAV. That is, the device must be able to perform its intended purpose, such as sensing, when it is not acting as a payload to the UAV. Similarly, when apart from the UAV, the IoMT device must be able to perform IoT functionality. Namely, the device must be able to collect data and connect wirelessly to a network.

#### **A.4.2 Measurable**

In order to verify the functionality of the IoMT devices, they must be tested in absence of the UAV. Specifically, the sensing functionality of sensors will be tested when the device is detached from the UAV and the short-range communication functionality will be verified using an IoT receiving compatible device other than the UAV.



### **A.4.3 Attainable**

For off-the-shelf IoT compatible devices, it is important to regularly test their functionality to ensure they are in working order. For microcontroller compatible devices, it is critical to first ensure that they are IoT operable before equipping them to the UAV. This guarantees that they maintain IoT functionality and are not reliant on the vehicle.

### **A.4.4 Relevance**

This objective will address the self-operable IoMT device part of the aim.

### **A.4.5 Timeframes**

This objective will be completed by the 30th of June.

## **Appendix B Stakeholders**

### **B.0.1 The University of Adelaide (UoA)**

The University of Adelaide is a key internal stakeholder of this project as they provide financial support and technical assistance/resource provision. Financial support includes \$200 student within the Honours Team 3296, whilst the technical assistance/resource provision includes workshop manufacturing training and use, equipment storage, and testing facilities. The University is interested in the development of the student's engineering competencies according to the Australian Qualifications Framework Level 8 and the Engineers Australia Stage 1 Competency Standard, and the potential reputation gain associated with the successful completion of this project.

### **B.0.2 Australian Department of Defence (ADoD)**

The Australian Department of Defence is an external stakeholder of this project who represent the clientele that may apply the project outcomes in real-world, defence-related scenarios. Such clientele are interested in the deployment practicality of this project with an emphasis on factors such as life-cycle cost, ease of integration, and maintenance requirements.

### **B.0.3 Defence Science and Technology Group (DSTG)**

The Defence Science and Technology Group, represented by Mr. David Roberts, are a major external stakeholder in this project. They have provided sponsorship for the project in the form of financial support, flight testing facilities and project management assistance. DSTG is invested in the Defence-related research outcomes of this project.

### **B.0.4 Multirotor Advisor (MA)**

The Project's multirotor advisor, Mr. Steele Phillips, is a Satellite Navigation Electronic Warfare Engineer at DSTG who will provide informal and occasional advice regarding the design, assembly, storage, and safety of the UAV platform. He is a relatively passive internal stakeholder and is interested in the development of a UAV platform that can be upgraded/modified in the future, and the acquisition of the UAV platform after the completion of the project.

### **B.0.5 Project Supervisor (PS)**

The Project's supervisor, Assoc. Prof. Rini Akmeliawati, is a crucial internal stakeholder as she will provide formal and frequent advice regarding the management of deliverables, technical assistance, and act as an interface to other University contacts and industry professionals. She is interested in the development of the student's engineering abilities and the completion of an innovative project with potential for future research.

### B.0.6 Honours Team 3296 (HT3296)

The Honours Team 3296 consists of the students: Daniel O'Connor, Patrick Capaldo, and Jason Huynh as critical internal stakeholders. The team has the most significant interest and power over the actions and outcomes of the project. Communication between the team and the internal stakeholders, as well as consideration of external stakeholders, is crucial to ensure the project remains within scope, time-frames, and delivers the expected outcomes.

Refer to Figure 38 to observe the relationship of power versus interest for each aforementioned stakeholder.

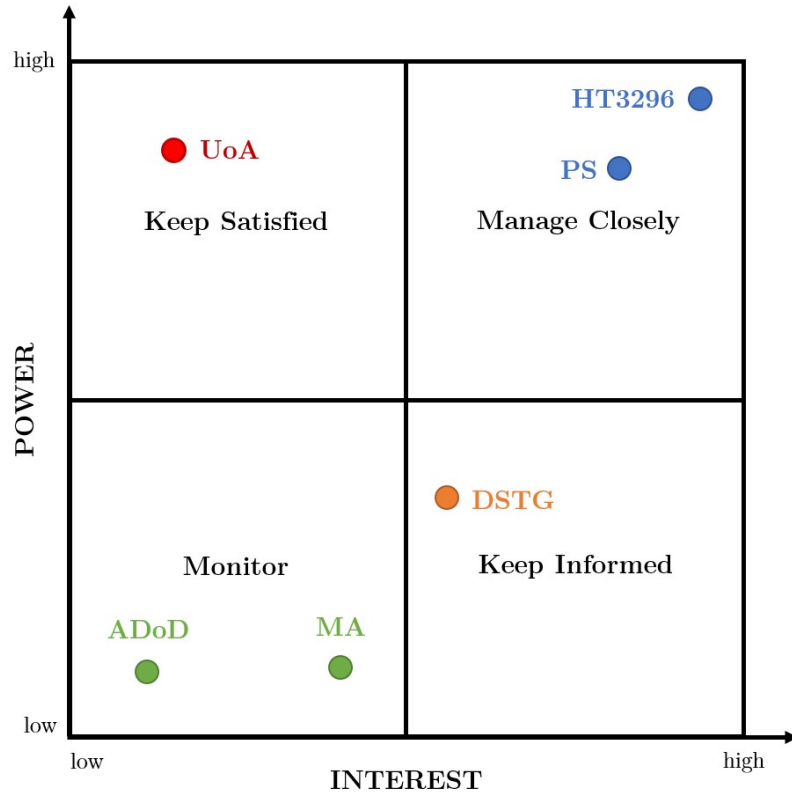


Figure 38: Power map of the six key stakeholders for this project.

## **Appendix C Project Failure Assessment**

In order to maintain system requirement and project objective quality, various project risks are identified which may hinder project success. Numerous mitigation strategies are developed in order to avoid minimise the impact of these risks.

Table 18: Project risks.

Code	Risk	Backward Traceability
R-01	The coronavirus pandemic causes widespread lock-downs resulting in the university shutting down indefinitely.	O-1, O-2, O-3, O-4
R-02	The project exceeds the allocated budget by the university and the sponsor resulting in an inability to fund components, necessary software, manufacturing processes and administration requirements.	O-1, O-2, O-3, O-4
R-03	The project exceeds the allocated deadline by the university for project delivery resulting in an improbable timeframe to complete components of the project.	O-1, O-2, O-3, O-4
R-04	Components necessary for manufacture of the UAV or payload experience long shipping delays which may ultimately delay the delivery of the project.	O-1, O-2, O-3, O-4
R-05	Malfunctioning electronic components in the UAV, IoMT payload or ground station communications system resulting in damage that cannot be quickly repaired.	O-1, O-2, O-3, O-4
R-06	Delays experienced in acquiring UAV flying licence by project team preventing the flight of vehicle.	O-1, O-2
R-06	Insufficient computing power to efficiently perform flight dynamics and calculations resulting in delayed flight decision making and ultimately inaccurate flight.	O-1
R-07	Radio frequency interference in short- or long-range communications paradigms resulting in inaccurate transmission and reception.	O-3
R-08	Guided landing system interference resultant of weather and environment conditions resulting in inaccurate identification of payload target. That is, light interference with cameras and infrared sensors.	O-2
R-09	Insufficient battery capacity during flight resulting in mid-flight low battery.	O-1, O-2, O-3
R-10	Helicopter rotors unable to provide sufficient lift due to mass and aerodynamic hindrances.	O-1, O-2
R-11	Mid-flight payload grasping system failure resulting in potential dropping of the payload.	O-2
R-12	Improper flying conditions resulting in significant flight disturbances which greatly impact the flight control system.	O-1
R-13	Mid-flight loss of UAV GPS location resulting in unknown position and therefore unknown navigation to target	O-1
R-14	Arrival at expected target location according to GPS positional data but undetected target by sensors thus creating confusion as to whether the UAV is near the target or not.	O-2
R-15	IoMT data not being received by UAV or any any IoT capable communications receiver.	O-3, O-4
R-16	Payload geometry incompatible with grasping mechanism resulting in inability to pick up payload.	O-2
R-17	Payload mass destabilises control of UAV resulting in inaccurate positional tracking and ill executed navigation.	O-1, O-2

Table 19: Risk mitigation strategies.

Code	Strategy	Mitigation	Backward Traceability
M-01	Reduction	Project work will continue from home and all meetings will be held virtually. If a state-wide lockdown is eminent, one member of the project team will be assigned to perform all ongoing manufacturing henceforth to avoid social contact. This will continue until restrictions are lifted.	R-01
M-02	Reduction, Transferral	Initial attempts to cut unnecessary costs will be made. If this is unsuccessful, discussions with the sponsor and university will occur to discuss the potential for an increased budget.	R-02
M-03	Reduction, Acceptance	As deadlines are approaching, time budgeting and increased project team work rate is necessary. If the deadline has passed, discussions will occur with project stakeholders regarding extending the deadline. If this is not possible, the current project state will be submitted.	R-03
M-04	Avoidance, Reduction	Parts to be ordered significantly in advance to avoid delays in component arrival. If delays are eminent, alternative sourcing arrangements will be investigated.	R-04
M-05	Avoidance	The electrical components will be tested and verified by University of Adelaide workshop staff prior to being installed in the UAV or communications infrastructure.	R-05
M-06	Transferral	A DSTG representative with an existing UAV flight licence will perform all flight testing required until a licence is acquired by a project team member.	R-06
M-07	Avoidance	All flight and transportation testing to be performed a significant distance from other sources of electromagnetic radiation to prevent radio frequency interference.	R-07
M-08	Avoidance	All flight testing will occur in clear, low wind weather with no glaring sunlight to avoid the potential for light and wind interference.	R-08, R-12
M-09	Avoidance	Fully-charged spare batteries on standby to prevent a situation where there is insufficient battery life. Moreover, the UAV will be in flight for no more than 80% of its expected battery life.	R-09
M-10	Avoidance	The flight dynamics shall be adequately modelled and calculated in order to ensure the system is operable before testing occurs.	R-10
M-11	Avoidance, Reduction	The grasping system is to be tested under strenuous circumstances to masses greater than that of the payloads in order to maintain confidence in its grasping ability. In the instance that it fails mid-flight, a parachute is to be deployed on the payload to minimise damage caused.	R-11
M-12	Reduction	The UAV shall remain stationary until GPS location has been received. If this does not occur after a period of time, the UAV shall make a slow descent until ground is reached.	R-13
M-13	Reduction	The UAV shall remain stationary and continue to search for the target using its sensors. If this does not occur after a period of time, the UAV shall make a slow descent until ground is reached.	R-14
M-14	Avoidance	The IoT functionality of the device shall be tested prior to flight to ensure it is operational and able to transmit data.	R-15
M-15	Avoidance	Within proof of concept paradigm, design payload and grasping for one orientation.	R-16
M-16	Avoidance	Design UAV to be compatible with various heavy payloads in line with the modular IoMT concept.	R-17

Table 20: Risk criticality matrix defined by likelihood and consequences for a project risk.

<b>Likelihood</b>	<b>Consequence</b>				
	Negligible	Minor	Modest	Major	Catastrophic
Probable	Low	Medium	Medium	High	High
Highly Likely	Low	Medium	Medium	High	High
Likely	Low	Low	Medium	Medium	Medium
Improbable	Low	Low	Low	Medium	Medium
Rare	Low	Low	Low	Low	Low

Table 21: Risk evaluation impacts.

<b>Risk</b>	<b>Likelihood</b>	<b>Consequence</b>	<b>Criticality</b>	<b>Mitigation</b>	<b>Final Criticality</b>
R-01	Likely	Major	Medium	M-01	Low
R-02	Improbable	Catastrophic	Medium	M-02	Medium
R-03	Improbable	Catastrophic	Medium	M-03	Medium
R-04	Likely	Major	Medium	M-04	Low
R-05	Likely	Major	Medium	M-05	Low
R-06	Likely	Catastrophic	High	M-06	Medium
R-07	Rare	Minor	Low	M-07	Low
R-08	Likely	Minor	Low	M-08	Low
R-09	Improbable	Major	Medium	M-09	Low
R-10	Improbable	Modest	Low	M-10	Low
R-11	Improbable	Major	Medium	M-11	Low
R-12	Likely	Modest	Medium	M-08	Low
R-13	Improbable	Major	Medium	M-13	Low
R-14	Improbable	Modest	Low	M-14	Low
R-15	Improbable	Minor	Low	M-15	Low

## **Appendix D Risk Assessments and Safe Operating Procedures**

For each test performed throughout the project, Risk Assessments and Safe Operating Procedures are prepared in order to ensure the safety of all participants involved with the testing. Moreover, the Risk Assessments and Safe Operating Procedures also provide a framework to ensure the safety of the equipment and any other external parties.

## HAZARD MANAGEMENT – SAFE OPERATING PROCEDURE (SOP)

**Only to be completed where required as a control measure under a Risk Assessment**

<p>A document setting out the requirements to carry out the work in a safe and healthy manner and in a logical sequence.</p> <p>It must be able to be easily read by those who need to know what has been planned.</p> <p>It is relevant to the following people:</p> <ul style="list-style-type: none"> <li>the worker carrying out the work; and</li> <li>the person who has management and control over the work.</li> </ul>	<p>A SOP, if identified as a control measure, is to:</p> <ul style="list-style-type: none"> <li>identify the work;</li> <li>specify/address the identified hazards relating to the work;</li> <li>describe the measures to be implemented to control the risks;</li> <li>take into account the circumstances at the workplace that may affect the way in which the work is carried out;</li> <li>take into account emergency management arrangements where applicable; and</li> <li>be communicated to all workers who carry out the work.</li> </ul>
---	---

<b>NAME OF THE TASK/ACTIVITY</b>	UAV PHORESIS HONOURS PROJECT	<b>DATE:</b> 07/09/2021
<b>LOCATION</b>	DST GROUP EDINBURGH	Insert photo (Optional)
<b>RISK ASSESSMENT (RA) NAME</b>	INDOOR FLIGHT TRIAL AND PAYLOAD TRANSPORTATION VERIFICATION	
<b>Residual risk rating on the RA</b>	<input checked="" type="checkbox"/> Low <input type="checkbox"/> Medium <input type="checkbox"/> High <input type="checkbox"/> Very High	
<b>Hazards identified on the RA</b>	TRIP, ELECTRIC SHOCK, LIPO BATTERY FIRE, SHARP CORNERS, COMMUNICATION INTERFERENCE	

**PERSONAL PROTECTIVE EQUIPMENT (BE SPECIFIC AND SPECIFY PPE TO BE WORN DURING THE TASK)  
(DELETE THE ROW IF NOT APPLICABLE)**



- Enclosed footwear:     Footwear that is resistant to spills of hazardous substances     Boots with steel caps  
 Other:

**DESCRIBE, IN SEQUENCE, STEPS TO COMPLETE THE ACTIVITY SAFELY**

**Pre-operational checks**

1. Ensure no uncontained liquids are nearby
2. Ensure no visible damage or faults to circuitry
3. Tripping hazards are eliminated

**Operational checks/steps to complete the activity from start to finish (including transport and waste disposal where relevant)**

1. Physically pre-arm UAV with on-board safety switch inside flight arena
2. All personnel to vacate flight arena after pre-arming of UAV
3. UAV is remotely armed after personnel have vacated flight arena
4. Monitor appropriate functioning of all systems
5. Ensure no persons are touching the magnet when magnetising or degmatising to avoid electric shock
6. Ensure UAV is operated by CASA certified drone pilot

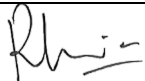
**On completion of work – steps to make safe (including clean up, any waste disposal & service/maintenance requirements)**

1. Ensure termination procedure is as expected
2. Remotely disarm UAV before any personnel enter flight arena
3. LiPo batteries stored in fireproof bags
4. UAV propellers removed and sheathed

**Emergency and Spill Procedures, Transport or storage requirements (where relevant), First aid/Medical**

1. If a spill is to occur, terminate device immediately and remove from area
2. If any personnel enter flight arena, activate emergency "kill" switch on UAV remote controller to de-activate propellers

**Prepared by**

People involved in the drafting of this SOP	D. O'CONNOR, J. HUYNH, P. CAPALDO		
Person authorising the SOP	Name:	R. AKMELIAWATI	Signature
	Position:	PROJECT SUPERVISOR AND ASSOCIATE PROFESSOR SCHOOL OF MECHANICAL ENGINEERING	

**This SOP must be reviewed after any incident/injury associated with this activity or when a Risk assessment is reviewed.**

File your completed SOP as instructed by the Supervisor/Person in control of the area/activity and retain the SOP in accordance with the State Records of SA, General disposal [Schedule](#) No. 30 issued under the State Records Act 1997. (Contact the University's [Records Management Office](#) for further assistance/information if required.)

HSW Handbook	Hazard Management	Effective Date:	1 December 2020	Version 4.0
Authorised by	Chief Operating Officer (University Operations)	Review Date:	1 December 2023	Page 1 of 1
Warning	This process is uncontrolled when printed. The current version of this document is available on the HSW Website.			



## HAZARD MANAGEMENT – RISK ASSESSMENT

This template or equivalent template can be used

Date: 15/04/2021

### MULTIPLE TASKS

(If you have not completed a risk assessment before refer to the [Handbook Chapter Appendix A](#) for guidance)

#### RECORD THE HIGHEST RESIDUAL RISK RATING

Ensure the appropriate level of authority to complete the activity can be evidenced. (e.g. a signature or formal approval attached)

- Low
- Medium
- High
- Very high

<b>Physical location(s) or Operational unit:</b>	<b>DST GROUP EDINBURGH</b>
<b>Names of workers involved in completing the risk assessment</b>	D. O'CONNOR, J. HUYNH, P. CAPALDO

#### **Supervisors/person in control of the area/activity**

- Ensure that the control measures address the hazards identified for each step in the process for this task.
- Ensure that there is a system for retaining this Risk assessment. (See section 5.1 of the Handbook chapter)
- Ensure that workers who undertake this task have access to this Risk assessment, are provided with the relevant, information, instruction and training required before they undertake the task. (This includes any other guidance material (e.g. Safe operating procedures) where required by this Risk assessment.)
- Ensure that if there is a requirement for instruction (Level 2 proficiency) and/or training (Level 3 competency/qualification) the information is added to the Training plan.

#### **Standard controls for this location** (e.g. Lab/workshop rules) (See definitions for information on [control banding](#))

The control measures listed must be applied by all workers when entering the location regardless of whether they are completing the task. The control measures must be specific. They do not need to be repeated under each task below.


DSTG rules apply at all times and all personnel must abide by any and all security procedures. All DSTG flight arena Safe Operating Practices also apply and must be abided by.

Hazard identification: Stop and think. What could cause harm from start to finish?	Assess the harm	What needs to be in place before you start?	Re-assess the level of risk
Identify and list each hazard that is part of this work process	Record how/when the worker is exposed to the hazard (e.g. what is the route of exposure when completing the task)	Calculate the risk rating without controls in place (See descriptor table overleaf)	The measures you select must address the hazard, be selected in accordance with the Hierarchy of Control and be clear to the worker. (Refer to the Hierarchy of Control <a href="#">Appendix A</a> page 6 for guidance.)
			i.e. the residual risk rating after controls are in place

Task 1:	Setting up of UAV			
<b>Arming of UAV</b>	Trip, shock, and collision hazard due to potential rotating propellers or magnetising and demagnetising magnet	<input checked="" type="checkbox"/> Low <input checked="" type="checkbox"/> Medium <input type="checkbox"/> High <input type="checkbox"/> Very high	<b>Physically pre-arm UAV inside the flight arena (one operator only), then all personnel to vacate flight arena, remotely arm the UAV using UAV remote controller</b>	<input checked="" type="checkbox"/> Low <input type="checkbox"/> Medium <input type="checkbox"/> High <input type="checkbox"/> Very high

Appendix B2 (Page 2 of 2)

Hazard identification: Stop and think. What could cause harm from start to finish?		Assess the harm	What needs to be in place before you start?	Re-assess the level of risk
Identify and list each hazard that is part of this work process	Record how/when the worker is exposed to the hazard (e.g. what is the route of exposure when completing the task)	Calculate the risk rating without controls in place (See descriptor table overleaf)	The measures you select must address the hazard, be selected in accordance with the Hierarchy of Control and be clear to the worker. (Refer to the Hierarchy of Control <a href="#">Appendix A</a> page 6 for guidance.)	i.e. the residual risk rating after controls are in place
<b>Task 2:</b>		<b>Flight of UAV</b>		
<b>Uncontrolled flight of UAV</b>	<b>Operator losing control of UAV during flight and risking potential collision</b>	<input type="checkbox"/> Low <input checked="" type="checkbox"/> Medium <input type="checkbox"/> High <input type="checkbox"/> Very high	<b>Ensure all operators are CASA certified flight pilots</b> <b>Ensure no personnel are inside flight arena after pre-arming of UAV</b>	<input checked="" type="checkbox"/> Low <input type="checkbox"/> Medium <input type="checkbox"/> High <input type="checkbox"/> Very high
<b>Personnel enter flight arena during flight</b>	<b>Personnel risking potential collision with UAV</b>	<input type="checkbox"/> Low <input checked="" type="checkbox"/> Medium <input type="checkbox"/> High <input type="checkbox"/> Very high	<b>Ensure no personnel are inside flight arena after pre-arming of UAV</b> <b>If any personnel are to enter flight arena, activate "kill" switch on UAV remote controller to de-activate propellers</b>	<input checked="" type="checkbox"/> Low <input type="checkbox"/> Medium <input type="checkbox"/> High <input type="checkbox"/> Very high
<b>Task 3:</b>		<b>Shut-down of UAV</b>		
<b>Personnel enter flight arena</b>	<b>Personnel risking potential collision with UAV</b>	<input checked="" type="checkbox"/> Low <input type="checkbox"/> Medium <input type="checkbox"/> High <input type="checkbox"/> Very high	<b>Ensure UAV is remotely disarmed before any personnel enter flight arena</b> <b>If any personnel are to enter flight arena, activate "kill" switch on UAV remote controller to de-activate propellers</b>	<input checked="" type="checkbox"/> Low <input type="checkbox"/> Medium <input type="checkbox"/> High <input type="checkbox"/> Very high
<b>Removal of LiPo batteries from UAV</b>	<b>LiPo battery fire</b>	<input checked="" type="checkbox"/> Low <input type="checkbox"/> Medium <input type="checkbox"/> High <input type="checkbox"/> Very high	<b>Ensure batteries are placed in fireproof bags after removing from UAV</b>	<input checked="" type="checkbox"/> Low <input type="checkbox"/> Medium <input type="checkbox"/> High <input type="checkbox"/> Very high

Authorisation for staff and student related tasks			
Residual risk rating	Authorisation	Name and signature (or attach evidence of authorisation)	
Low & medium risk	Supervisor/Person in control of the area/activity	R. AKMELIAWATI	
High risk	Head of School/Branch		
Very high risk	Executive Dean/Divisional Head		

HSW Handbook	Hazard Management	Effective Date:	1 December 2020	Version 4.0
Authorised by	Chief Operating Officer (University Operations)	Review Date:	1 December 2023	Page 2 of 3
Warning	This process is uncontrolled when printed. The current version of this document is available on the HSW Website.			

**Proof of hazard identification and risk assessment is required for this task**

- File your completed Risk assessment as instructed by the Supervisor/Person in control of the area/activity
- Ensure there is a system for retaining formal Risk assessments in accordance with the State Records of SA, General disposal [Schedule No. 30](#) issued under the State Records Act 1997. (Contact the University's [Records Management Office](#) for further assistance/information if required.)

**For activities with a Residual risk rating of high or very high risk**

- The Head of School/Branch or Executive Dean/Divisional Head is to raise a risk under the [University's Risk management framework](#) through the [University Risk Register](#).

**DESCRIPTORS FOR ASSESSING THE LEVEL OF RISK**

Assess the level of risk based on the likelihood of an incident occurring and the consequence			
Likelihood Table		Consequences Table	
<b>Almost certain</b>	There is an expectation that an event/incident will occur.	<b>Severe</b>	Injury resulting in death, permanent incapacity.
<b>Likely</b>	There is an expectation that an event/incident <b>could occur</b> but not certain to occur.	<b>Major</b>	Injury requiring extensive medical treatment (e.g. hospitalisation) or activities could result in a Notifiable occurrence.
<b>Possible</b>	This expectation lies somewhere in the midpoint between "could" and "improbable".	<b>Moderate</b>	Injury requires formal medical treatment (e.g. hospital outpatient/doctors visit).
<b>Unlikely</b>	There is an expectation that an event/incident is doubtful or <b>improbable</b> to occur.	<b>Minor</b>	Injury requires first aid treatment.
<b>Rare</b>	There is no expectation that the event/incident will occur.	<b>Negligible</b>	Injury requires minor first aid (e.g. bandaid), short term discomfort (e.g. bruise, headache), no medical treatment.

The level of risk will increase as the likelihood of harm and its severity increases										
Likelihood of exposure	Consequences – level of seriousness of the injury following exposure to the hazard(s) -									
	Negligible		Minor		Moderate		Major		Severe	
Almost certain	<input type="checkbox"/>	Medium	<input type="checkbox"/>	High	<input type="checkbox"/>	Very High	<input type="checkbox"/>	Very High	<input type="checkbox"/>	Very High
Likely	<input type="checkbox"/>	Medium	<input type="checkbox"/>	Medium	<input type="checkbox"/>	High	<input type="checkbox"/>	Very High	<input type="checkbox"/>	Very High
Possible	<input type="checkbox"/>	Low	<input type="checkbox"/>	Medium	<input type="checkbox"/>	High	<input type="checkbox"/>	High	<input type="checkbox"/>	Very High
Unlikely	<input type="checkbox"/>	Low	<input type="checkbox"/>	Low	<input type="checkbox"/>	Medium	<input type="checkbox"/>	Medium	<input type="checkbox"/>	High
Rare	<input type="checkbox"/>	Low	<input type="checkbox"/>	Low	<input type="checkbox"/>	Low	<input type="checkbox"/>	Medium	<input type="checkbox"/>	Medium

HSW Handbook	Hazard Management	Effective Date:	1 December 2020	Version 4.0
Authorised by	Chief Operating Officer (University Operations)	Review Date:	1 December 2023	Page 3 of 3
Warning	This process is uncontrolled when printed. The current version of this document is available on the HSW Website.			

## Appendix E IoMT Payload Iterative Development

The first stage in the two device Bluetooth HC-05 connection is the establishment of the master-slave hierarchy. Although the master-slave hierarchy is more significant when connecting with numerous devices, it is still a requirement for HC-05 connectivity. The HC-05 is initially connected to an Arduino Uno by connecting the HC-05 VCC and ground pins to the Arduino 5V and ground ports, respectively. The TX and RX pins on the HC-05 are connected to the opposite RX and TX ports on the Arduino. Through the Arduino IDE Serial Monitor, which allows for commands to be sent directly to the HC-05 module from the user, the HC-05 is set to initialisation mode and the two devices are paired. In the pairing of the devices, one is selected to be the master and the other the slave. In this hierarchy, a master can communicate to numerous slaves whereas a slave can only communicate to its master.

The next iteration in HC-05 connection is Boolean communication between the devices whilst connected to a fixed-location power source, such as a computer. In the initial stages, the power source used is a computer connected to the Arduino Uno through an ethernet cable. Boolean communication is achieved through the implementation of a button on each device's circuitry. The button is connected to an Arduino Uno digital input port and thus when it is pressed, the Arduino reads a "1" and when it is not pressed, the Arduino reads a "0". As the two devices maintain a connection, this Boolean input can be communicated from one device to the other through a selected baud rate. The baud rate determines the speed at which information is transferred. In order to maintain stable communication, both devices must send and receive at the same baud rate. The HC-05 default baud rate for Bluetooth communication is 9600. In order to demonstrate when a Boolean signal has been received by the second device, each device has an LED which is connected to an Arduino digital output port where the output port state is set to whatever signal is being received. Hence, when a button is pressed on one device, a "1" signal is transmitted to the other device. Upon receipt of the message, the output of the LED is set to "1" thus turning it on. The physical implementation of this iteration is demonstrated in Figure 39.

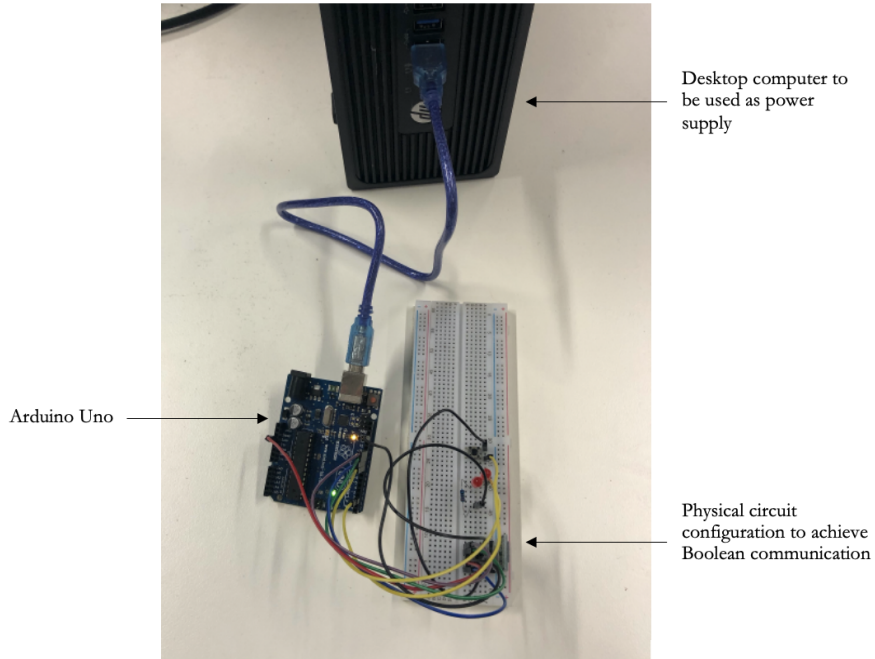


Figure 39: Physical implementation of LED integrated boolean communication with an external power supply.

The third development iteration then arises with the implementation of string and integer communication. After establishing communication between a selected baud rate of 9600, the Arduino IDE Serial Monitor can be utilised to send string and integers between the devices. In real-time messages can be sent and received from one device to the other. This is demonstrated in Figure 40 in which an example message communication is demonstrated.

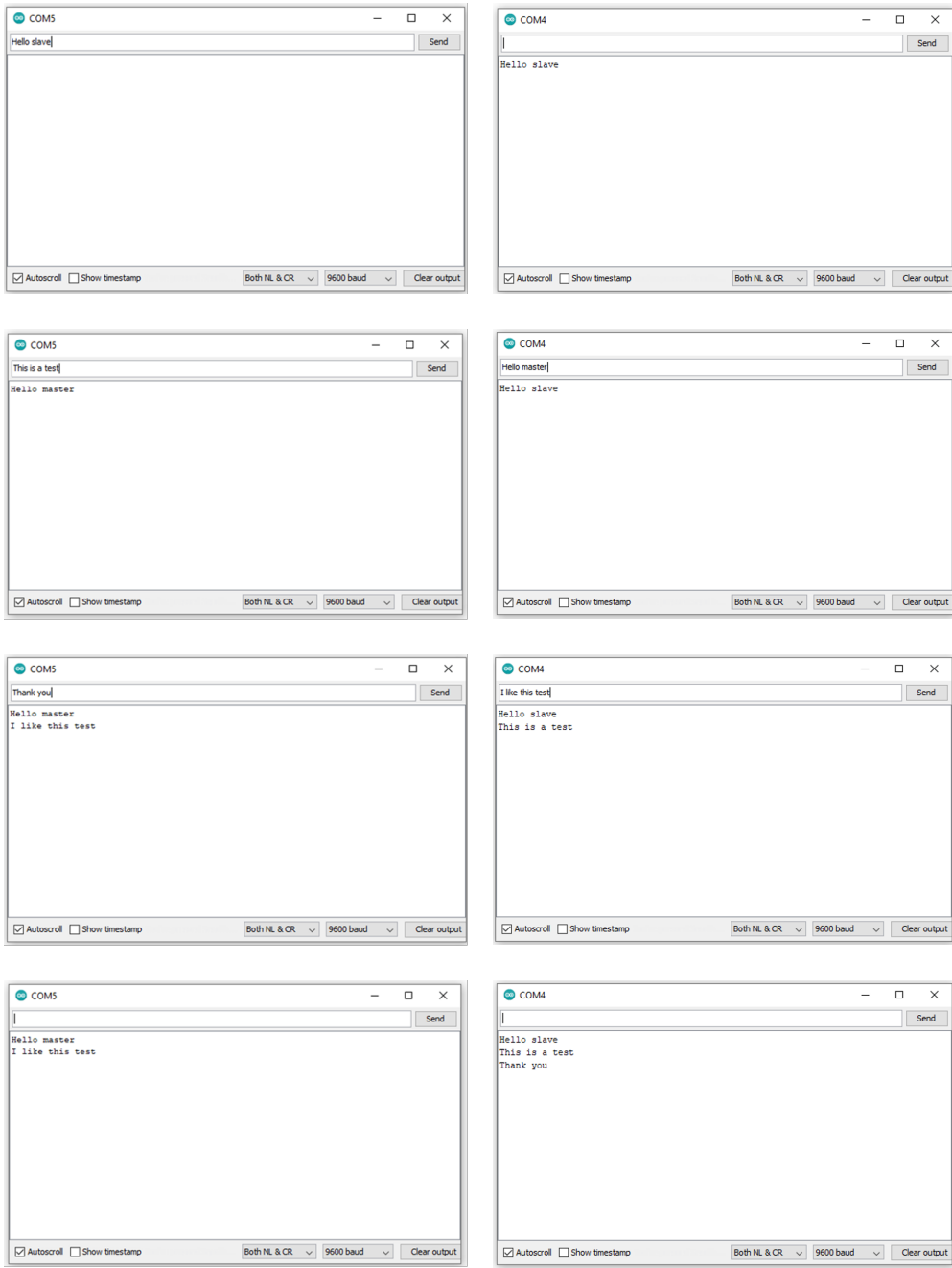


Figure 40: String communication between master (left) and slave (right) HC-05 modules.

The fourth iteration extends the Boolean communication to a stage where the devices no longer have to be plugged into a computer for a power source. By connecting a 9V battery to the  $V_{in}$  Arduino port, the circuit can receive its required power supply and as such, the circuit can operate independently of a computer and ultimately achieve portability. As the devices are now portable, a problem is encountered when the devices are brought in range, establish a connection, and then go out of range. When the devices go out of range, they remain in the “connected” mode and as such cannot be “re-connected” as they do not search for a device to connect to. The fifth iteration rectifies this issue. On the master device, a transistor is connected to the voltage pin of the HC-05 chip and a digital output port of the Arduino. When a signal has not been received for a nominated 30 second period of time, the state of the transistor is briefly changed, thus disconnecting and reconnecting power to the HC-05 module and essentially hard-resetting the device. This is implemented in the device’s code as shown in Figure 41. This causes the master device to "search for a device" and ultimately reconnect to the slave device. This also achieves system requirement R.2.6 which states that the UAV and payload must remain in constant communication. The master device was selected to be the device with the reset functionality after re-connection time testing. The final physical and circuit implementations of the master and slave devices are shown in Figures 42 and 43, respectively.

```
void reset_chip()
{
  digitalWrite(BTPowerPin, LOW);
  // have a small delay to allow the transistor to register a change in control
  delay(500);
  digitalWrite(BTPowerPin, HIGH);
  // have a small delay before resetFunc so the previous process isn't interrupted
  delay(500);
}
```

Figure 41: Arduino function that changes the state of the transistor in order to disconnect and re-connect power to the HC-05 module.

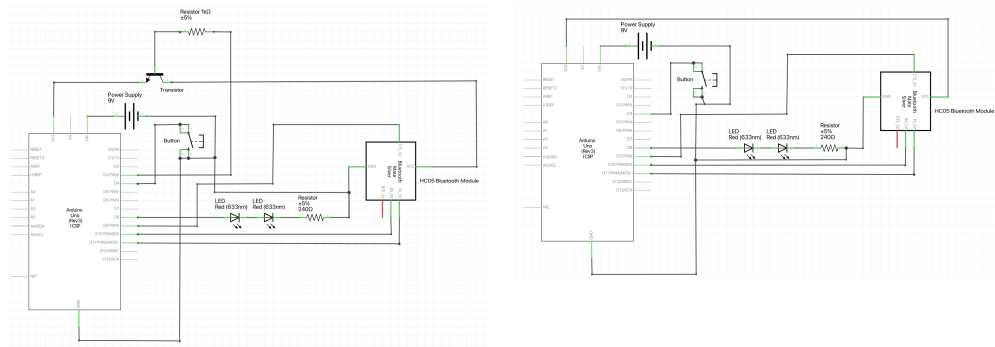


Figure 43: Circuit implementation of portable master (left) and slave (right) devices with re-connect functionality.

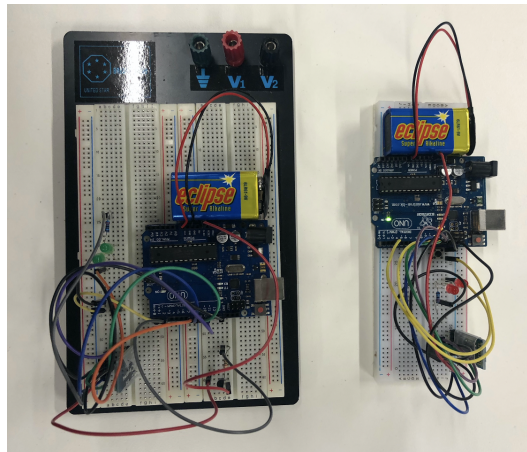


Figure 42: Physical implementation of portable master (left) and slave (right) devices with re-connect functionality.



## Appendix F MQ-2 Smoke Gas Detector Sensor Module Data Sheet

# User Manual

For

## MQ-2 Smoke Gas Detector Sensor Module For Arduino (ME084)



### Description:

MQ-2 gas sensor sensitive material used in the clean air low conductivity tin oxide (SnO<sub>2</sub>). When there is the environment in which the combustible gas sensor, conductivity sensor with increasing concentration of combustible gases in air increases. Using a simple circuit to convert the change in conductivity of the gas concentration corresponding to the output signal. MQ-2 gas sensor high on gas, propane, hydrogen sensitivity of detection of natural gas and other flammable vapors are also very good. This sensor can detect a variety of flammable gas, is a low-cost sensors for a variety of applications.

### Specification

- Power supply needs: 5V
- A gas, natural gas, city gas, smoke better sensitivity.
- There are four screw holes for easy positioning ;
- Has a long life and reliable stability
- Rapid response and recovery characteristics
- DO output: TTL digital 0 and 1 (0.1 and 5V)
- Detectable concentration: 300-10000ppm

## PinOut

Pin	Description
Vcc	Power supply 5V/DC
Gnd	Ground
D0	Digital Output pin

## Example

In this example, we use the digital output pin D13 to sense the change of environment gas concentration. When the gas concentration arrive at some level, the buzzer is ring.

Wire connection as below:

Vcc-----5V  
Gnd-----Gnd  
D0-----A0

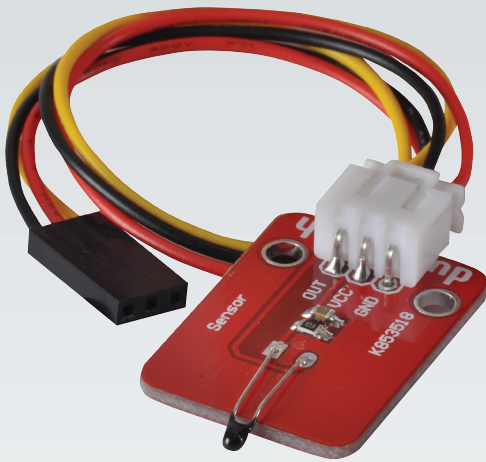
\*\*\*\*\*Code Begin\*\*\*\*\*

```
const int sensorPin= 0;
const int buzzerPin= 13;
int smoke_level;

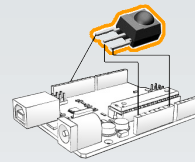
void setup() {
  Serial.begin(9600);
  pinMode(sensorPin, INPUT);
  pinMode(buzzerPin, OUTPUT);
}
void loop() {
  smoke_level= analogRead(sensorPin);
  Serial.println(smoke_level);
  if(smoke_level > 200){
    digitalWrite(buzzerPin, HIGH);
  }
  else{
    digitalWrite(buzzerPin, LOW);
  }
}
```

\*\*\*\*\*Code End\*\*\*\*\*

Appendix G XC-4438 Microphone Module Data  
Sheet



# Analog Temperature Sensor



■ Type: Module  
 Application: Add On Module  
 Measure Temperature

Dimensions: 33(L) x 16(W) x 9(H)mm

## Analog Temperature Sensor Overview:

This module provides a simple way to measure temperature. The module outputs an analog voltage that varies directly with temperature. Connect it straight to one of your DuinoTECH analog inputs.

Specifications	
	Analog Temperature Sensor
Operating Voltage	0VDC - 5VDC
Protocol	Analog
Dimensions	33(L) x 16(W) x 9(H)

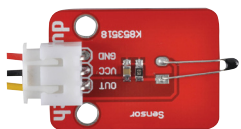
Pinout		
Module	Duinotech	Function
VCC	5V	Power Supply
OUT	A0	Analog output from Module
GND	GND	Ground Connection

What is included: 1 x Analog Temperature Module  
 1 x Breakout cable

Essential Accessories: Plug to Plug Jumper Lead (WC6024)

Optional Accessories:

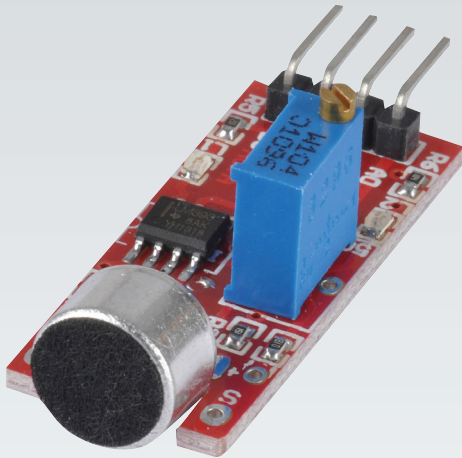
## Analog Temperature Sensor Sample Projects:



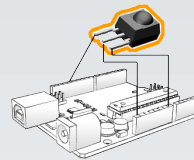
## Did you know:

The small size of the thermistor on this module means it responds quickly to changes in temperature

## Appendix H XC-4494 Analogue Temperature Sensor Module Data Sheet



# Microphone Module



- Type: Module
- Application: Add On Module  
Measure Sound level with your arduino. Combine with SD card and create a simple audio recorder.
- Dimensions: 43(L) x 16(W) x 13(H)mm

## Microphone Module Overview:

Our range would not be complete without a microphone sensor module. This unit is highly sensitive with the added advantage of having two outputs. An analogue output for real time microphone voltage signal, and a digital output for when the sound intensity reaches its threshold. Great to turn your Duinotech into a voice recorder or vox.

What is included: 1 x Microphone Module

Essential Accessories: Jumper Leads (WC6028)

Optional Accessories: SD Card Module

## Specifications

Microphone Module	
Sensitivity	Ajdustable via trim pot.
Operating Voltage	0-5VDC(analog)
Supply Voltage	5VDC
Dimensions	43(L) x 16(W) x 13(H)
Additional Features	Digital Threshold Comparater

## Pinout

PIN	DUINO	Function
AO	AO	Analog Output
G	GND	Ground Connection
+	SV	SV Supply
DO	D8	Digital Output

## Microphone Module Sample Projects:



## Did you know:

Vox is the name given to a voice operated switch and can be used to activate a device when a sound is detected



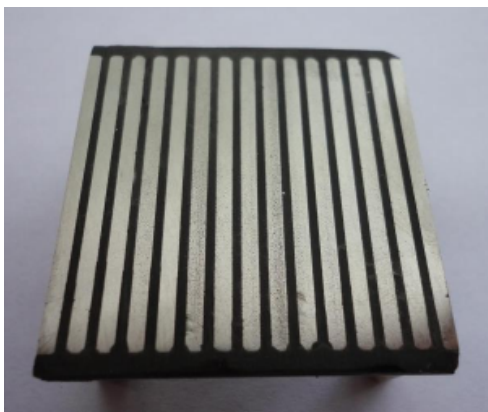
## Appendix I Electro Ferromagnet Data Sheet

# OpenGrab EPM v3

- Overview
  - Theory of operation
  - Applications
  - Features
- Mechanical properties
  - Version 3R5C and newer
  - Version 3R4B and older
- Characteristics
- Human-machine interface
  - Push button
  - External button
  - LED indication
- RCPWM interface
- UAVCAN interface
  - Mode and status codes
  - Services
  - Messages
  - CAN bus characteristics
  - DIP switch
- UART interface
- Links

## Overview

The OpenGrab EPM v3 is an electropermanent magnet, combining the advantages of electro and permanent magnets. The device creates a very strong magnetic contact with a ferrous target. It supports [UAVCAN](#), RCPWM and push button operation. OpenGrab EPM v3 has been developed by NicaDrone in cooperation with Zubax Robotics.



## Appendix J SITL Simulation

The following is a detailed guide of utilising ArduCopter, QGroundControl, and FlightGear software platforms to simulate the operation of the UAV via a SITL architecture. The purpose of this task is to allow the students to familiarise themselves with the control software that will also be used in the hardware-based operation of the drone, and to test fundamental UAV behaviours such as its endurance and response to adverse environmental conditions, such as strong winds and turbulence.

### J.1 Ubuntu, ArduPilot, QGroundControl, FlightGear Installation

To install the operating software and three programs responsible for constructing a multirotor SITL simulation capability, the following steps are suggested to be enacted:

1. Install Ubuntu 20LTS on VirtualBox
  - (a) Tutorials for this installation process are readily available online and hence will not be reiterated in this report. Refer to Tucakov (2020) and Bose (2019) to download and install Ubuntu 20LTS and VirtualBox, respectively.
  - (b) Within VirtualBox, allocate sufficient RAM and disk-drive memory to run the SITL simulations. For this application, 8GB of RAM and 40GB of disk-drive memory was allocated.
2. Install ArduPilot/ArduCopter:
  - (a) Update packages with command: `sudo apt update && sudo apt full-upgrade`
  - (b) Install Git with command: `sudo apt install git`
  - (c) Clone the master branch of the ArduPilot Git project with command: `cd ~ && git clone https://github.com/ArduPilot/ardupilot.git`
  - (d) Update submodules of the ArduPilot project with command: `cd ~/ardupilot && git submodule update --init --recursive`
  - (e) From "ardupilot" directory, run the environment installer with command: `Tools/environment_install/install-prereqs-ubuntu.sh -y`
  - (f) Logout of, and log back into, the user's Ubuntu 20LTS account to enable any changes to user permissions
  - (g) Download the ArduCopter branch with the following commands:
    - i. `cd ~`
    - ii. `rm -rf ardupilot`
    - iii. `git clone --branch Copter-4.0 https://github.com/ArduPilot/ardupilot.git`
    - iv. `cd ardupilot && git submodule update --init --recursive`
  - (h) Build the ArduCopter SITL environment from the "ardupilot" directory with the following commands:

- i. `./waf configure --board SITL`
  - ii. `./waf copter`
3. Install QGroundControl on Ubuntu 20LTS: Instructions readily available online and will not be reiterated in this report.
  4. Install FlightGear on Ubuntu 20LTS: Instructions readily available online and will not be reiterated in this report.

## J.2 ArduCopter Launch

To launch the hexacopter multirotor with a console, 2D map, and On-Screen Display (OSD), the following steps are suggested to be enacted:

1. Start Ubuntu on VirtualBox
2. Navigate: Files > Home > ardupilot
3. Navigate: Right click "ArduCopter" and click "Open in Terminal"
4. Select frame type and launch the vehicle:
  - (a) To view all types of frames, run command: `sim_vehicle.py --help`
  - (b) For a hexarotor (and starting with a ground station console window, map, and OSD), run command: `sim_vehicle.py -f hex --console --map --osd`
  - (c) Code for that SITL vehicle will then compile
5. Wait for "IMU0 is using GPS" and "IMU1 is using GPS" to appear in the console (this ensures the drone has a 3D location fix)
6. Takeoff:
  - (a) Run command: `mode guided`
  - (b) Run command (arm the vehicle's throttle control): `arm throttle`
  - (c) Run command (command the vehicle to ascend to an altitude of 50m above sea-level, this value can be changed): `takeoff 50`

## J.3 Add Custom Location

To add a custom GPS location to the possible flight areas, the following steps are suggested to be enacted:

1. Files > ardupilot > Tools > autotest > locations.txt
2. Add a new row to the text file with format: `[name] = [lat (degrees)], [lon (degrees)], [height above sea level (m)], [heading (degrees)]`

## J.4 Modify Vehicle Parameters

To alter the UAV's parameters, such as battery voltage or capacity, the following steps are suggested to be enacted:

1. Start in the "`~/ardupilot/ArduCopter`" terminal running the simulation
2. To change battery parameters (e.g., 4S batteries (16.8V) with 20 Amp-hours of capacity):
  - (a) Run command: `param set SIM_BATT_VOLTAGE 16.8`
  - (b) Run command: `param set BATT_CAPACITY 20000`

## J.5 Modify Environmental Parameters

To change environmental parameters that influence the UAV, such as wind speed or turbulent accelerations, the following steps are suggested to be enacted:

1. Start in the "`~/ardupilot/ArduCopter`" terminal running the simulation
2. To change wind parameters (e.g., turbulence of  $3\text{ m/s}^2$  will induce random accelerations of  $3\text{ m/s}^2$  onto the UAV during simulated flight):
  - (a) To see wind parameters, run command: `param show SIM_WIND*`
  - (b) Run command: `param set SIM_WIND_TURB 3`

## J.6 ArduPilot and QGroundControl Launch at Location and Fly

To launch and fly the UAV at a specific location using ArduPilot as the autopilot and QGroundControl to command the flight path of the UAV, as shown in Figure 5, the following steps are suggested to be enacted:

1. In directory "`~/ardupilot/ArduCopter`" run command:  
`sim_vehicle.py -L St_Kilda -f hexa --console --map`
2. Wait for "IMU0 is using GPS" and "IMU1 is using GPS" to appear in console (this ensure the drone has a 3D location fix)
3. Takeoff:
  - (a) Run command: `mode guided`
  - (b) Run command (arm the vehicle's throttle control): `arm throttle`
  - (c) Run command (command the vehicle to ascend to an altitude of 50m above sea-level, this value can be changed): `takeoff 50`
4. Run (or double click): `QGroundControl.AppImage`

5. Fly the UAV: Left click on QGC map and select "Go to location", the slide the toggle to verify the command
6. Return to home: Click 'Return' on the left menu on QGC and verify the command. The UAV will return to it's home location with the heading remaining the same as from it's previous command
7. Land the UAV: Click 'Land' on the left menu of QGC and verify the command. The UAV will return to ground level

## J.7 ArduPilot, QGroundControl, and FlightGear Launch at Location and Fly

To launch and fly the UAV at a specific location using ArduPilot as the autopilot and QGroundControl to command the flight path of the UAV (as shown in Figure 5), the following steps are suggested to be enacted:

1. With ArduPilot DEACTIVATED and QGroundControl DISCONNECTED
2. Navigate to "`~/ardupilot/ArduCopter`"
3. Open FlightGear with command: `../Tools/autotest/fg_quad_view.sh`
4. In directory "`~/ardupilot/ArduCopter`" run command (to fly at custom location "St\_Kilda"):
 

```
sim_vehicle.py -L St_Kilda -f hexa --console --map
```
5. Wait for "IMU0 is using GPS" and "IMU1 is using GPS" to appear in console (this ensure the drone has a 3D location fix)
6. Takeoff:
  - (a) Run command: `mode guided`
  - (b) Run command (arm the vehicle's throttle control): `arm throttle`
  - (c) Run command (command the vehicle to ascend to an altitude of 50m above sea-level, this value can be changed): `takeoff 50`
7. Run (or double click): `QGroundControl.AppImage`
8. Fly the UAV: Left click on QGC map and select "Go to location", the slide the toggle to verify the command
9. Return to home: Click 'Return' on the left menu on QGC and verify the command. The UAV will return to it's home location with the heading remaining the same as from it's previous command
10. Land the UAV: Click 'Land' on the left menu of QGC and verify the command. The UAV will return to ground level

## J.8 Download ArduPilot Logs

To record and store the log files from an ArduPilot-only flight, the following steps are suggested to be enacted:

1. Open the " /ardupilot/ArduCopter" terminal running the simulation
2. Check the log list by running command: `log list`
3. Run command: `log download [log number] [filename and location]`

## J.9 Download QGroundControl Logs

To record and store the log files from a QGroundControl and ArduPilot flight, the following steps are suggested to be enacted:

1. Click 'Q' on QGC > Analyze Tools > Log Download > Refresh
2. Select the logs to download (most recent will be from the most recent flight)
3. Select "Download"
4. When prompted for a directory, this will be where it stores the log it's about to download. The default location is "home/\$USER\$". This could be changed to be stored in a designated "flight logs" folder if desired
5. After downloaded, click 'Erase All' to clean the memory cache

## J.10 Setup a Shared Folder between Ubuntu 20LTS and Windows

To establish a shared memory location between the virtual machine where the simulations are run and recorded, and the host Windows machine, the following steps are suggested to be enacted:

1. On Windows create a new folder in any location
2. On POWERED OFF Oracle VM VirtualBox > Machine > Settings > Shared Folders > Add new shared folder > find and select the Windows folder path > Select auto-mount to ensure it starts automatically
3. POWER ON the VM.
4. Start terminal
5. Verify user by running command: `whoami`
6. From home, run command: `sudo adduser $USER$ vboxsf`
7. Restart the VM

## J.11 Analyse Logs with Mission Planner

To analyse the log files in the GCS, Mission Planner, the following steps are suggested to be enacted:

1. Move logs to Windows:
  - (a) Copy to shared folder, or;
  - (b) Copy to shared cloud service (e.g., Google Drive)
2. Open Mission Planner > Data
3. Then in the left, grey, horizontal menu, navigate to "DataFlash Logs"
4. Select "Auto Analysis"
5. Find the desired log file and open it
6. The following analysis will describe the outputs of several tests by comparing the input control to the UAV response.

## J.12 Create a Flight Path with QGroundControl

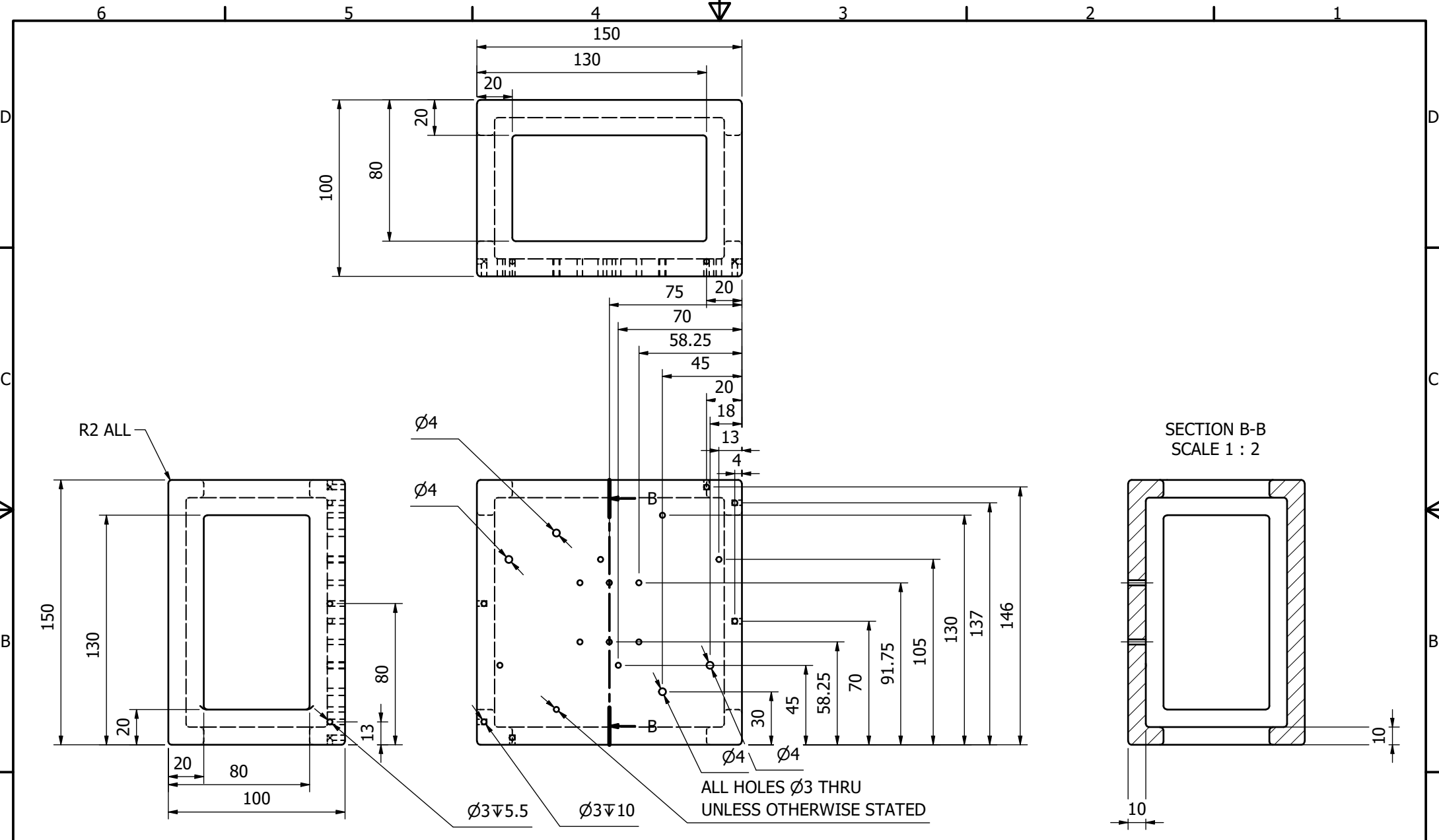
To create and save (for offline use) a flight path with QGroundControl, the following steps are suggested to be enacted:

1. Open QGroundControl
2. Select "Plan" from left menu
3. Select "Blank" for an empty template
4. Start with a "Takeoff" node by selecting "Takeoff" from the left menu
5. Select "Waypoint" from the left menu
6. Begin creating the series of waypoints for the UAV to follow by left clicking around the QGC map. After creating a singular waypoint, modify the altitude, hold time, flight speed using the right menu.
7. Finish the plan with a "Return to home" by clicking "Return" in the left menu.
8. Optional - Upload and fly:
  - (a) If the ArduPilot simulation is already running, upload the flight plan by clicking the "Upload" or "Upload required" button at the top of QGC.
  - (b) Click "Fly" on the left menu and verify the mission to begin the flight path
  - (c) The drone will now fly the specified flight path
9. Save the flight path:

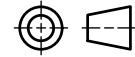


- (a) Click "File" on the left menu > "Save As..." and choose the desired save location (e.g., in the shared folder)
- (b) This file can be uploaded offline to quickly start a predetermined flight (also can be used on Mission Planner)

## Appendix K Technical Drawings

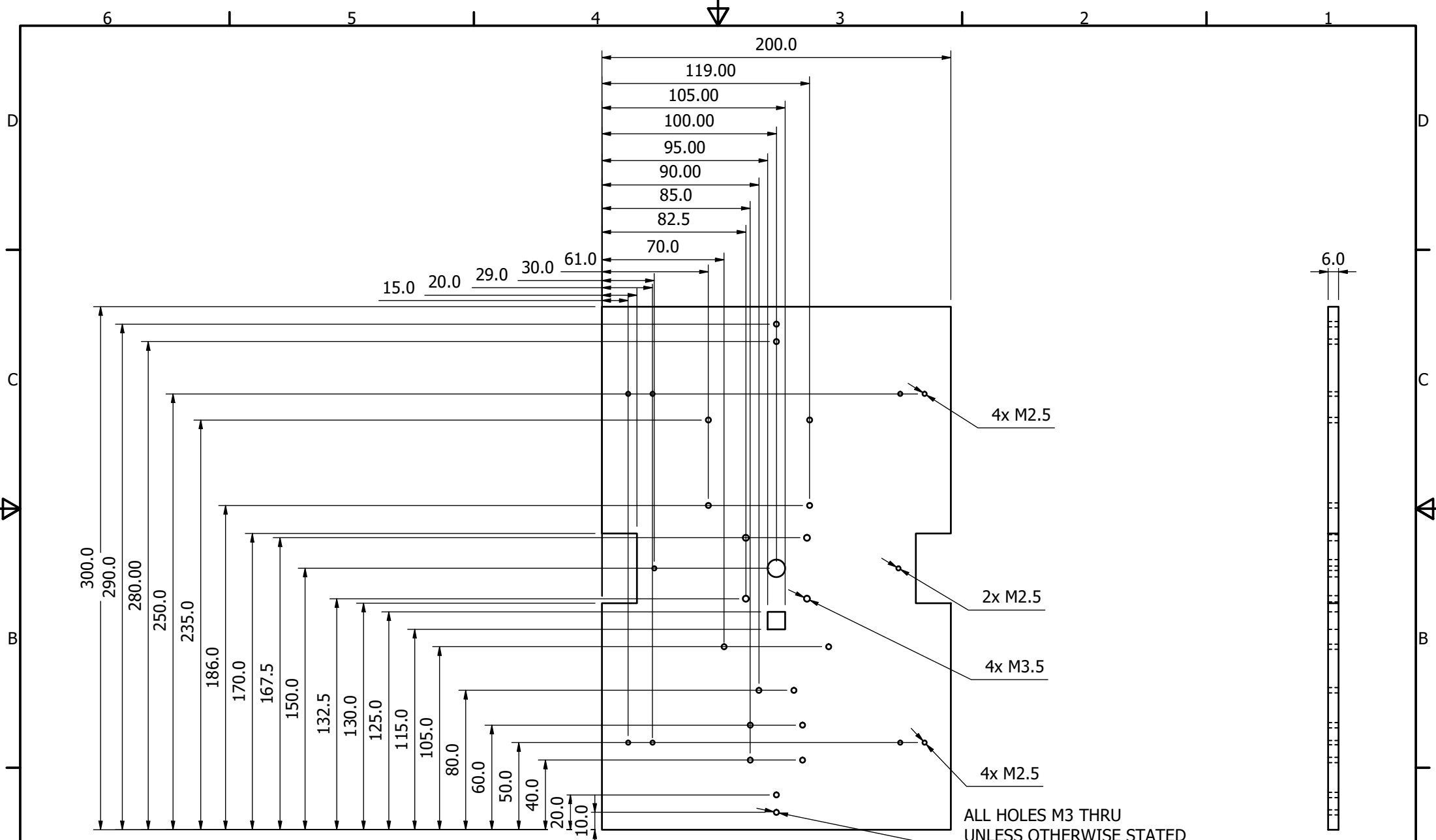


UNLESS STATED OTHERWISE  
 GENERAL TOLERANCE:  
 LINEAR: ± 0.3  
 ANGULAR: ± 1°  
 REMOVE BURRS & SHARP EDGES  
 3.2 / ALL OVER.

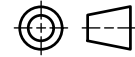
DO NOT SCALE  
  
 THIRD ANGLE PROJECTION  
 DIMENSIONS IN  
 MILLIMETERS  
 DRAWING STANDARD  
 AS1100

DESIGNED D. O'Connor	DATE 1/09/2021
DRAWN D. O'Connor	DATE 1/09/2021
CHECKED P. CAPALDO	DATE 1/09/2021
APPROVED J. HUYNH	DATE 1/09/2021
MATERIAL ABS Plastic	

PROJECT UAV PHORESIS	
TITLE Payload Casing	
PART NUMBER PRT01	REVISION 1
QTY 1	MASS 0.200 kg
SCALE 1:2	SHEET 1 of 1
A3	

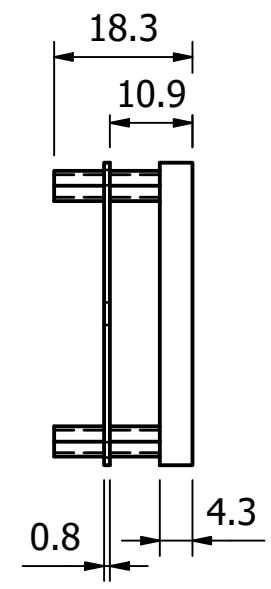
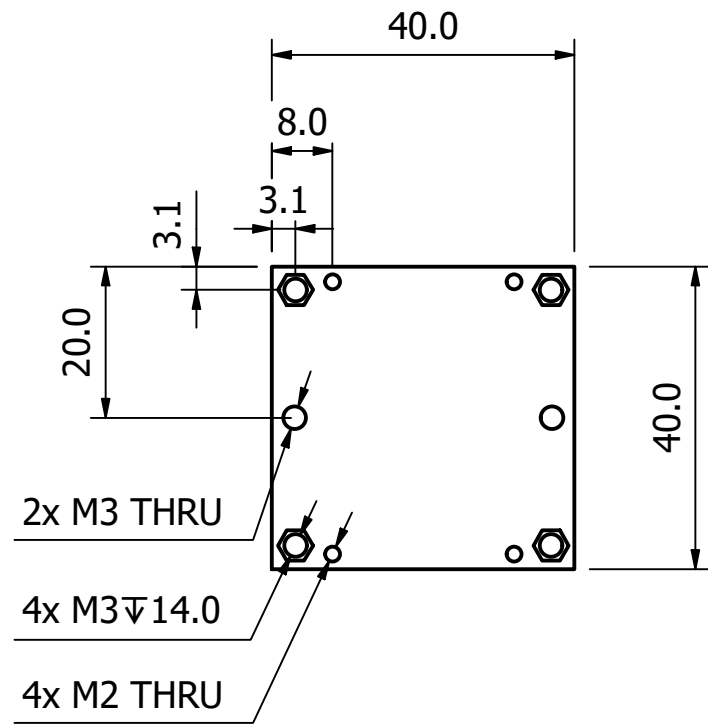
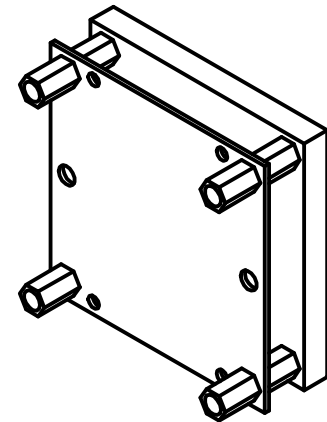


UNLESS STATED OTHERWISE  
 GENERAL TOLERANCE:  
 LINEAR: ± 0.3  
 ANGULAR: ± 1'  
 REMOVE BURRS & SHARP EDGES  
 3.2 / ALL OVER.

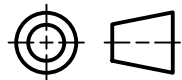
DO NOT SCALE  
  
 THIRD ANGLE PROJECTION  
 DIMENSIONS IN  
 MILLIMETERS  
 DRAWING STANDARD  
 AS1100

DESIGNED D. O'CONNOR	DATE 1/09/2021
DRAWN D. O'CONNOR	DATE 1/09/2021
CHECKED P. CAPALDO	DATE 1/09/2021
APPROVED J. HUYNH	DATE 1/09/2021
MATERIAL Acrylic	

PROJECT UAV PHORESIS	
TITLE <b>MOUNTING PLATE</b>	
PART NUMBER <b>PRT02</b>	REVISION <b>1</b>
QTY 1	MASS 0.200 kg
SCALE 1:2	SHEET 1 of 1
<b>A3</b>	



UNLESS STATED OTHERWISE  
 GENERAL TOLERANCE:  
 LINEAR:  $\pm 0.3$   
 ANGULAR:  $\pm 1'$   
 REMOVE BURRS & SHARP EDGES  
 3.2  $\checkmark$  ALL OVER.

DO NOT SCALE  
  
 THIRD ANGLE PROJECTION  
 DIMENSIONS IN  
 MILLIMETERS  
 DRAWING STANDARD  
 AS1100

DESIGNED J. HUYNH	DATE 1/09/2021
DRAWN J. HUYNH	DATE 1/09/2021
CHECKED D. O'CONNOR	DATE 1/09/2021
APPROVED P. CAPALDO	DATE 1/09/2021
MATERIAL Generic	

PROJECT UAV PHORESIS	
TITLE GRIPPER MOUNT	
PART NUMBER PRT03	REVISION 1
QTY 1	MASS 0.100 kg
SCALE 1 : 1	SHEET 1 of 1
A4	

## Appendix L IoMT Sensor Payload Code

### L.1 Smoke Detector Sensor Payload

```
int smokeA0=A0;
float sensorValue;

void setup()
{
  Serial.begin(9600);
  delay(500); //boot
  pinMode(smokeA0,INPUT);
  Serial.println("Smoke Detector Sensor Activated");
}
void loop()
{
  sensorValue=analogRead(smokeA0);
  if(sensorValue > 300)
  {
    Serial.println("Smoke detected");
  }
  else
  {
    Serial.println("No smoke detected");
  }
  delay(2000); // wait 2s for next reading
}
```

## L.2 Sound Sensor Payload

```
int sound_pin=9;
float sensorValue;

void setup()
{
  Serial.begin(9600);
  delay(500); //boot
  pinMode(sound_pin,INPUT);
  Serial.println("Sound Sensor Activated");
}

void loop()
{
  sensorValue=digitalRead(sound_pin);
  if(sensorValue == HIGH)
  {
    Serial.println("Sound detected");
  }
  else
  {
    Serial.println("No sound detected");
  }
  delay(500); // wait 2s for next reading
}
```

### L.3 Temperature Sensor Payload

```
#include <math.h>
#include <string.h>

int tempA0=A0;
float sensorValue;
char ch=248;

String temp_convert(int input_value) {
  double output_value;
  String output_value_str;
  output_value = log(((10240000/input_value) - 10000));
  output_value = 1 / (0.001129148 + (0.000234125 + (0.0000000876741
    * output_value * output_value ))* output_value );
  output_value = output_value - 273.15; // Convert Kelvin to Celcius

  output_value_str=String(output_value,2);
  return output_value_str;
}

void setup()
{
  Serial.begin(9600);
  delay(500); //boot
  pinMode(tempA0,INPUT);
  Serial.println("Temperature Sensor Activated");
  delay(1000);
}

void loop()
{
  sensorValue=analogRead(tempA0);
  Serial.println("Temperature = "+temp_convert(sensorValue)+"C");
  delay(2000);
}
```



## Appendix M Raspberry Pi Sensor Data Receiving Code

```
#!/usr/bin/python3

import serial
import os
import time
import datetime

if os.path.exists('/dev/rfcomm0') == False:
    path = 'sudo rfcomm bind 0 98:D3:C1:FD:A0:63'
    os.system (path)
    time.sleep(1)

ser = serial.Serial(
    port='/dev/rfcomm0',
    baudrate=9600,
    parity=serial.PARITY_ODD,
    stopbits=serial.STOPBITS_TWO,
    bytesize=serial.SEVENBITS
)
ser.isOpen()
curr_time = datetime.datetime.now() + datetime.timedelta(hours=8.5)
curr_time = curr_time.strftime("%d-%m-%Y %H:%M:%S")
print("Payload sensor message log as of " + curr_time + "\n\n")
logname = "sensor_log_"+curr_time+".txt"
log = open(logname, "a+")
log.write("Payload sensor message log as of "+curr_time+"\n\n")
log.close()

while 1 :
    recv = ''
    user_input = ''
    if user_input == 'exit':
        ser.close()
        exit()
    else:
        tic = time.time()
        while time.time() - tic < 15 and ser.inWaiting() == 0:
            time.sleep(1)

        if ser.inWaiting() > 0:
            recv = ser.readline()
```

```
if recv != '':
    curr_time = datetime.datetime.now() + datetime.timedelta(hours=8.5)
    curr_time = curr_time.strftime("%d-%m-%Y %H:%M:%S")

    print("Sensor message received at "+curr_time+"\n"+str(recv, 'utf-8')+"\n")
    log = open(logname, "a+")
    log.write("Sensor message received at "+curr_time+"\n"+str(recv, 'utf-8')+"\n")
    log.close()
```

## Appendix N Work Breakdown Structure and Gantt Chart

Table 22: Progress key of the WBS.

Completed	Ongoing	To Be Commenced
-----------	---------	-----------------

Table 23: Administration-based tasks of the WBS.

Section	Progress [%]	Responsible	Deliverable	Commence	Due
1.	100	All	Project Charter	04/03	26/03
1.1.	-	JH	Abstract	04/03	11/03
1.2.	-	All	Introduction	04/03	19/03
1.2.1.	-	JH	Background/Context	04/03	11/03
1.2.2.	-	PC	Stakeholders	10/03	19/03
1.2.3.	-	PC	Motivation/Purpose	10/03	19/03
1.2.4.	-	DOC	Project Aim	10/03	19/03
1.2.	-	All	Literature Overview	10/03	19/03
1.2.1.	-	PC	Platform Selection	10/03	19/03
1.2.2.	-	DOC	Payload-UAV Communication	10/03	19/03
1.2.3.	-	DOC	Guided Landing	10/03	19/03
1.2.3.	-	JH	Grasping Mechanism	10/03	19/03
1.3.	-	DOC, PC	Project Objectives	10/03	19/03
1.4.	-	JH	Resources Required	10/03	19/03
1.5.	-	DOC, PC	Project Management	10/03	19/03
1.5.1.	-	PC	Work Breakdown Structure	10/03	19/03
1.5.2.	-	DOC	Gantt Chart	10/03	26/03
1.6.	-	DOC	Project Failure Assessment	10/03	26/03
1.7.	-	JH	Budget	10/03	26/03
1.8.	-	DOC	Conclusion	10/03	26/03
1.9.	-	PC	Meeting Agenda and Minutes	10/03	26/03
2.	100	All	Preliminary Report	02/04	04/06
2.1.	-	JH	Introduction	02/04	18/04
2.2.	-	All	Problem Definition	02/04	18/04

2.2.1.	-	JH	System Context	02/04	18/04
2.2.2.	-	PC	Stakeholders	02/04	18/04
2.2.3.	-	DOC	Scenario-Based Needs Analysis	02/04	18/04
2.2.4.	-	All	User Needs	02/04	18/04
2.2.5.	-	All	System Requirements	02/04	18/04
2.3.	-	All	Literature Review	18/04	02/05
2.3.1.	-	PC	UAV Platform Selection	18/04	02/05
2.3.1.	-	JH	Loaded Multirotor Transportation	18/04	02/05
2.3.2.	-	DOC	Autonomous Landing	18/04	02/05
2.3.4.	-	DOC	Short-Range Communication	18/04	02/05
2.4.	-	All	Theory	02/05	13/05
2.4.1.	-	PC	Airframe, Motor, and Propeller Selection	02/05	13/05
2.4.2.	-	JH	Dynamics of a Multirotor UAV with a Suspended Load	02/05	13/05
2.4.3.	-	DOC	Bluetooth Enabled Short-Range Communication	02/05	13/05
2.4.4.	-	PC	SITL Simulation	02/05	13/05
2.5.	-	All	Design and Methodology	13/05	23/05
2.5.1.	-	DOC	Bluetooth Based Communication System	13/05	23/05
2.5.2.	-	JH	Gripping Mechanism	13/05	23/05
2.5.3.	-	DOC	Payload Casing	13/05	23/05
2.6.	-	PC	UAV Platform Selection	13/05	23/05
2.7.	-	DOC	Conclusion	23/05	04/06
2.8.	-	PC	Future Work	23/05	04/06
2.9.	-	All	Executive Summary	23/05	04/06
3.	100	All	Seminar	10/09	24/09
3.1.	-	All	Presentation Slides	10/09	24/09
3.2.	-	All	Rehearsal	10/09	24/09
3.3.	-	JH	Collecting Hardware for Display	10/09	22/09
3.4.	-	All	Present to Supervisor	16/09	20/09
3.5.	-	All	Present Seminar	24/09	29/09
4.	100	All	Video	01/10	08/10
4.1.	-	All	Record Personal Footage	01/10	08/10
4.2.	-	All	Record Footage Voice-Over	01/10	08/10

4.3.	-	All	Edit Video and Audio Together	01/10	08/10
4.4.	-	All	Submit Video	08/10	08/10
5.	100	All	Ingenuity	01/10	26/10
5.1.	-	All	Collect Hardware for Display	01/10	22/10
5.2.	-	All	Apply for VIP Guest Tour Recognition	01/10	22/10
5.3.	-	All	Design and Submit Poster	01/10	10/10
5.4.	-	All	Design Stall Layout	01/10	22/10
5.5.	-	All	Submit Risk Assessment	18/10	22/10
5.6.	-	All	Present at Ingenuity	25/10	26/10
6.	100	All	Final Report	14/05	29/10

Table 25: Designing-, building-, testing- and execution-based tasks of the WBS.

Section	Progress [%]	Responsible	Deliverable	Commence	Due	Backwards Traceability
1.	100	All	Platform Selection	21/03	10/04	RR-01, 02, 03
1.1.	-	PC	Airframe, Motors and Propellers	21/03	02/04	RR-01, 02
1.2.	-	DOC	Power Supply	21/03	02/04	RR-02
1.3.	-	DOC	Guided Landing	21/03	02/04	RR-03
1.4.	-	DOC	UAV-Payload Communication	21/03	10/04	RR-03
1.5.	-	JH	UAV-Ground Station Communication	21/03	10/04	RR-03
1.6.	-	PC	Flight Control	21/03	10/04	RR-03
1.7.	-	PC	Assessment of Platform in Accordance with the 'Five Eyes' directives	21/03	10/04	RR-01, 02, 03
2.	100	All	Design	10/04	26/05	RR-01, 02, 03, 04, 05, 07, 08, 09, 10, 11
2.1.	-	All	Mechanical	10/04	26/05	RR-01, 03, 04, 05, 07, 09, 10
2.1.1.	-	JH	Gripping Mechanism	10/04	26/05	RR-01, 03, 04, 05, 07, 09, 10
2.1.2.	-	DOC, PC	Payload Casing	17/04	26/05	RR-03, 05, 07, 09
2.2.	-	DOC, JH	Electrical	10/04	26/05	RR-03, 04, 05, 10
2.2.1.	-	DOC	Payload Sensor System	10/04	17/04	RR-04, 07, 08, 09, 10
2.2.2.	-	DOC	Payload-UAV Communication	10/04	17/04	RR-04, 05, 10
2.2.3.	-	JH	Ground Station-UAV Communication	17/04	24/04	RR-03, 10
2.2.4.	-	JH	UAV Power Supply	17/04	24/04	RR-01, 02, 04, 07, 10
2.2.5.	-	JH	Payload Power Supply	17/04	24/04	RR-04, 10
2.2.6.	-	JH	Independent Payload Operation	17/04	01/05	RR-04, 09, 10

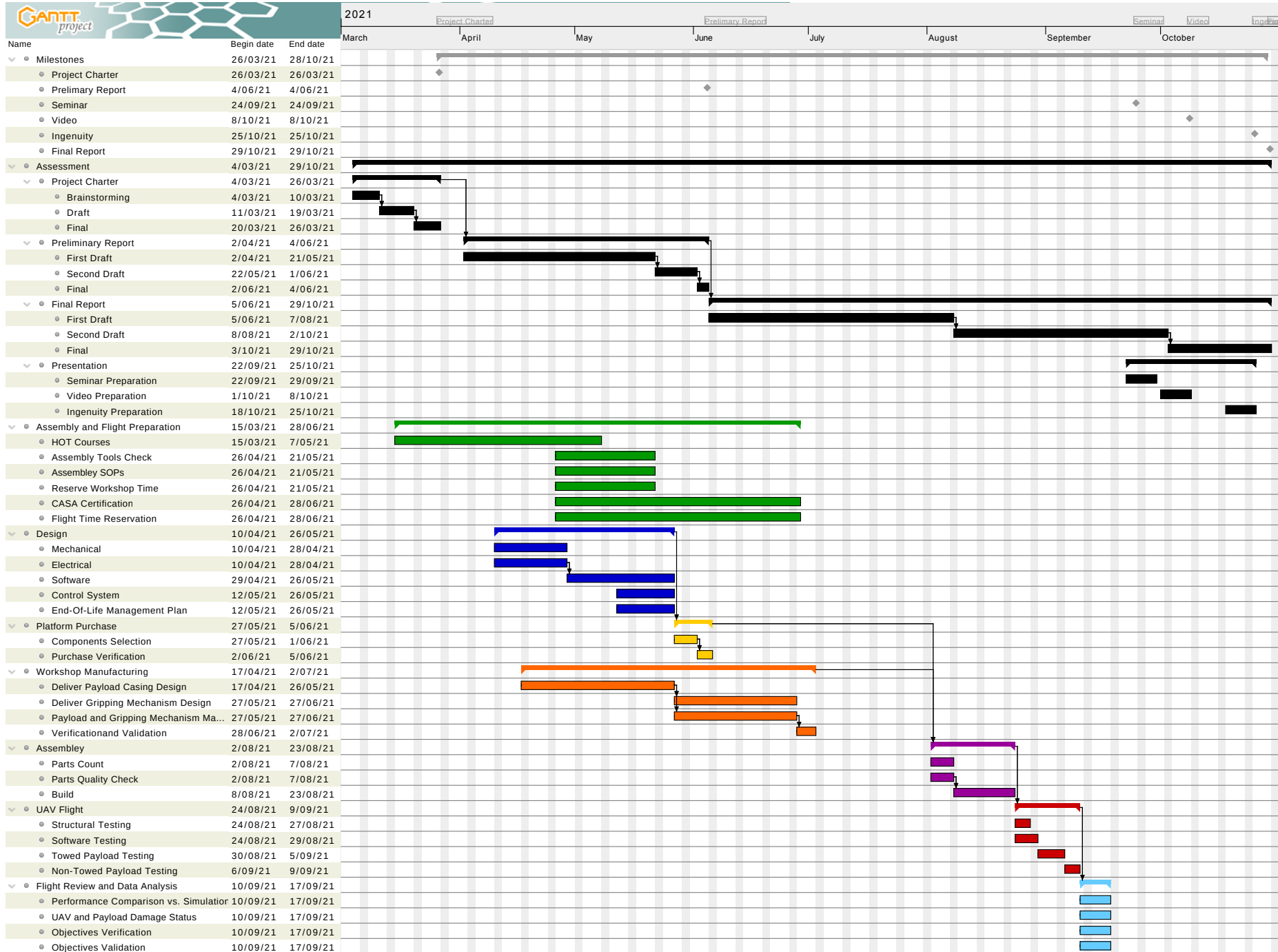
2.2.7.	-	JH	Payload-UAV Autonomous Connectivity	17/04	26/05	RR-03, 04, 09, 10
2.3.	-	All	Software	28/04	26/05	RR-03, 08, 11
2.3.1.	-	DOC	Payload-UAV Communication	28/04	26/05	RR-01, 03, 04
2.3.2.	-	PC	Ground Station-UAV Communication	28/04	26/05	RR-01, 03
2.3.3.	-	PC	Simulation Testing	28/04	26/05	RR-08, 11
2.3.3.1.	-	PC	Platform Selection	28/04	02/05	RR-08
2.3.3.2.	-	PC	Flight Controller to Virtual UAV	05/05	26/05	RR-08
2.3.3.3.	-	PC	UAV Endurance	05/05	12/05	RR-08, 11
2.3.3.4.	-	PC	Payload Endurance	12/05	19/05	RR-08, 11
2.3.4.	-	All	Default Multirotor Control	12/05	26/05	RR-03, 08, 11
2.3.5.	-	All	Towed Payload Multirotor Control	12/05	26/05	RR-03, 08, 11
2.4.	-	All	End-of-Life Management Plan	12/05	26/05	RR-01, 02, 03, 04
3.	100	JH	Platform Purchase	26/05	07/06	RR-01, 02, 03, 04
3.1.	-	JH	Platform Components Selection	26/05	07/06	RR-01, 02, 03
3.1.1.	-	JH	Propellers	26/05	07/06	RR-02
3.1.2.	-	JH	Motors	26/05	07/06	RR-02
3.1.3.	-	JH	Airframe	02/06	07/06	RR-01
3.1.4.	-	JH	Flight Controller	02/06	07/06	RR-03
3.1.5.	-	JH	Payload and UAV Communication	02/06	07/06	RR-03
3.2.	-	JH	Component Approval	02/06	07/06	-
3.3.	-	JH	Purchase Verification	02/06	07/06	RR-01, 02, 03, 04
3.4.	-	JH	Receive Components	07/06	25/07	RR-01, 02, 03, 04
4.	100	All	Assembly and Flight Preparation	15/03	21/05	RR-03, 04, 05, 06, 07, 08, 09, 10
4.1.	-	All	Establish Ranged and Dynamic UAV, Payload, and Ground-Station Communication	15/03	30/07	RR-03, 04, 08

4.2.	-	All	Hands-On-Training (HOT) Course(s) for Workshop Access	15/03	07/05	RR-05, 06, 09, 10
4.3.	-	All	Assembly Tools Check	26/04	21/05	RR-05, 09, 10
4.4.	-	All	Assembly Safe Operating Procedures	26/04	21/05	RR-05, 06, 09, 10
4.5.	-	All	Reserve Workshop Time and Resources	26/04	21/05	RR-05, 09, 10
4.6.	-	PC JH	Reserving a UAV Pilot with a CASA UAV License	26/04	28/06	RR-06
4.7.	-	PC JH	Reserving Flight Time on Defence-Owned Property	26/04	28/06	RR-06
5.	100	All	Workshop Manufacturing	02/08	23/08	RR-01, 02, 03, 04, 05, 07, 09, 10
5.1.	-	DOC	Deliver Payload Casing Design to Workshop Team	17/04	26/05	RR-04, 07
5.2.	-	All	Payload and Gripping Mechanism Verification and Validation	26/06	30/06	RR-01, 02, 03, 04, 05, 07, 09, 10
6.	100	All	UAV Assembly	02/08	23/08	RR-01, 02, 03, 04, 05, 07, 09, 10
6.1.	-	DOC	Parts Count	02/08	07/08	RR-01, 02, 03, 04
6.2.	-	PC	Parts Quality Check	02/08	07/08	RR-01, 02, 03, 04, 05, 07, 09, 10
6.3.	-	All	Build	07/08	23/08	RR-01, 02, 03, 04, 05, 07, 09, 10
7.	100	All	Flight	24/08	20/09	RR-06, 08, 09, 10
7.1.	-	All	Structural Testing	24/08	27/08	RR-05, 09, 10
7.2.	-	All	Software Testing	24/08	29/08	RR-08
7.3.	-	PC, JH	Take-Off, Hover, Translation, and Landing Without Towed Payload	30/08	05/09	RR-06, 08



7.4.	-	PC, JH	Take-Off, Hover, Translation, and Landing With Towed Payload	06/09	09/09	RR-06, 08
8.	100	All	Flight Review and Data Analysis	09/09	16/09	RR-01, 02, 03, 04, 05, 08
8.1.	-	All	Performance Comparison Against Simulations	09/09	16/09	RR-06, 08
8.2.	-	All	UAV and Payload Damage Status	24/08	16/09	RR-01, 02, 03, 04, 08
8.3.	-	All	Objectives Verification	09/08	16/09	-
8.4.	-	All	Objectives Validation	09/08	16/09	-

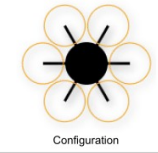
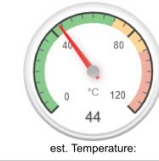
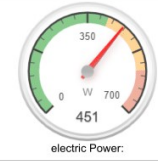
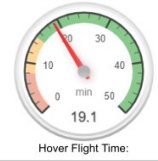
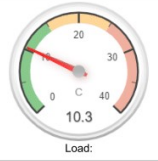
## Gantt Chart



## Appendix O Detailed Flight Characteristics

This appendix overviews the various components required as input parameters to eCalc and the resulting calculations. The input components, displayed in Appendix P, were used to specify the UAV platform and total mass of the unloaded (Figures 44 and 45) and loaded (Figures 46 and 47) configurations. Furthermore, average atmospheric conditions of Adelaide in May, 2020 (field elevation, air temperature, pressure) were sourced from the Bureau of Meteorology (BoM 2020).

<b>General</b>	Model Weight: 1020 g incl. Drive 36 oz	# of Rotors: 6 flat	Frame Size: 810 mm 31.89 inch	FCU Tilt Limit: 40°	Field Elevation: 50 m.ASL 164 ft.ASL	Air Temperature: 15 °C 59 °F	Pressure (QNH): 1022.5 hPa 30.19 inHg	
<b>Battery Cell</b>	Type (Cont. / max. C) - charge state: LiPo 10000mAh - 15/25C - normal	Configuration: 4 S 2 P	Cell Capacity: 10000 mAh 20000 mAh total	max. discharge: 85%	Resistance: 0.0025 Ohm	Voltage: 3.7 V	C-Rate: 15 C cont. 25 C max	Weight: 217 g 7.7 oz
<b>Controller</b>	Type: Hobbywing FlyFun 40A-6s	Current: 40 A cont. 60 A max	Resistance: 0.013 Ohm	Weight: 44 g 1.6 oz		<b>Accessories</b>	Current drain: 3.856 A	Weight: 4324 g 152.5 oz
<b>Motor</b>	Manufacturer - Type (Kv) - Cooling: T-Motor - MN4010-9 (580) - good	KV (w/o torque): 580 rpm/V Prop-Kv-Wizard	no-load Current: 1.3 A @ 10 V	Limit (up to 15s): 580 W	Resistance: 0.042 Ohm	Case Length: 30.5 mm 1.2 inch	# mag. Poles: 24	Weight: 112 g 4 oz
<b>Propeller</b>	Type - yoke twist: T-Motor CF - 0°	Diameter: 15 inch 381 mm	Pitch: 5 inch 127 mm	# Blades: 2	PConst / TConst: 1.15 / 1.0	Gear Ratio: 1 : 1		<input type="button" value="calculate"/>



<b>Remarks:</b>	<b>Battery</b>	<b>Motor @ Optimum Efficiency</b>	<b>Motor @ Maximum</b>	<b>Motor @ Hover</b>	<b>Total Drive</b>	<b>Multicopter</b>
	Load: 10.35 C	Current: 22.87 A	Current: 33.85 A	Current: 8.27 A	Drive Weight: 2939 g	All-up Weight: 5344 g
	Voltage: 13.77 V	Voltage: 13.82 V	Voltage: 13.33 V	Voltage: 14.42 V		103.7 oz
	Rated Voltage: 14.80 V	Revolutions*: 7432 rpm	Revolutions*: 6869 rpm	Revolutions*: 3933 rpm	Thrust-Weight: 2.4 : 1	add. Payload: 5693 g
	Energy: 296 Wh	electric Power: 316.0 W	electric Power: 451.0 W	Throttle (log): 39 %	Current @ Hover: 49.61 A	200.8 oz
	Total Capacity: 20000 mAh	mech. Power: 272.3 W	mech. Power: 383.0 W	Throttle (linear): 52 %	P(in) @ Hover: 734.2 W	max Tilt: 40 °
	Used Capacity: 17000 mAh	Efficiency: 86.2 %	Power-Weight: 506.4 W/kg	electric Power: 119.3 W	P(out) @ Hover: 606.0 W	max. Speed: 43 km/h
	min. Flight Time: 4.9 min		229.7 W/lb	mech. Power: 101.0 W	Efficiency @ Hover: 82.5 %	26.7 mph
	Mixed Flight Time: 15.5 min		Efficiency: 84.9 %	Power-Weight: 137.4 W/kg	Current @ max: 203.07 A	est. Range: 4082 m
	Hover Flight Time: 19.1 min		est. Temperature: 44 °C	62.3 W/lb	P(in) @ max: 3005.5 W	2.54 mi
	Weight: 1736 g		111 °F	Efficiency: 84.7 %	P(out) @ max: 2297.9 W	est. rate of climb: 6.7 m/s
	61.2 oz			est. Temperature: 23 °C	Efficiency @ max: 76.5 %	1319 ft/min
		<b>Wattmeter readings</b>	Current: 203.1 A	73 °F		68.41 dm <sup>2</sup>
		Current: 13.77 V	Voltage: 13.77 V	specific Thrust: 7.47 g/W		1060.36 in <sup>2</sup>
		Power: 2796.7 W		0.26 oz/W		<input type="button" value="check"/>

Figure 44: UAV platform unloaded configuration parameter inputs and basic performance characteristics.

UAV PHORESIS Unloaded Configuration - eCalc - xcopterCalc

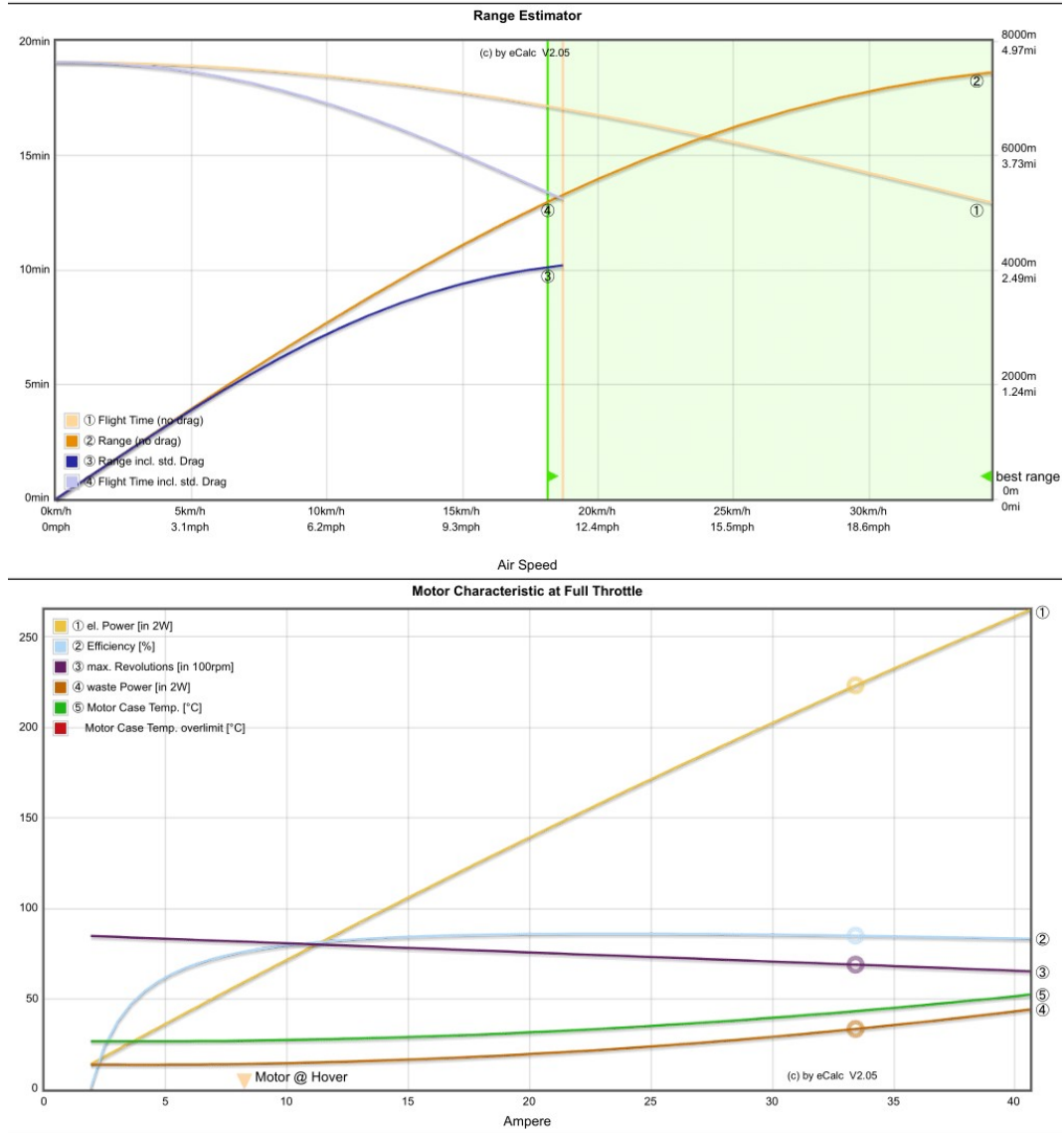
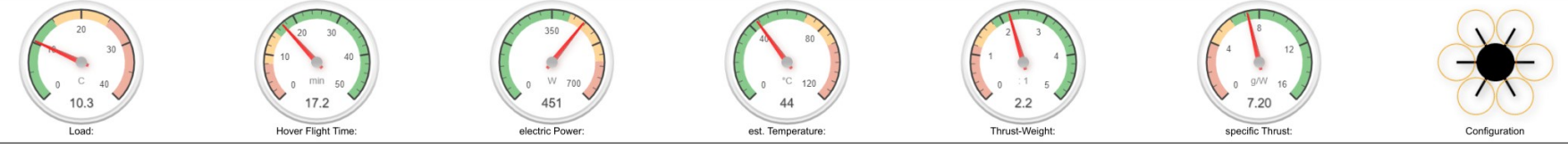


Figure 45: UAV platform unloaded configuration range estimations and motor characteristics at full throttle.

<b>General</b>	Model Weight: 1020 g <small>incl. Drive</small> 36 oz	# of Rotors: 6 flat	Frame Size: 810 mm 31.89 inch	FCU Tilt Limit: 40°	Field Elevation: 50 mASL 164 ftASL	Air Temperature: 15 °C 59 °F	Pressure (QNH): 1022 hPa 30.19 inHg	
<b>Battery Cell</b>	Type (Cont. / max. C) - charge state: LiPo 10000mAh - 15/25C - normal	Configuration: 4 S 2 P	Cell Capacity: 10000 mAh 20000 mAh total	max. discharge: 85%	Resistance: 0.0025 Ohm	Voltage: 3.7 V	C-Rate: 15 C cont. 25 C max	Weight: 218 g 7.7 oz
<b>Controller</b>	Type: Hobbywing FlyFun 40A-6s	Current: 40 A cont. 60 A max	Resistance: 0.013 Ohm	Weight: 45 g 1.6 oz		<b>Accessories</b>	Current drain: 3.856 A	Weight: 4731 g 166.9 oz
<b>Motor</b>	Manufacturer - Type (Kv) - Cooling: T-Motor - MN4010-9 (580) - good	KV (w/o torque): 580 rpm/V	no-load Current: 1.3 A @ 10 V	Limit (up to 15s): 580 W	Resistance: 0.042 Ohm	Case Length: 30.5 mm 1.2 inch	# mag. Poles: 24	Weight: 112 g 4 oz
<b>Propeller</b>	Type - yoke twist: T-Motor CF - 0°	Diameter: 15 inch 381 mm	Pitch: 5 inch 127 mm	# Blades: 2	PConst / TConst: 1.15 / 1.0	Gear Ratio: 1 : 1		<input type="button" value="calculate"/>




Remarks:		Motor @ Optimum Efficiency	Motor @ Maximum	Motor @ Hover	Total Drive	Multicopter
<b>Battery</b>	Load: 10.34 C	Current: 22.87 A	Current: 33.83 A	Current: 9.25 A	Drive Weight: 2955 g	All-up Weight: 5751 g
	Voltage: 13.77 V	Voltage: 13.82 V	Voltage: 13.33 V	Voltage: 14.38 V		202.9 oz
	Rated Voltage: 14.80 V	Revolutions*: 7432 rpm	Revolutions*: 6869 rpm	Revolutions*: 4081 rpm	Thrust-Weight: 2.2 : 1	add. Payload: 5265 g
	Energy: 296 Wh	electric Power: 316.0 W	electric Power: 450.9 W	Throttle (log): 42 %	Current @ Hover: 55.52 A	185.7 oz
	Total Capacity: 20000 mAh	mech. Power: 272.3 W	mech. Power: 382.9 W	Throttle (linear): 54 %	P(in) @ Hover: 821.7 W	max Tilt: 40 °
	Used Capacity: 17000 mAh	Efficiency: 86.2 %	Power-Weight: 470.4 W/kg	electric Power: 133.1 W	P(out) @ Hover: 676.7 W	max. Speed: 43 km/h
	min. Flight Time: 4.9 min		213.4 W/lb	mech. Power: 112.8 W	Efficiency @ Hover: 82.4 %	26.7 mph
	Mixed Flight Time: 14.3 min		Efficiency: 84.9 %	Power-Weight: 142.9 W/kg	Current @ max: 203.01 A	est. Range: 3794 m
	Hover Flight Time: 17.2 min		est. Temperature: 44 °C	64.8 W/lb	P(in) @ max: 3004.5 W	2.36 mi
	Weight: 1744 g		111 °F	Efficiency: 84.7 %	P(out) @ max: 2297.3 W	est. rate of climb: 6.2 m/s
	61.5 oz			est. Temperature: 24 °C	Efficiency @ max: 76.5 %	1220 ft/min
		<b>Wattmeter readings</b>	Current: 202.98 A	75 °F		Total Disc Area: 68.41 dm <sup>2</sup>
		Voltage: 13.77 V	Voltage: 13.77 V	specific Thrust: 7.20 g/W		1060.36 in <sup>2</sup>
		Power: 2795 W	Power: 2795 W	0.25 oz/W		with Rotor fail: 

Figure 46: UAV platform loaded configuration parameter inputs and basic performance characteristics.

UAV PHORESIS Loaded Configuration - eCalc - xcopterCalc

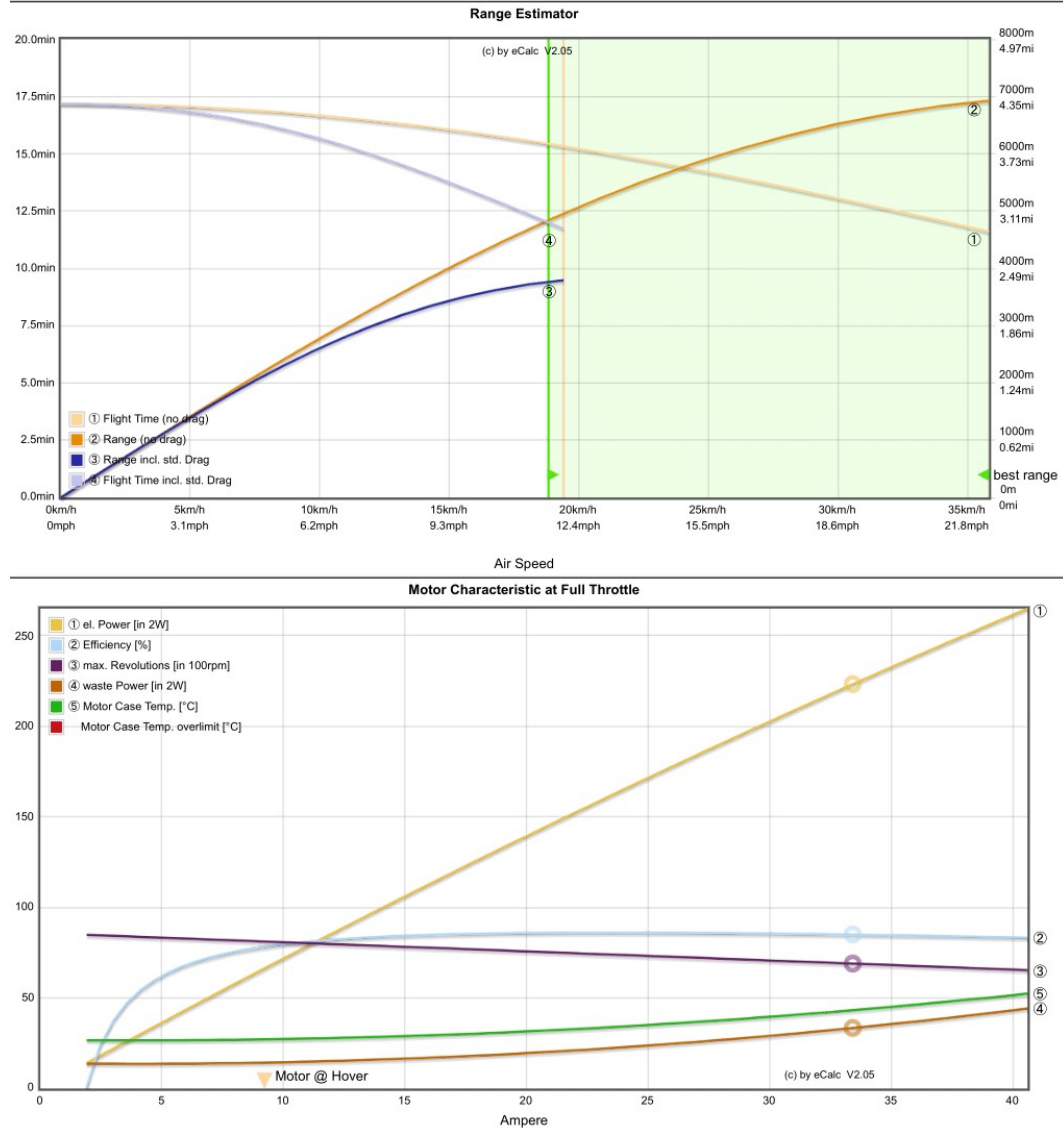


Figure 47: UAV platform loaded configuration range estimations and motor characteristics at full throttle.





## Appendix P Mass Estimation

Table 27: UAV on-board mass estimation, noting that the mass of certain small components are not available.

Item Identifier	Item Description	Quantity	Mass [g]
Ma.1	<b>Flight Control System</b>		
Ma.1.1	Cube Orange Standard Set (ADS-B Carrier Board)	1	200
Ma.1.2	Here3 GPS	1	50
Ma.1.3	Foxtech GPS Folding Antenna Mount Holder	1	38
Ma.1.4	RFD900x Modem Bundle	1	350
Ma.1.5	PIXHAWK2 to RFD900 Telemetry Cable - 300mm	1	10
Ma.1.6	Raspberry Pi 4	1	46
Ma.1.7	Battery Eliminator Circuit	1	16
Ma.1.8	Receiver Antenna Mount	1	6.6
Ma.2	<b>Airframe</b>		
Ma.2.1	Tarot T810 CF Folding Hexacopter(TL810A)	1	1020
Ma.2.2	T810/T960 gimbal mount kit(TL96014)	1	200
Ma.2.3	TL96016 Rubber Damper Ring (12mm Dia.)	6	36
Ma.2.4	TL96013-02 Upgraded Landing Skids for T810	1	275
Ma.2.5	T-Motor MN4010 580kV	6	822
Ma.2.6	NS15x5 Prop-2PCS/PAIR	6	126
Ma.2.7	Propeller Quick Detach CW&CCW	3	18
Ma.3	<b>On-board Power</b>		
Ma.3.1	Turnigy Graphene Professional 10000mAh 4S 15C LiPo Pack w/ XT90	2	1872
M.3.2	Tarot T810/T960 mount dual battery under the seat(TL96018)	2	97.92
Ma.4	<b>Camera System</b>		
Ma.4.1	Caddx Turtle V2	1	12
Ma.4.2	Micro Minim On Screen Display (OSD) with KV Team Mod	1	1.8
Ma.4.3	25-200-600mW Adjustable Power Video Transmitter (SPMVT1000)	1	9.9
Ma.4.4	IR Sensor	1	21.5
Ma.4.5	Lidar Rangefinder	1	50
Ma.4.6	Electro Ferromagnet	1	65
Ma.5	<b>Payload</b>		
Ma.5.1	IR Beacon	1	200
Ma.5.2	Ferrous Plate	1	12.88
Ma.5.4	Arduino & Bluetooth Module	1	25
	<b>Total On-Board Mass</b>		<b>5751</b>
	<b>On-Board Mass, Excluding Payload</b>		<b>5344</b>

## Appendix Q Budget Breakdown

Table 28: Itemised list of anticipated direct project expenditure.

Item	Source	Backward Traceability	Price per Unit [\$]	Quantity	Total [\$]
Telemetry Cables for Smart Port Radios	Amazon	O-3	26.3	1	26.3
FPV Camera	Phaser FPV	O-2	67.72	1	67.72
GPS Mast	Fox Tech	O-1, O-3	32.37	1	32.37
Tarot T810 CF Folding Hexacopter(TL810A)	Fox Tech	O-1, O-2	846.2	1	846.2
Gimbal Rail	Fox Tech	O-1, O-2	17.59	1	17.59
Hobbywing XRotor 40A ESC(no BEC)	Fox Tech	O-1, O-2	12.49	9	112.41
Propeller Quick Detach CWCCW	Fox Tech	O-1, O-2	3.84	8	30.72
Battery Tray	Fox Tech	O-1, O-2	4.745	2	9.49
TL96016 Rubber Damper Ring (12mm Dia.)	Helipal	O-1, O-2	9.77	6	58.62
TL96013-02 Upgraded Landing Skids for T810	Helipal	O-1, O-2	116.54	1	116.54
25-200-600mW Adjustable Power Video Transmitter (SP-MVT1000)	Horizon Hobby	O-2	39.99	1	39.99
VTX Antenna	Horizon Hobby	O-2	13.99	1	13.99
RP Controller	Next FPV	O-1, O-3	399.95	1	399.95
RP Controller Receiver	Next FPV	O-1, O-3	89.95	1	89.95
Balance Charger	RC Mart	O-1, O-2, O-3	219.4	1	219.4
T-Motor MN4010 580kV	T-Motor	O-1, O-2	86.9	9	782.1
NS15x5 Prop-2PCS/PAIR	T-Motor	O-1, O-2	73.75	9	663.75
IR Sensor	IR-LOCK	O-2	152.73	1	152.73
IR Beacon	IR-LOCK	O-2	210.48	1	210.48
Pixhawk cable	IR-LOCK	O-2	7.64	1	7.64
Lidar Rangefinder	IR-LOCK	O-2	358.01	1	358.01
Electro ferromagnet	NicaDrone	O-2	159.99	1	159.99
Ferrous Target Square 10 pack	NicaDrone	O-2	14	1	14
9v battery	Bunnings	O-4	5.49	1	5.49
Turnigy 2200mAh 3S 25C LiPo Pack	HobbyKing	O-4	19.23	1	19.23
Turnigy High Quality 16AWG Silicone Wire 10m (Red)	HobbyKing	O-1	11.66	1	11.66

Turnigy High Quality 16AWG Silicone Wire 10m (Black)	HobbyKing	O-1	11.66	1	11.66
Turnigy High Quality 10AWG Silicone Wire 10m (Red)	HobbyKing	O-1	41.15	1	41.15
Turnigy High Quality 10AWG Silicone Wire 10m (Black)	HobbyKing	O-1	41.15	1	41.15
Crescent 150 x 3.6mm Black Cable Ties - 100 Pack	HobbyKing	O-1	2.65	2	5.3
Double Sided Tape (Clear) 25mm x 1m	HobbyKing	O-1	5.24	2	10.48
Male-to-Male Silicone Servo Leads 26AWG (JR) 130mm 5pcs/bag	HobbyKing	O-1	6.96	1	6.96
30CM Servo Lead Extension (Futaba) 26AWG (10pcs/set)	HobbyKing	O-1	4.65	1	4.65
HobbyKing Receiver Antenna Mount Dual 45deg With Direct Or Clip Mount	HobbyKing	O-3	1.53	1	1.53
3.5mm Gold Compact Connector (10pairs)	HobbyKing	O-1	1.97	6	11.82
Graphene Battery Strap 300 x 20mm (3 Pcs)	HobbyKing	O-1	7	4	28
Turnigy Graphene Professional 10000mAh 4S 15C LiPo Pack w/ XT90	HobbyKing	O-1	167.23	4	668.92
XT90 Battery Harness 10AWG for 2 Packs in Parallel	HobbyKing	O-1	12.11	1	12.11
4mm bullets	HobbyKing	O-1	4.71	12	56.52
Lithium Polymer Charge Pack 25x33cm JUMBO Sack	HobbyKing	O-1	7.23	2	14.46
Turnigy® Fire Retardant LiPoly Battery Bag (Zippered) (200x155x95mm) (1pc)	HobbyKing	O-1	6.48	2	12.96
XT90 Silicone Charged and Discharged Indicator Caps (5pairs)	HobbyKing	O-1	4.47	2	8.94
Micro Minim On Screen Display (OSD) with KV Team Mod	HobbyKing	O-1	8.62	1	8.62
Cube Orange Standard Set (ADS-B Carrier Board)	Bask Aerospace	O-1, O-2	473	1	473
Here3 GPS	Bask Aerospace	O-1, O-2	215.45	1	215.45
RFD900x Modem Bundle	Bask Aerospace	O-1, O-3	312.5	1	312.5
RFD900X Modem	Bask Aerospace	O-1, O-3	131.45	2	262.9
900MHz 2dBi Straight Monopole Antenna	Bask Aerospace	O-1, O-3	6.55	1	6.55
900MHz 2dBi Right Angle Monopole Antenna	Bask Aerospace	O-1, O-3	6.55	1	6.55
900MHz 3dBi Dipole Antenna	Bask Aerospace	O-1, O-3	7.65	4	30.6
PIXHAWK2 to RFD900 Telemetry Cable - 300mm	Bask Aerospace	O-1, O-3	4.95	3	14.85
PL2-6S BEC / 2 x 5.3V-3A / With CFK Enclosure	Bask Aerospace	O-1, O-3	91.74	1	91.74
PL - FC cable for Cube / Pixhawk2.1 / MolexClik-Mate2.0-6p / 150mm	Bask Aerospace	O-1, O-3	10	2	20

PL-200 Sensorboard / 2 x 10cm 10AWG / With CFK Enclosure	Bask Aerospace	O-1, O-3	69.55	1	69.55
Raspberry Pi 4 Model B 2GB	Core Electronics	O-3, O-4	66.92	2	133.84
Raspberry Pi 4 Model B 4GB	Core Electronics	O-3, O-4	92.4	1	92.4
Pimoroni Pibow Coupé 4 Ninja (Raspberry Pi 4 only)	Core Electronics	O-3, O-4	18.95	3	56.85
Arduino Uno R3	Core Electronics	O-3, O-4	39	3	117
USB Cable A-B for Arduino	Core Electronics	O-3, O-4	2.18	3	6.54
Bluetooth Module (HC-05)	Core Electronics	O-3, O-4	13.2	3	39.6
Raspberry Pi 4 Power Supply (Official) - USB-C 5.1V 15.3W (White)	Core Electronics	O-3, O-4	16.45	3	49.35
USB MicroSD Card Reader/Writer - MicroSD / MicroSDHC / MicroSDXC	Core Electronics	O-3, O-4	13.42	1	13.42
MicroSD Memory Card - 16GB Class 10	Core Electronics	O-3, O-4	14	1	14
Micro-HDMI To Standard HDMI 1M Cable	Core Electronics	O-3, O-4	7.65	3	22.95
<b>Total</b>					<b>7471.85</b>

Table 29: Quantifiable in-kind contributions for the project.

<b>Item</b>	<b>Source</b>	<b>Backward Traceability</b>	<b>Price per Unit [\$]</b>	<b>Quantity</b>	<b>Total [\$]</b>
Autodesk Inventor 1-Year Licence	University of Adelaide	O-2, O-4	3223	3	9669
Microsoft 365 1-Year Licence	University of Adelaide	O-1, O-2, O-3, O-4	99	3	297
MATLAB 1-Year Licence	University of Adelaide	O-1, O-2	1320	3	3960
<b>Total</b>					<b>13926</b>

Table 30 is approximately constructed with consideration that David Roberts (DSTG representative) was provided monthly project updates and was involved with arranging flight testing at the DSTG Flight Test Range.

Table 30: In-kind labour contributions for the project.

<b>Stakeholder</b>	<b>Role</b>	<b>Hours per Week</b>	<b>Hours Worked</b>	<b>Hourly Rate [\$]</b>	<b>Total [\$]</b>
Patrick Capaldo	Student	14	490	50	24500
Jason Huynh	Student	14	490	50	24500
Daniel O'Connor	Student	14	490	50	24500
Rini Akmeliawati	Supervisor	3	105	150	15750
David Roberts	DSTG Representative		20	150	3000
Workshop Staff			10	50	500
Steele Phillips	Multicopter Advisor	1	35	150	5250
<b>Total</b>					<b>98000</b>